The Efficacy of LY293558 in Blocking Seizures and Associated Morphological, and Behavioral Alterations Induced by Soman in Immature Male Rats and the Role of the M1 Muscarinic Acetylcholine Receptor in Organophosphate Induced Seizures

by

Steven Lawrence Miller

Dissertation submitted to the Faculty of the
Neuroscience Graduate Program
Uniformed Services University of the Health Sciences
In partial fulfillment of the requirements for the degree of
Doctor of Philosophy, 2014

UNIFORMED SERVICES UNIVERSITY, SCHOOL OF MEDICINE GRADUATE PROGRAMS
Graduate Education Office (A 1045), 4301 Jones Bridge Road, Bethesda, MD 20814

FINAL EXAMINATION/PRIVATE DEFENSE FOR THE DEGREE OF DOCTOR OF PHILOSOPHY
IN THE NEUROSCIENCE GRADUATE PROGRAM

Name of Student: Steven Lawrence Miller

Date of Examination: January 30, 2015

Time: 10:00am

Place: C2095

DECISION OF EXAMINATION COMMITTEE MEMBERS:

	PASS	FAIL
Dr. Joseph McCabe DEPARTMENT OF ANATOMY, PHYSIOLOGY AND GENETICS Committee Chairperson	✓	
Dr. Maria Braga DEPARTMENT OF ANATOMY, PHYSIOLOGY AND GENETICS Dissertation Advisor	✓	
Dr. Ann Marini DEPARTMENT OF NEUROLOGY Committee Member	✓	
Dr. Thomas Flagg DEPARTMENT OF ANATOMY, PHYSIOLOGY AND GENETICS Committee Member	✓	
Dr. Fereshteh Nugent DEPARTMENT OF ANATOMY, PHYSIOLOGY AND GENETICS Committee Member	✓	

UNIFORMED SERVICES UNIVERSITY, SCHOOL OF MEDICINE GRADUATE PROGRAMS
Graduate Education Office (A 1045), 4301 Jones Bridge Road, Bethesda, MD 20814

APPROVAL OF THE DOCTORAL DISSERTATION IN THE
NEUROSCIENCE GRADUATE PROGRAM

Title of Dissertation: "The Efficacy of LY293558 in Blocking Seizures and Associated Morphological, and Behavioral Alterations Induced by Soman in Immature Male Rats and the Role of the M1 Muscarinic Acetylcholine Receptor in Organophosphate Induced Seizures"

Name of Candidate: Steven Lawrence Miller
Doctor of Philosophy Degree
January 30, 2015

DISSERTATION AND ABSTRACT APPROVED:

DATE:

Joseph McCabe 2/11/15
Dr. Joseph McCabe
DEPARTMENT OF ANATOMY, PHYSIOLOGY AND GENETICS
Committee Chairperson

1/30/15
Dr. Maria Braga
DEPARTMENT OF ANATOMY, PHYSIOLOGY AND GENETICS
Dissertation Advisor

1/30/15
Dr. Ann Marini
DEPARTMENT OF NEUROLOGY
Committee Member

1/30/15
Dr. Thomas Flagg
DEPARTMENT OF ANATOMY, PHYSIOLOGY AND GENETICS
Committee Member

1/30/15
Dr. Fereshteh Nugent
DEPARTMENT OF ANATOMY, PHYSIOLOGY AND GENETICS
Committee Member

ACKNOWLEDGMENTS

One of the most important lessons I have learned in my career in science so far is that science is a team effort. I could not be where I am today without the help of everyone I have met during my career thus far. Thank you to my CSU Fresno faculty who really started my career and instilled my passion for science and my curiosity: Drs. Jason Bush, James Prince, Madhusudan Katti, Eric Pearson, David Frank and Fred Schreiber. And, to Rowena Chu who started my "at-the-bench" training.

I truly appreciate Drs. Sharon Juliano and He Li for giving me the opportunity to rotate in their labs before I decided upon doing my dissertation work in the lab of Dr. Maria Braga. Thank you Dr. Braga for your extensive training you have provided to me from the day that I joined your lab. Your mentorship has been a critical part of propelling me through the neuroscience program at USUHS and I believe that I have excelled because of it. Thank you for accepting me into your lab and for your guidance in training me to become a principal investigator. I believe a great deal of my future success will result from the extensive career advice you have given me, thank you so much.

Thank you to Drs. Vassiliki Aroniadou-Anderjaska, Volodymyr Pidoplichko and Taiza Figueiredo. You have all been invaluable members in my hands-on training and a special thanks to you Dr. Figueiredo who helped me conduct so many experiments up at Aberdeen Proving Grounds. Thank you to my collaborator Dr. James Apland for his guidance in the difficult field of research that we work in. And, thank you to his former laboratory technician, Andrew Borrell for his enthusiasm in helping me conduct experiments at Aberbeen Proving Grounds. Thank you to the other current and previous

lab members of the Braga lab including Drs. Eric Prager, Camila Almeida-Suhett, Franco Rosetti, as well as Katia Rosetti and Adriana Souza.

Thank you to the members of my dissertation committee which include my chair, Dr. Joseph McCabe, as well as Drs. Ann Marini, Fereshteh Nugent and Thomas Flagg. I have greatly appreciated the support and encouragement you've all provided.

The graduate education office has provided support I have been immensely appreciative of. Thank you to Drs. Lee Metcalf and Gregory Mueller for the providing the specialized support the PhDs-in-training need.

To my many friends, you have all been instrumental in helping me finish out one of the greatest challenges of my life. Thank you all for your support and know that you will forever have my love, gratitude and appreciation for it: Drs. Aimee Starosciak, Kristen Hamilton, Eric Prager, LTC Jennifer Coyner, MAJ John Buonora, Jeremy Ullmann, Clifton Dalgard, Anna Zecharia; Stephen Nasto, Andrew Smith, Chris Franklin, Elizabeth Watson, Sam Moseley, Fiona Brabazon, Steve Dash, Josh Royall, Michael Neill, Mike Rutherford, Stephanie Eftimiades, Justin Jung, Alex Biacsi, Maria Carrizales, Ryan Shepard, all of my classmates, my friends from the Society for Neuroscience, and my friends from both years of the Molecular Neuroanatomy Course in 2013 and 2014. Thank you all for your unwavering belief in me.

To my family: Ashly McHatton, Westley Firschein, Miles Firschein, Marshall Torre, Lawrence Miller and to my mother, Lynn Gygax, it is unclear to me where I would be without you all. I cannot think of a group of people who believe in me more than you and have made tremendous sacrifices to ensure that I made it to where I am. Thank you is completely inadequate, I love you all so much.

DEDICATION

I dedicate this work to Lynn Gygax, the best mother any son could ask for. No one is more selfless than you in putting my needs in front of yours. Thank you from the bottom of my heart for all that you've done for me.

The author hereby certifies that the use of any copyrighted material in the thesis manuscript entitled:

The Efficacy of LY293558 in Blocking Seizures and Associated Morphological and Behavioral Alterations Induced by Soman in Immature Male Rats and the Role of the M1 Muscarinic Acetylcholine Receptor in Organophosphate Induced Seizures

is appropriately acknowledged and, beyond brief excerpts, is with the permission of the copyright owner.

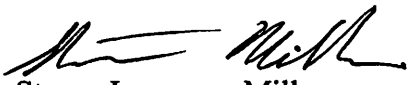

Steven Lawrence Miller
Program in Neuroscience
Department of Anatomy, Physiology & Genetics
Uniformed Services University
02/20/2015

ABSTRACT

Title of Dissertation: The Efficacy of LY293558 in Blocking Seizures and Associated Morphological, and Behavioral Alterations Induced by Soman in Immature Male Rats and the Role of the M1 Muscarinic Acetylcholine Receptor in Organophosphate Induced Seizures

By

Steven L. Miller, Doctor of Philosophy, 2015

Thesis directed by: Dr. Maria Braga, D.D.S., Ph.D.,

Professor, Department of Anatomy, Physiology, and Genetics

Department of Psychiatry, Program in Neuroscience

Poisoning by organophosphorous compounds (OPs) can produce severe symptoms including seizures or status epilepticus (SE), and if left untreated results in long-term brain damage and neuropsychiatric symptoms or death. OPs produce their toxic effects by irreversibly inhibiting the enzyme acetylcholinesterase (AChE), which subsequently causes a hyperstimulation of the muscarinic acetylcholine receptors (mAChRs) and the nicotinic acetylcholine receptors (nAChRs). The use of OP nerve agents in attacks in Syria recently highlighted the importance of developing treatments for all ages, but specifically, this attack highlighted the importance of developing treatments for seizures induced by OP intoxication for children. We developed an immature rat model appropriate for testing novel anticonvulsants against the nerve agent

soman. Using postnatal day 21 male rats (P21), we found them to be highly susceptible to seizure induction and mortality induced by soman exposure. Soman exposure in P21 rats produced profound reduction in the activity of AChE in numerous brain regions but suggested that this reduction must occur specifically in the basolateral amygdala (BLA) to produce seizures as animals that did not experience seizures still retained higher AChE activity within the BLA. Seizures, if treated within 20 min or 60 min post-soman exposure could be arrested with the administration of atropine sulfate (ATS) or the GluK1-subunit containing Kainate (GluK1KR)/α-Amino-3-hydroxy-5-methyl-4-isoxazolepropionic Acid (AMPA) Receptor Antagonist LY293558, respectively. We also found an additional GluK1KR antagonist, UBP302 to be efficacious in arresting soman-induced seizures when treatment was administered at 60 min post-exposure. Delayed posttreatment with LY293558 blocked volumetric reductions in the amygdala and hippocampus induced by soman exposure that was observed 30 or 90 days post-soman exposure in rats that did not receive LY293558 treatment. LY293558 treatment prevented an increase in anxiety-like behavior and deficits in fear conditioning at 30 days post-soman exposure. These results provide a rodent model relevant to the pediatric population for studying novel anticonvulsants for soman intoxication and identify treatments that are efficacious against soman-induced seizures and in preventing the associated long-term effects.

Hyperstimulation of mAChRs, within the BLA, is thought to be responsible for seizure induction following OP intoxication. To date, it has not been elucidated what specific subtypes of mAChRs are involved in seizure induction, nor how their stimulation produces an excitatory state. We found that the OP paraoxon (POX), through stimulation

of the M_1 mAChR subtype, facilitates a net increase in the ratio of spontaneous excitatory postsynaptic currents to spontaneous inhibitory postsynaptic currents within the BLA. We also found that antagonizing M_1 mAChRs *in vivo* in rats suppressed the severity of seizures induced by either POX or soman, indicating a critical role for these receptors for seizure induction following OP intoxication.

TABLE OF CONTENTS

LIST OF TABLES

LIST OF FIGURES

CHAPTER 1: Introduction

Over 1,400 civilians were killed by rockets loaded with military-grade sarin during attacks in Damascus, Syria. The victims of this attack, which occurred in August, 2013, resulted in the death of 426 children and exemplifies one of the deadliest uses of chemical weapons in recent history (81). Nerve agents, like sarin, are categorized as OP compounds and also include some widely used pesticides. OPs can be extremely lethal upon exposure; approximately 10% of people exposed to an OP will die from the acute toxic side effects resulting from exposure (26; 60), indicating the significant public health concern of OP exposure.

OP compounds exert their toxic effects through their action as irreversible inhibitors of the enzyme AChE in the peripheral and central nervous system. Irreversible inhibition of AChE indirectly results in a "cholinergic crisis" and induces a collection of symptoms, including salivation, lacrimation, urination, defecation, gastrointestinal motility, emesis, and miosis. In cases of severe poisoning, or if treatment is not immediately administered, respiratory distress/failure and seizures/SE may result. Following the binding of an OP compound to AChE, a biochemical process referred to as "aging" occurs, where the OP becomes permanently bound to AChE, resulting in an inability to restore AChE enzymatic activity. Time to AChE aging widely varies depending on the OP compound, but nerve agents, especially the nerve agent soman, display extremely short times to AChE aging, which makes the window for therapeutic intervention limited.

BIOCHEMICAL MECHANISM OF OP ACTION

AChE is a critically important enzyme in the peripheral and central nervous system due to its role in the termination of cholinergic neurotransmission. The canonical role of AChE is the catalytic hydrolysis of acetylcholine (ACh) into acetate and choline (272). AChE contains a catalytic triad of histidine, glutamate and serine deep within the core of the enzyme and requires that the substrate for hydrolysis travel down into the enzyme to be hydrolyzed (263; 272). OPs act as a substrate for AChE; once they interact with the enzyme, the phosphorous group on the OP forms a covalent bond with the serine residue within the active site (144). AChE can spontaneously recover its activity with the OP potentially dissociating, but the rate at which AChE can recover activity varies depending on the particular AChE-OP conjugate. If bound long enough to an OP, the active site of AChE undergo dealkylation, which in turn makes this AChE-OP conjugate permanent and AChE permanently inactive (144). The half-time to AChE aging varies widely by the specific OP studied, but the rate of aging for AChE-OP conjugates is highest for the nerve agent class of OPs (265). The aging half-time from the binding of soman to human AChE has been reported to be as fast as 1.87 min which makes soman one of the most lethal nerve agents (251) and is the nerve agent studied in this dissertation.

PROPERTIES OF ORGANOPHOSPHATES: NERVE AGENTS AND PESTICIDES

Pesticides and nerve agents share a similar, primary mechanism of action: the irreversible inhibition of AChE. Both pesticides and nerve agent organophosphates pose a high risk to humans due to their potency and exert toxic effects through all potential routes of exposure. However, the biochemical, chemical and physical properties of these compounds vary dramatically and must be considered to understand the differences in

their relative toxicity. See Table 1 for a comparison of the relative toxicities between pesticides and nerve agents.

Table 1. Physical and Toxicological Properties of Nerve Agents and Pesticides.

	Tabun	Sarin	Soman	VX	Parathion	Dichlorvos	Chlorpyrifos	Malathion
OP Classification	Nerve Agent	Nerve Agent	Nerve Agent	Nerve Agent	Pesticide	Pesticide	Pesticide	Pesticide
Subclassification	G-Series	G-Series	G-Series	V-Series	Diethyl	Diethyl	Dimethyl	Dimethyl
Molecular Weight (g/mol)	162.13	140.09	182.17	267.37	291.26	220.28	350.59	330.36
Vapor Pressure (mm Hg at 20°C)	490	22,000	3,900	10.5	6.68×10^{-6}	1.2×10^{-2}	1.9×10^{-5}*	3.38×10^{-6}
Rat Dermal LD50 (mg/kg)	18	N/A	N/A	N/A	6.8-49.4	75-107	202	>4,400
Rat Oral LD50 (mg/kg)	3.7	0.55	N/A	0.012	2-22	56-80	155	1000-1375
Human Dermal LD50 (mg/70 kg)	1	0.7	0.35	0.001-0.006	N/A	N/A	N/A	N/A
Human Oral LD50 (mg/70 kg)	N/A	8-12	7-12	5	50-200	500-1000	grams	grams

References: (24; 206; 211; 245; 285). *mm Hg at 25°C.

Organophosphate Pesticides

Organophosphate pesticides are categorized into two groups: diethyl and dimethyl pesticides. Commonly used dimethyl pesticides include dichlorvos and malathion whereas commonly used diethyl pesticides include chlorphyrifos and parathion. Of these pesticides, the World Health Organization (WHO) ranks parathion as the most hazardous, while dichlorvos, chlorpyrifos, and malathion are less hazardous (144). Hazard rankings are determined by the WHO based on dermal and oral acute toxicity in the rat, where dermal medial lethal dose (LD_{50}) values dictate the hazardous classification of a pesticide (123). Additionally, if toxic effects in humans are found to be more pronounced, pesticides are classified into more hazardous categories (310). Enhanced toxicity of diethyl pesticides can be explained by a relatively slow spontaneous reactivation of AChE following diethyl pesticide binding to the active site of AChE (100). This also explains why dimethyl pesticides are classified as less toxic or hazardous due to the faster spontaneous reactivation of AChE (100). Some of the OP pesticides require a metabolic conversion to the active, toxic metabolite. Following exposure to these pesticides, liver oxidases rapidly convert these compounds to an 'oxon' form, which is the form that binds to and irreversibly inhibits AChE (286). The precursor, parent compounds are relatively inactive and exert minimal toxicity on their own prior to conversion into their oxon form (287). Some of the parent compounds are not substrates that are capable of interacting with AChE until metabolic conversion to the oxon form (287). Parathion, for example, is converted by oxidative metabolism to paraoxon and is highly toxic compared to the parent compound (286). Synthesized in 1944, parathion is one of the most lethal pesticides (287) and has been used as a chemical weapon in war (189). Specifically, the Rhodesian Army produced a lethal mixture of parathion by mixing it with dimethyl

sulfoxide to contaminate clothing left for guerilla rebels to find and wear during the Rhodesian war (189). Parathion is rarely used in agriculture due to its severe, acute toxicity in humans, persistence in the environment, and is easily replaced by effective pesticides that are less toxic to humans (135). Given its high toxicity, and shared mechanism of action to nerve agents; the active metabolite paraoxon was used for pharmacological studies in this dissertation.

Organophosphate Nerve Agents

OP nerve agents differ in their toxicity compared to OP pesticides for a variety of reasons: 1) nerve agents do not require metabolic conversion into an active, toxic form in order to act as a substrate for AChE and result in the irreversible inhibition of AChE, 2) AChE aging time is far more rapid for nerve agents than pesticides, and 3) the potency of nerve agents is dramatically higher compared to pesticides, as doses that are required for lethal action are far smaller. These characteristics of nerve agents make treatment challenging as the onset to the most severe symptoms including respiratory distress and seizures can occur rapidly.

MECHANISM OF ORGANOPHOSPHATE-INDUCED SEIZURES

Following AChE inhibition, synaptic levels of ACh increase drastically and cause a hyperstimulation of the ACh receptors: the mAChRs and the nAChRs. In cases of severe poisoning, profound inhibition of AChE in the brain can induce long-lasting seizures or SE. Animal models demonstrate that, if these seizures are not arrested, severe brain damage results (12; 13; 89). Seizures are a common symptom in severely poisoned individuals, as seen in the patients exposed to sarin following the Tokyo Subway attacks by the Japanese terrorist group Aum Shinrikyo (202; 205). SE induced by nerve agents is

notoriously difficult to treat. Evidence from experimental models suggest that the longer an episode of nerve agent induced-SE lasts, the greater the resulting brain damage and associated symptoms.

Seizures induced by severe poisoning by OPs are a biochemical consequence of the irreversible inhibition of AChE, which in turn leads to a dramatic increase in synaptic ACh. A three-phase model of seizure initiation and maintenance following organophosphate poisoning proposed by Shih and Mcdonough (181) suggests that the increase in synaptic ACh initiates seizure activity, primarily through the hyperstimulation of mAChRs. Neuropharmacological evidence supports this hypothesis as pre- or rapid post-treatment with nonselective mAChR antagonists such as atropine sulfate or scopolamine exert potent anticonvulsant efficacy (153; 181; 259; 261; 266). However, as seizure activity continues over time, treatment with mAChR antagonists exert either no or little anticonvulsant efficacy and require dramatically higher doses in order to do so. Following an early phase of seizure activity mediated primarily by the increase in ACh in peripheral and central synapses, excitatory amino acids appear to sustain and reinforce ongoing seizure activity induced by OPs (181).

The development of successful immediate or delayed post-treatment of OP-induced seizures/SE requires an understanding of the mechanism by which AChE inhibition results in seizure induction, and experimental models that are relevant to all populations and ages to test novel therapies. While evidence suggests mAChRs play a critical role in seizure induction following OP poisoning, a clear mechanism for seizure induction and their maintenance remains to be elucidated. Additionally, a majority of the literature examining the long-term effects of organophosphates has largely been

examined in adult laboratory animals. Dramatic differences exist in the induction, maintenance, and treatment of seizure activity in the immature brain. However, no experimental models currently exist to examine 1) the long-term effects of these seizures in immature animals, 2) if novel therapies can arrest OP-induced seizures/SE in immature animals, 3) whether novel anticonvulsants are successful in blocking any associated long-term side effects of OP-induced SE, and 4) how seizures are induced by OPs in the immature brain. To address this gap, this dissertation has aimed to develop a rodent model relevant to the pediatric population for testing treatments to arrest seizures induced by the nerve agent soman, to verify whether new treatments can protect against the associated long-term toxic effects; and determine the cellular and molecular mechanism for seizure induction following severe OP poisoning.

TREATMENT OF OP-EXPOSURE

Following decontamination of the victim of OP intoxication, several pharmacological treatments are currently available depending on the severity of intoxication, symptoms present, and time at which therapies are administered.

Atropine

Atropine, a nonselective muscarinic receptor antagonist, is one of the first lines of care in the treatment of OP intoxication and is used as a countermeasure against the hyperstimulation of muscarinic receptors in the periphery (24). While animal studies suggest that atropine may be efficacious as an anticonvulsant, it has low availability to the central nervous system and may only be efficacious if given immediately after the onset of seizure activity, which is unrealistic for mass casualty scenarios (182). Atropine is extremely effective in alleviating some of the severe peripheral symptoms associated

with OP intoxication, including apnea, and bronchoconstriction, and can induce a drying of secretions associated with mAChR hyperstimulation (24). Tolerance for atropine may be very high as it has been estimated that in cases of severe OP intoxication, a safe therapeutic range can be 35-210 mg per 70 kg in humans (24). This recommended dose is much higher than the standard carried in the United States military nerve agent antidote kits which contains 2.1 mg atropine sulfate (184). Doses of atropine contained in autoinjectors designed for adult treatment following OP exposure have been found to be well-tolerated in children. During the Persian Gulf Crisis, for example, the Medical Corps of the Israeli Defense Forces distributed autoinjectors to the Israeli population containing antidotes to nerve agent exposure, including atropine. A total of 410 children unintentionally poisoned themselves with these atropine autoinjectors and were evaluated in two separate studies (7; 142) but only a small number of cases presented with symptoms of severe atropine poisoning but no deaths resulted.

Oximes

Oximes are also first line treatment for OP poisoning and are used in both clinical and military settings. Oximes are nucleophilic compounds that attack the phosphorous bond created between the AChE-OP adduct within the active site of AChE (145; 240). This reaction can restore the activity of AChE if the enzyme has not already undergone the aging process. Unfortunately, oximes do not exert broad-spectrum efficacy in restoring AChE function for all AChE-OP adducts. In the United States, pralidoxime chloride (2-PAM) is the standard civilian and military treatment used after OP intoxication; 2-PAM is predominantly effective in restoring AChE function when sarin or VX is the OP bound to the enzyme, but is relatively ineffective in restoring function

when the OP is tabun, cyclosarin or soman (240). These compounds are typically incapable of penetrating the blood-brain barrier and as a result have little efficacy as anticonvulsants (240). However, development of new oxime compounds with broad spectrum efficacy in restoring AChE function, which are capable of crossing the blood-brain barrier, is an active area of investigation and has yielded promising results with the compound MMB4 (46; 240).

Anticonvulsants

Atropine is only an effective anticonvulsant against seizures induced by OP exposure when administered rapidly following seizure induction; typically within the first 20 minutes (153; 261; 266). This may be due to a transition from mAChR-mediated seizure activity to glutamate-receptor hyperactivation that sustains ongoing seizure activity for OP-induced seizures (181). The United States Food and Drug Administration (FDA) approved diazepam for the treatment of seizures induced by OPs. Enhancing the activity of the inhibitory γ-aminobutyric acid A-receptor ($GABA_AR$) has been consistently used as a therapeutic approach for the treatment of seizures. Thus, the commercially available anticonvulsant, diazepam was investigated as a potential treatment for OP-induced seizures and has been implemented as the standard anticonvulsant in military autoinjectors designed for treatment of OP intoxication (181). Though numerous studies suggest that diazepam is an effective anticonvulsant for nerve agent-induced seizures, none of these studies found a complete protection of brain damage associated with nerve agent-induced seizures (37; 39; 65; 110; 115; 128; 129; 161-163; 169; 178; 180; 195; 218; 256; 257). Corroborating these findings, our group has found that diazepam administered 1 h following soman exposure offers either no or

minimal neuroprotection against seizure-induced cellular loss, depending on the brain structure studied (13). Diazepam treatment suppresses the initial episode of SE induced by soman exposure, but over a 24 h period diazepam treatment offers no protection against the total duration of SE. In juxtaposition, diazepam can enhance the 24 h duration of SE if treatment is delayed to 2 h post-soman exposure and it was found to increase the number of returning convulsive seizures (13).

It has been suggested that during a later phase of OP-induced seizure activity, ongoing activity is primarily mediated by the excitatory amino acid receptors (181), and as such, antagonists to the N-methyl-D-aspartate (NMDA) receptor have been thoroughly investigated. This has been substantiated by recent research suggesting the NMDA receptor antagonist MK-801 exerts some anticonvulsant efficacy against nerve agent-induced seizures and this efficacy increases when treatment is delayed to further timepoints (256). However, MK-801 is ineffective in blocking seizure induction or arresting seizure activity when administered soon after induction by soman (43; 256). As the sole treatment for seizures induced by soman in rats, high dose treatment of MK-801 increased mortality or enhanced the lethal effects of soman (256). In this study, Shih also found that treatment with MK-801 at doses necessary to exert anticonvulsant efficacy actually produces numerous adverse events including severe respiratory depression (256).

A novel class of glutamate receptor antagonists, GluK1KR antagonists, are promising candidates for arresting seizures and protecting the brain against the neuropathology associated with nerve agent exposure. GluK1KR antagonists have been found to block the induction or arrest ongoing seizures induced by pilocarpine–a nonselective mAChR agonist that has comparable mechanisms of action for seizure

induction and maintenance following exposure (269; 284). Topiramate, an anticonvulsant that has antagonistic properties for the GluK1KRs, suppresses excitability in the BLA (41), a key structure involved in the induction of seizures induced by OP exposure (227). Our group and others have hypothesized a critical role for GluK1KRs in maintaining and reinforcing further seizure activity during an episode of OP-induced SE. As such, we have investigated the role of GluK1KR antagonists as treatments for nerve agent-induced SE at delayed timepoints. Stopping seizures induced by nerve agents at delayed timepoints following seizure induction (e.g. 1 h post-seizure onset) is extremely difficult, but model realistic windows for therapeutic intervention for mass casualty scenarios involving civilians or military personnel.

LY293558, a GluK1KR/AMPA receptor antagonist; and UBP302, a GluK1KR antagonist, are promising candidates for the treatment of OP-induced SE. When SE is induced by soman in adult male rats and treatment is delayed to 1 h post-soman exposure, LY293558 treatment: 1) increases survival to 100% , 2) reduces the initial episode of SE, 3) reduces the duration of SE over a 24 hr period, 4) protects against neuronal loss in BLA and CA1 at 1 and 7 d post-soman exposure, and 5) protects against the loss of interneurons in the BLA at 7 d post-soman exposure (12; 89). By comparison, UBP302 administration 1 h post-soman exposure: 1) increases survival to 96%, 2) reduces the initial episode of SE, 3) reduces the duration of SE over a 24 h period, 4) reduces neuronal loss in the BLA and CA1 at 1 and 7 d post-soman exposure, 5) protects against the loss of interneurons in the BLA at 7 d post-soman exposure, and 6) protects against the development of anxiety-like behavior induced by soman exposure (13). These results indicate that GluK1KR antagonist may be leading candidate in the treatment of OP-

induced SE as they are highly effective in increasing survival, arresting SE, and protecting against neuropathology and behavioral deficits induced by OP exposure. While both LY293558 and UBP302 show similar effectiveness, LY293558 reaches peak brain levels more rapidly following administration (12) and can arrest SE more rapidly following soman exposure. As such, LY293558 is the primary GluK1KR antagonist used in the experiments described below.

LONG-TERM NEUROTOXICOLOGICAL EFFECTS OF OP EXPOSURE

Long-Term Toxicological Effects in Humans

What is known about the long-term effects of nerve agents in humans has largely been derived from the long-term studies conducted on patients exposed to sarin in the early 1990's in Japan. Largely, the long-lasting symptoms resulting from sarin exposure are neuropsychiatric in nature (118), although some memory impairments have been reported (198; 200; 204). The most common diagnosis or clinical finding in long-term studies is the presentation of post-traumatic stress disorder (PTSD). A variety of studies that performed long-term follow-ups found a higher frequency of PTSD or suspected diagnoses of PTSD in sarin-exposed patients than in the general population, which was positively correlated with the severity of sarin exposure (134; 194; 200; 203; 204).

Gray and white matter analyses have been conducted on a collection of patients exposed to sarin from the attacks (238; 314). In one study, 38 patients treated for severe sarin intoxication had structural MRI scans and variety of structural alterations were identified up to six years post-sarin intoxication (314). In addition to widespread white matter integrity disruption in the parietal lobe, temporal lobe and brainstem, gray matter volume was reduced in the insular cortex, temporal cortex and the hippocampus (314).

Notably, the authors also found that the volume of insular white matter was positively correlated with serum cholinesterase (ChE) suggesting that more pronounced structural alterations are directly correlated to the severity of sarin intoxication (314). In a separate structural study of victims of the sarin attacks, 25 patients were scanned for differences in the volume of the amygdala and hippocampus. Remarkably, only patients who currently or had a history of PTSD displayed reductions in bilateral volumes of the amygdalae and specifically, a reduction in the volume of the left amygdala, which was negatively correlated with PTSD severity (238). Given the critical role of the amygdala in regulating anxiety and emotional processing (219; 221); along with the function of the hippocampus in memory processes (239), reductions in the volumes of these structures may impair their function and explain the observed, long-term clinical sequela of sarin poisoning.

Long-Term Toxicological Effects in Animals

The long-term consequences of OP and specifically nerve agent poisoning have been studied exhaustively in a variety of laboratory species including guinea pigs, mice and rats (70; 74; 90; 166; 188; 218; 228; 233). Exposing guinea pigs to sublethal (0.6 or 0.8 X LD_{50}) doses of soman resulted in anxiety-like behavior that persisted up to 3 months following a single exposure (166). Similarly, in mice exposed to soman, anxiety-like behavior was observed up to 3 months post-exposure and responses in both cue and context dependent fear conditioning were impaired (74). Additionally, both mice and rats have been found to have long-term deficits in performance on behavioral measures of learning and memory (90; 233). These behavioral studies suggest that a single, acute exposure to an OP can cause long-lasting anxiety and behavioral deficits.

Gross neuropathology is a common finding following OP-induced seizures in animals (12-14; 23; 62; 69; 89; 132; 133; 158; 176; 178; 181; 194; 216; 218; 228). The presence and severity of observed neuropathology appears to be directly related to the expression of seizures and their duration (177; 227; 228; 258). Of the variety of brain structures damaged following OP-induce seizures, which include the amygdala, hippocampus, entorhinal cortex, neocortex, piriform cortex, and thalamus, the amygdala, hippocampus and piriform cortex sustain the most severe damage (12-15; 53; 62; 70; 76; 89; 216). Given the role of the amygdala in regulating anxiety and its role in mediating cue-dependent fear conditioning, along with the role of the hippocampus in mediating context-dependent of fear conditioning and mediating some behavioral tasks of learning and memory, it would suggest that the neuropathology routinely observed in these structures following an OP exposure may explain the long-term behavioral impairments.

Acute neuropathology from OP-induced seizures may be long-lasting and could explain the long-term neuropsychiatric symptoms observed in humans following sarin poisoning. In mice receiving a convulsive dose of soman, the number of cells in the amygdala is still reduced compared to controls up to 90 days post-soman exposure (70) and correlates with impairments in amygdala-dependent behaviors such as cue-dependent fear conditioning, lasting up to 30 days post-exposure and increases in anxiety-like behavior up to 90 days post-exposure (74). Long-term neuropathology and impairments in hippocampal-dependent behaviors are also evident following soman intoxication. A single injection of soman in mice reduces the number of cells in the CA1 subfield of hippocampus by 50% and this reduction persists up to 90 days post-exposure (68). More severe intoxication by soman produces greater weight loss in mice and correlates the

extent of neuropathology observed in CA1 (90); as well as impairments in T-maze or the Morris water maze task up to 90 days post-exposure (90). Animal models provide an excellent means to study the mechanisms and time-course of the neuropathology and behavioral alterations resulting from OP intoxication. Information obtained from these studies may help in the development of novel treatments for OP intoxication, but limited studies have been performed to understand the effects of OPs, especially the effects of nerve agents on immature animals. This information is critically important for the development of treatments suitable for children during mass casualty scenarios involving nerve agent intoxication.

CHILDREN AND OP POISONING

Unlike adults, children require special consideration in the poisoning and treatment following intoxication by OPs. Children are highly susceptible to the toxic effects of OPs due to a variety of physiological, developmental and medical reasons. In the event of dermal exposure to OPs, children are poisoned faster and more severely due to thinner skin with a greater permeability compared to adults and a larger surface-area to body mass ratio (116). Greater respiratory minute volume – the total air either inhaled or exhaled in one minute – and their height, where vapor density of volatilized OPs is greatest, also make them more vulnerable to respiratory exposure (116). Levels of AChE in the brain are also lower compared to that of adults rats (Miller et al., Unpublished), characteristic of incomplete development of the cholinergic system (75), and therefore lower doses of OPs can elicit more severe symptoms. This is especially true in regards to seizures due to the increased susceptibility to seizure induction in children (1; 113). Standard decontamination methods, which do not include the use of heated water may

result in hypothermia following the decontamination of children also due to their higher surface-area to body-mass ratio (116). Medical guidelines for the treatment of children following nerve agent poisoning do not have a national consensus and therefore would likely result in chaos, overwhelming first responders and causing a high mortality rate for children during a mass casualty scenario involving nerve agents (92).

Given the special considerations for treating children intoxicated by OPs, it is surprising that more basic research has not been conducted in this area. To our knowledge, only one study has investigated developmental effects of nerve agent intoxication in animal models. Specifically, this study by Sterri and Colleagues (279) examined the mortality rates of rats exposed to varying doses of soman across development. They found that younger rats were more susceptible to death following soman exposure at lower doses when compared to adult rats only one to three weeks older (279). For example, in their study, when post-natal day 5 (P5) rats were exposed to 20 μg/kg soman (s.c.) this caused 100% mortality, but this same dose only resulted in a 25% mortality rate in P12 rats (279). This single study in rats and the deaths of the 426 children during the sarin attack in Syria highlight the importance of investigating the mechanisms of OP action in immature animals to develop treatment for children. With this knowledge, treatments may be developed to protect against the acute and long-term side effects associated with OP exposure.

CONCLUSIONS

The effects of OPs, their mechanism of action, treatment, as well as the acute and long-term effects are well studied in adult animals and humans. Though it is well accepted that the mechanism of action by which OPs induce their toxicity, and in

particular seizures, is through the inhibition of AChE and the subsequent hyperstimulation of mAChRs and nAChRs, the specific receptors responsible for seizure induction remain to be elucidated. The standard of care for seizures induced by OPs is diazepam, but recent evidence suggests diazepam may increase SE duration and mortality rate (13) and it is unclear if this therapy would be efficacious in children or protect them against the long-term effects associated OP-induced seizures. Therefore, the purpose of this dissertation is to develop a rodent model of nerve agent exposure that is relevant to the pediatric population. In particular, in immature rats we will: 1) test novel anticonvulsants to arrest seizures induced by nerve agents; 2) study the long-term deleterious effects associated with nerve agent induced seizures; 3) study whether novel anticonvulsants protect against these long-term neuropathological effects resulting from nerve agent-induced seizures; and 4) clarify the molecular and cellular mechanism by which OPs induce seizure activity.

CHAPTER 2: A Rat Model of Nerve Agent Exposure Applicable to the Pediatric Population: The Anticonvulsant Efficacies of Atropine and GluK1 Antagonists

Steven L. Miller[a,c], Vassiliki Aroniadou-Anderjaska[a,b,c], Taiza H. Figueiredo[a] , Eric M. Prager[a,c], Camila P. Almeida-Suhett[a,c], James P. Apland[d], Maria F.M. Braga[a,b,c*]

[a]Department of Anatomy, Physiology, and Genetics, [b]Department of Psychiatry, and [c]Program in Neuroscience, Uniformed Services University of the Health Sciences, 4301 Jones Bridge Road, Bethesda, MD 20814, USA
[d]Neurotoxicology Branch, U.S. Army Medical Research Institute of Chemical Defense, Aberdeen Proving Ground, Maryland, 21010, USA

*Corresponding Author:
Maria F.M. Braga, D.D.S., Ph.D.
Department of Anatomy, Physiology, and Genetics
F. Edward Hébert School of Medicine,
Uniformed Services University of the Health Sciences
4301 Jones Bridge Road
Bethesda, MD 20814, USA
Phone: (301) 295-3524
Fax: (301) 295-3566
Email: maria.braga@usuhs.edu

ABSTRACT

Inhibition of AChE after nerve agent exposure induces SE, which causes brain damage or death. The development of countermeasures appropriate for the pediatric population requires testing of anticonvulsant treatments in immature animals. In the present study, exposure of P21 rats to different doses of soman, followed by probit analysis, produced an LD_{50} of 62 μg/kg. The onset of SE was accompanied by a dramatic decrease in brain AChE activity; rats who did not develop SE had significantly less reduction of AChE activity in the basolateral amygdala than rats who developed SE. ATS at 2 mg/kg, administered 20 min after soman exposure ($1.2XLD_{50}$), terminated seizures. ATS at 0.5 mg/kg, given along with an oxime within 1 min after exposure, allowed testing of anticonvulsants at delayed time-points. The AMPA/GluK1 receptor antagonist LY293558, or the specific GluK1 antagonist UBP302, administered 1 h post-exposure, terminated SE. There were no degenerating neurons in the soman-exposed P21 rats, but both the amygdala and the hippocampus were smaller than in control rats at 30 and 90 days post-exposure; this pathology was not present in rats treated with LY293558. Behavioral deficits present at 30 days post-exposure, were also prevented by LY293558 treatment. Thus, in immature animals, a single injection of atropine is sufficient to halt nerve agent-induced seizures, if administered timely. Testing anticonvulsants at delayed time-points requires early administration of ATS at a low dose, sufficient to counteract only peripheral toxicity. LY293558 administered 1 h post-exposure, prevents brain pathology and behavioral deficits.

INTRODUCTION

Nerve agents are potent, OP toxins that act primarily by inhibiting the activity of AChE. The resulting accumulation of acetylcholine at synaptic junctions produces peripheral cholinergic crisis (excessive salivation, lacrimation, rhinorrhea, bronchorrhea, cardiorespiratory suppression, eventual muscle paralysis, etc.), and, in the brain, induces seizures and SE. Without timely pharmacological intervention, death will ensue, or if death is prevented but the SE is not controlled, brain damage will result, with long-term neurological and behavioral consequences (13; 14; 74; 88-90; 228; 229; 315). The nerve agent sarin that was released during a terrorist attack in Syria, in August 2013, resulted in the death of over 1,400 civilians, 426 of which were children (81). Mass casualties during terrorist attacks that employ nerve agents are expected to disproportionately affect children due to their greater body surface area-to-body mass ratio, increased skin permeability, faster respiration rate, breathing at a level where nerve agent vapor density would be highest, and an increased susceptibility to seizures (1). The higher vulnerability of children necessitates the availability of effective countermeasures that will protect their lives.

Pharmacological treatments to counteract nerve agent toxicity exist for the adult population, and the scientific community is actively seeking to improve them by testing the efficacy of novel compounds in mitigating both the short-term and the long-term health consequences of nerve agent exposure. Specifically, for the control of the peripheral effects of nerve agent exposure, the FDA has approved the use of atropine, a muscarinic receptor antagonist, along with an oxime (2-PAM), which reactivates the inhibited AChE (24; 25; 168; 297). In addition, diazepam has been approved for the cessation of nerve agent-induced SE. Improvements to this regimen are likely to be made

in the future, as more effective anticonvulsants are being discovered (12; 49; 88; 89; 97), and, as recent studies suggest, diazepam does not protect against brain damage and behavioral deficits associated with nerve agent exposure (13; 196), while other anticonvulsant compounds have high neuroprotective efficacy (13). Due to the nature of the research, nerve agent studies can be carried out only in animal models. Do the findings from studies in adult animals apply to the young age as well, and only the dose has to be adjusted according to body weight? There is very limited information on immature animals, and although it is possible that adult and immature animals or humans would respond similarly to pharmacological countermeasures against nerve agents, the differences between a developing brain and an adult brain, and their implications, must be considered. For example, the cholinergic system–which plays a central role in the mechanisms of nerve agent action– is still at a developing stage in early postnatal life (75). In addition, differences in the blood-brain barrier (BBB) between developing and adult animals (243; 294) could affect the pharmacokinetics of the injected drugs. Furthermore, there is evidence suggesting that immature animals differ from adult animals both in seizure susceptibility and in the extent and nature of neuropathology that seizures can induce (30; 113; 277; 302); it is unclear what type of neuropathology nerve agents induce in immature animals, and, therefore, it is also unclear what is the nature of neuroprotection expected by drugs that terminate nerve agent-induced seizures in immature animals.

In the present study, we describe findings in P21 rats. It is difficult to precisely ascertain the corresponding age in humans. If we use the conversion factor for the early developmental phase (10; 250), P21 would correspond to about a 6-month-old human;

however, because the developmental stage of the brain in the two species must be taken into account (8), and synaptogenesis–which is a basic parameter of brain development–is completed within the first 3 weeks of life in the rat and about 3.5 years in the human (230), a P21 rat may correspond to a human close to 4 years of age. In the P21 rats, we determined the LD_{50} of the nerve agent soman, measured AChE activity after soman exposure in brain regions that play an important role in seizure generation, and determined the effects of atropine administration on ongoing SE. In addition, because we have shown previously in young-adult rats that antagonists of kainate receptors containing the GluK1 subunit (formerly known as GluR5Rs, see (66; 124)) are very effective anticonvulsants and neuroprotectants against soman exposure (12; 13; 89), we also examined the efficacy of these compounds in the immature, P21 rats.

MATERIALS AND METHODS

Animals

Sprague-Dawley rats were obtained from Charles River Laboratories (Wilmington, MA). Male, immature rats (weighing 50-60g at the time of soman exposure on P21) were housed in groups of 5 with a surrogate mother and weaned on the day of experiments. Young-adult male rats (150-200g at the time of soman exposure) were housed in pairs until the day of experiments. All rats were provided with food and water ad libitum. Experiments were carried out with the approval of the Institutional Animal Care and Use Committees of the Uniformed Services University of the Health Sciences and the U.S. Army Institute of Chemical Defense.

Seizure induction and assessment

Rats were exposed to soman (pinacoyl methylphosphonofluoridate; obtained from the Edgewood Chemical Biological Center, Aberdeen Proving Ground, Edgewood, MD) diluted in cold physiological saline, by subcutaneous injection over the right hind-quarter. The LD_{50} was determined for the immature rats (see next section), and the two age-groups (immature and young-adult rats) were administered a dose that corresponded to 1.2 X $LD_{50.}$ Seizures were classified according to a minimally modified version of the Racine scale (232) as we have previously described (89): stage 0, no behavioral response; stage 1, behavioral arrest; stage 2, oral/facial movements, chewing, head nodding; stage 3, unilateral/bilateral forelimb clonus without rearing, Straub tail, extended body posture; stage 4, bilateral forelimb clonus plus rearing; stage 5, rearing and falling; and stage 6, full tonic seizures. Following soman injection, rats that went on to develop Stage 3 seizures or above were considered to have SE.

Median lethal dose determination

Using the log-probit method (164), we determined the LD_{50} of soman for the immature rats. P21 rats were randomly assigned into five groups of ten animals per group. Animals in each group received doses ranging from 40 to 70 μg/kg soman.

Groups and drug treatments

Another group of P21 male rats were administered 1.2 X LD_{50} soman (74.4 μg/kg, s.c.) followed by 0.5 mg/kg ATS (i.m) and 125 mg/kg HI-6 (i.p.) at 1 min post-soman exposure; HI-6 is a bispyridinium oxime that reactivates inhibited acetylcholinesterase, primarily in the periphery (131; 186). At 60 min after soman injection, these rats were administered the GluK1/AMPA receptor antagonist LY293558 (20 mg/kg, i.m.; kindly provided by Raptor Pharmaceutical Corp., Novato, CA; Bleakman et al., 1996), or the GluK1 receptor antagonist UBP302 (250 mg/kg, i.p.; Tocris, Bristol, UK; (190)), or the drug vehicle.

Acetylcholinesterase assay

Following soman exposure, rats that went on to develop SE were sacrificed immediately (at the onset of SE). Rats that did not develop SE were sacrificed 20 min after soman exposure. Total AChE activity was measured in the prelimbic cortex, BLA, piriform cortex, and hippocampus, using an established spectrophotometric protocol (83; 207). Rats were anesthetized with 3-5% isoflurane and rapidly decapitated. The brain was removed and placed in ice-cold phosphate buffer (0.1 M, pH 8.0). Coronal brain slices (500 μm-thick) containing the prelimbic cortex (Bregma 5.16 mm to 2.52 mm), BLA (Bregma -2.28 mm to -3.72 mm), piriform cortex (Bregma -1.72 mm to -3.00 mm), and hippocampus (Bregma -2.28 mm to -4.68 mm) were cut using a vibratome (series 1000;

Technical Products International, St. Louis, MO). The subsequent procedure has been described previously (227; 228). Briefly, each structure was isolated by hand and placed in an Eppendorf tube. They were homogenized in phosphate buffer (0.1M, pH 8.0) + Triton 10%, centrifuged, and the supernatant was placed into a separate Eppendorf tube. Glutathione was used to construct a standard curve in the presence of DTNB [5.5'-dithio-bis(2-nitrobenzonic acid)]. Then, tissue homogenate supernatants (10 µL per well) were added to either 10 µL eserine or ethoprozine, in the presence of 5 µL acetylthiocholine (1 µM) and 175 µL DTNB (1 mM; all purchased from Sigma-Aldrich, St. Louis, MO). Samples were read by the Softmax Pro 5.2 kinetics every 20 sec for 4 min. The total butyrylcholinesterase inhibition was subtracted from the absorbance sample to provide a difference score, which was multiplied by the slope and intercept of the standard curve to provide the total AChE activity. AChE specific activity was calculated by dividing the total activity by the calculated protein concentration assayed by the Bradford method (40) using a protein assay dye reagent (Biorad, Cat # 500-006).

Fixation and tissue processing

One day, 7, 30, or 90 days after soman administration, groups of rats were deeply anesthetized with pentobarbital (75–100 mg/kg, i.p.) and transcardially perfused with PBS (100 ml) followed by 4% paraformaldehyde (200 ml). The brains were removed and postfixed overnight at 4°C, then transferred to a solution of 30% sucrose in PBS for 72 h, and frozen with dry ice before storage at 80°C until sectioning. A 1-in-5 series of sections from the rostral extent of the amygdala to the caudal extent of the entorhinal cortex was cut at 40 µm on a sliding microtome. One series of sections was mounted on slides (Superfrost Plus; Daigger, Vernon Hills, IL) in PBS for Nissl staining with cresyl violet.

Two adjacent series of sections were also mounted on slides for Fluoro-Jade C (FJC) staining.

FJC staining and analysis

FJC (Histo-Chem, Jefferson, AR) was used to identify irreversibly degenerating neurons (247) in the brains of P21 soman-exposed rats, at 24 h and 7 days after exposure, as described previously (12; 89). Mounted sections were air-dried overnight and then immersed in a solution of 1% sodium hydroxide in 80% ethanol for 5 min. The slides were then rinsed for 2 min in 70% ethanol and 2 min in distilled water (dH_20), and then incubated in 0.06% potassium permanganate solution for 10 min. After a 2 min rinse in dH_20, the slides were transferred to a 0.0001% solution of FJC dissolved in 0.1% acetic acid for 10 minutes. Following three 1-minute rinses in dH_20, the slides were dried on a slide warmer, cleared in xylene for at least 1 min, and coverslipped with DPX (Sigma-Aldrich). To assess the extent of neurodegeneration, we used a series of adjacent Nissl-stained sections to trace the regions of interest. The tracings from the Nissl-stained sections were superimposed on the FJC-stained sections, using the Stereo Investigator 9.0 (MicroBrightField, Williston, VT). The rating system used to assess the extent of neurodegeneration has been described previously (14; 89).

Volumetric analysis

Volumetric analysis was performed 30 and 90 days after soman exposure. Nissl-stained sections containing the hippocampal formation (sections were 400 µm apart) or the amygdala (sections were 200 µm apart) were used to estimate stereologically the volume of these structures based on the previously described Cavalieri principle (Gundersen et al., 1988). Sections were viewed with a Zeiss Axioplan 2ie fluorescent

microscope with a motorized stage (Oberkochen, Germany), interfaced with a computer, running StereoInvestigator 9.0 (MicroBrightField, Williston, VT). The hippocampus and the amygdala were identified on slide-mounted sections under a 2.5x objective, based on the atlas of Paxinos and Watson (215), and traced using the Stereo Investigator 9.0. The volume was calculated by using the stereological probe called Cavalieri Estimator. An overlay of a rectangular lattice with a grid size of 300 µm was placed over the brain region (amygdala or hippocampus) tracings, and each point marked was counted to estimate the volume. For each animal, the coefficient of error (CE) was calculated to assure sufficient accuracy of the estimate (CE < 0.05).

Context- and cue-dependent fear conditioning

Fear conditioning took place 30 or 90 days after soman exposure. Rats were placed in Context A, which was a rodent-conditioning chamber made of Plexiglas and metal grid floor (Coulbourn Instruments, Lehigh Valley, PA, USA). The chamber was dimly illuminated by a single house-light (2–3 lux) and enclosed within a sound-attenuating chamber (background dB = 55). The chamber was cleaned between testing runs with a 70 % EtOH solution and thoroughly dried. Prior to presentation of the stimuli, rats were left to explore the chamber for 5 min. Then, they were presented with three pairings of an auditory conditioning stimulus (CS; 5 kHz, 75 dB, 20 s) that co-terminated with a foot-shock unconditioned stimulus (US; 1.0 mA, 500 ms); the intervals between CS presentations were random. One and two days after the fear conditioning, rats were placed in Context A for 20 min, with no presentations of CS or US, in order to test for context-dependent fear acquisition. Three and four days after the fear conditioning, rats were placed into a novel context (Context B), and were presented with twenty auditory

CS (5 kHz, 75 dB, 20 s) at random intervals and without electric shock, in order to test for cue-dependent fear acquisition. Context B consisted of plastic flooring covered with fresh bedding; it had a geometry different from that of context A, contained different spatial cues (red and black tape), and was cleaned with 1 % acetic acid solution. Freezing behavior during testing of context or cue-dependent fear acquisition was scored from digitized videos. Freezing was defined as the absence of all movements except those related to respiration (Fanselow, 1980). For the cue-dependent test, freezing was scored only during the CS presentations, while for the context-dependent test, freezing was scored throughout the session. Total freezing time during test sessions was used as a measurement of the extent of fear acquisition (the impact of the fear conditioning).

The open field test

Thirty and 90 days after soman exposure, anxiety-like behavior was assessed in the open field apparatus (40X40X30 cm clear Plexiglas arena), as described previously (17; 228). One day prior to testing (on day 29 or 89 after soman exposure), animals were acclimated to the apparatus for 20 min. On the test day, the rats were placed in the center of the open field, and activity was measured and recorded for 20 min, using an Accuscan Electronics infrared photocell system (Accuscan Instruments Inc., Columbus, OH). Data were automatically collected and transmitted to a computer equipped with "Fusion" software (from Accuscan Electronics). Locomotion (distance traveled in cm), total movement time, and time spent in the center of the open field were analyzed. Anxiety behavior was measured as the ratio of the time spent in the center over the total movement time, expressed as a percentage of the total movement time.

Statistical analysis

All data are expressed as mean ± standard error. Differences in latency to seizure onset between adult and P21 rats were tested for statistical significance using the Student's *t*-test. Results from the AChE assay were analyzed using either One-way ANOVA followed by Dunnett's post-hoc test, or one-way ANOVA followed by Tukey HSD post hoc test. Results from the behavioral seizures were analyzed using MANOVA followed by Bonferroni post-hoc test. One-way ANOVA with a Dunnett's post hoc test was used to analyze the results from the behavioral tests and from the volumetric analysis. Statistical analyses were made using the software package PAWS SPSS 22 (IBM, Armonk, NY, USA). Differences were considered significant with $p < 0.05$. Sample size "n" refers to the number of animals.

RESULTS

Calculation of the LD_{50} of soman in immature P21 male rats

The doses of soman (40-70 μg/kg, n = 10 rats/dose) and the corresponding mortality rates (Table 2) were the input data for the log-probit method of calculating the LD_{50}. Using the probit analysis function of the IBM SPSS Statistics 20 package, the estimated dose of soman expected to result in 50% mortality rate was calculated to be 62.02 μg/kg. The estimated soman doses and mortality rates (Table 3) were used to produce a dose-response curve for soman in P21 male rats (Fig. 1).

Table 2. Input Data for Log-Probit Analysis

Soman Dose (μg/kg)	Number of Rats	Mortality Rate
40	10	0%
55	10	40%
57.5	10	30%
62.5	10	50%
70	10	70%

Table 3. 95% Confidence Limits for Estimated Dose from Probit Analysis.

Estimated Mortality	Soman Dose Estimate (μg/kg)	Lower Bound	Upper Bound
.010	38.085	14.149	46.280
.020	40.325	16.924	47.951
.030	41.814	18.956	49.054
.040	42.970	20.640	49.909
.050	43.934	22.117	50.622
.060	44.771	23.455	51.243
.070	45.519	24.691	51.799
.080	46.199	25.851	52.306
.090	46.826	26.951	52.777
.100	47.411	28.002	53.219
.150	49.911	32.767	55.157
.200	51.991	37.045	56.872
.250	53.845	41.040	58.552
.300	55.566	44.817	60.340
.350	57.210	48.353	62.398
.400	58.815	51.557	64.926
.450	60.411	54.325	68.130
.500	62.023	56.633	72.148
.550	63.679	58.561	77.027
.600	65.407	60.235	82.802
.650	67.241	61.771	89.582
.700	69.231	63.258	97.594
.750	71.444	64.776	107.258
.800	73.991	66.407	119.332
.850	77.076	68.272	135.306
.900	81.140	70.606	158.672
.910	82.153	71.172	164.919
.920	83.268	71.788	171.993
.930	84.512	72.468	180.132
.940	85.923	73.230	189.689
.950	87.561	74.105	201.222
.960	89.525	75.140	215.687
.970	92.001	76.425	234.926
.980	95.398	78.158	263.217
.990	101.008	80.948	314.959

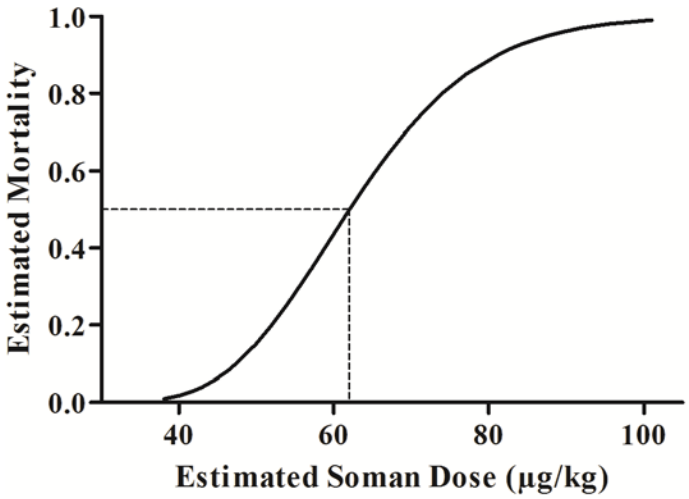

Figure 1. Determination of the LD_{50} of soman for P21 male rats. Fifty rats (10 rats per dose) were injected subcutaneously with soman at the following doses (µg/kg): 40, 55, 57.5, 62.5, and 70. Mortality rates were recorded at 24 hr following soman injection and used as the input data into the log-probit method of the IBM SPSS Statistics 20 package to determine the LD50. The plot shows the predicted mortality rates at different doses of soman at P21. The LD50 was 62.02 µg/kg (dashed line; $p = 0.00414$).

Latency to seizure onset and comparison with adults

Soman, at 1.2 X LD_{50}, was administered to 191 P21 rats (74.4 µg/kg), of whom 156 developed SE, as well as to 24 young-adult rats (132 µg/kg), of whom 16 developed SE. Mortality rates depended on the treatment and are reported below in the appropriate section. The latency to initiation of generalized seizures (stage 3 of the Racine scale) was significantly shorter in the P21 rats (2.15 ± 0.31 min, n = 20) compared to the young-adults (8.94 ± 0.25 min, n = 16, $p < 0.001$, Fig. 2).

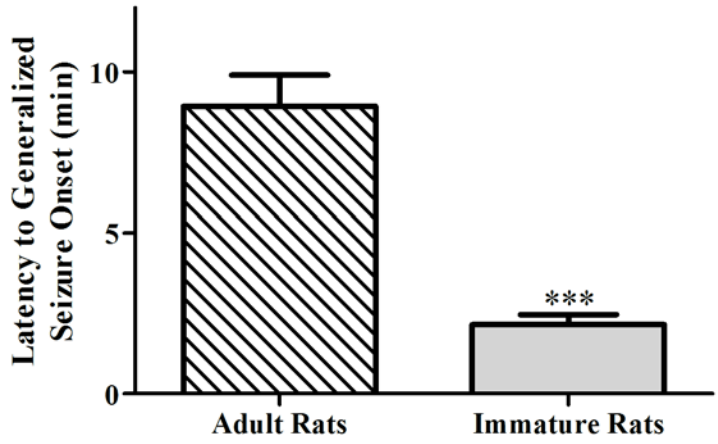

Figure 2. The latency to SE onset after soman injection is shorter in P21 rats compared to adults. P21 rats (n = 12) and young-adult rats (n = 20) were injected with the appropriate soman dose corresponding to 1.2 X LD50. ***$p < 0.001$ (Student's t-test).

Baseline AChE Activity in immature rats and comparison with adult rats

Baseline AChE activity (in nmol/min/ng) in the prelimbic cortex, BLA, piriform cortex, and hippocampus was measured in naïve P21 rats (n = 5) and compared with young-adult rats (n = 15). As in the young-adult rats ((228), and Fig. 3), AChE activity in the immature rats was significantly higher in the BLA (932.5 ± 132.2) than in the prelimbic cortex (193.3 ± 11.8), piriform cortex (250.8 ± 37.2), and hippocampus (196.8 ± 16.7; $p < 0.001$, Fig. 3). Between the two age groups, there was no statistically significant difference for the BLA (932.5 ± 132.2 for the P21 group and 1134.8 ± 92.1 for the adult group; $p = 0.244$), but in the prelimbic cortex (193.3 ± 11.8 in the P21 rats and 351.8 ± 32.4 in the adults; $p < 0.001$), piriform cortex (250.9 ± 37.2 in the P21 rats and 473.4 ± 58.6 in the adults; $p < 0.01$), and hippocampus (196.8 ± 16.7 in the P21 rats and 425.2 ± 45.0 in the adults; $p < 0.001$), AChE activity was significantly lower in the P21

rats (Fig. 3).

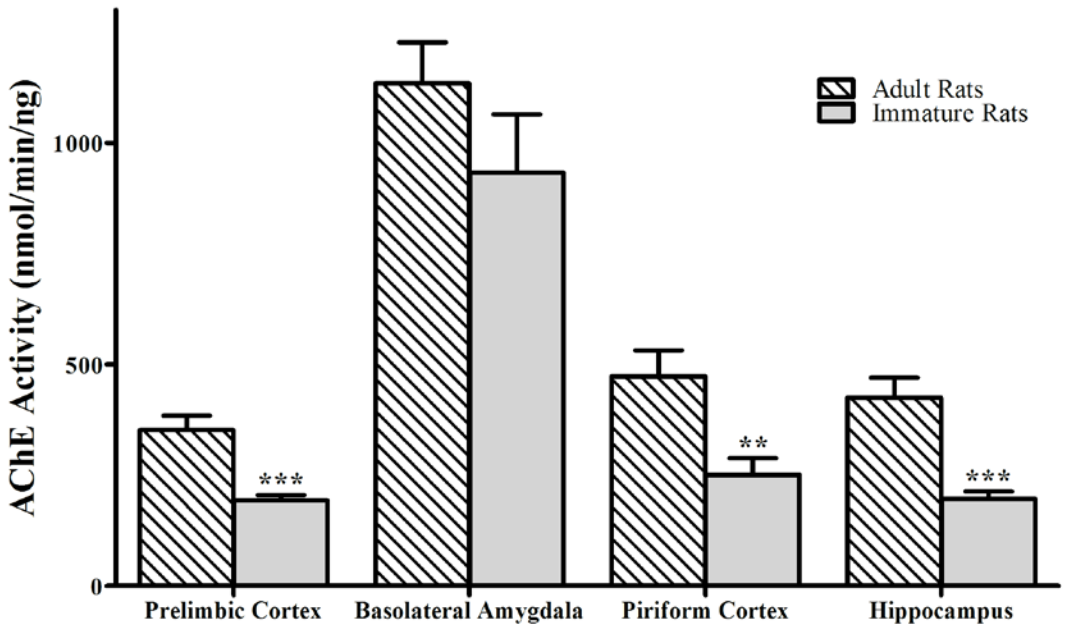

Figure 3. Baseline AChE activity in P21 rats is lower in the prefrontal cortex, piriform cortex and hippocampus, but not in the amygdala, compared to adult rats. For P21 rats, n = 5, and for the young-adult rats, n = 15. $^{**}p < 0.01$, $^{***}p < 0.001$ (Student's t-test).

Inhibition of AChE activity in the basolateral amygdala plays a critical role in seizure induction following exposure of immature rats to soman

The AChE activity in the prelimbic cortex, BLA, piriform cortex, and hippocampus of naïve P21 rats (Control Group, n = 5) was compared to that of P21 rats that were exposed to soman but did not develop seizures (No-SE Group, n = 7; AChE activity was measured at 20 min after soman injection) and P21 rats that were exposed to soman and developed seizures (SE-Onset Group, n = 7; AChE activity was measured at the onset of stage 3 seizures). We found that, compared to the control group (for control values see baseline activity in the immature group in the previous section), AChE activity was significantly lower in all four brain regions in the rats that were exposed to soman ($p < 0.001$; Fig. 4). In the No-SE group, AChE activity was 12.2 ± 7.2 nmol/min/ng in the

prelimbic cortex, 360.4 ± 33.7 in the basolateral amygdala, 36.2 ± 24.2 in the piriform cortex, and 29.7 ± 17.4 in the hippocampus. In the SE-Onset group, AChE activity was 13.4 ± 3.2 in the prelimbic cortex, 100.1 ± 30.3 in the basolateral amygdala, 15.9 ± 3.1 in the piriform cortex, and 4.9 ± 0.8 in the hippocampus The only significant difference between the SE-Onset group and the No-SE group was the greater reduction of AChE activity in the basolateral amygdala of the former group ($p < 0.05$; Fig. 4).

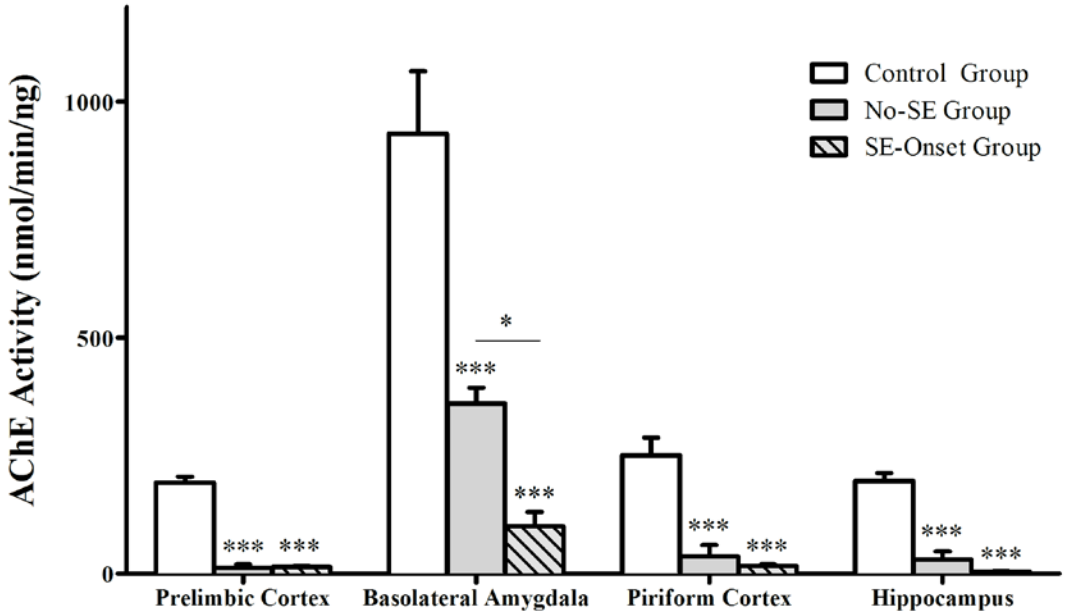

Figure 4. Reduction of AChE activity in P21 rats after injection of 1.2 X LD_{50} soman. Soman-exposed rats that did not develop SE were sacrificed 20 min after soman injection (No-SE group, n = 7). Rats that developed SE were sacrificed at the onset of SE (SE-onset group, n = 7). The soman-exposed rats had significantly lower AChE activity in all brain regions, compared to the control group (n = 5). AChE activity in the basolateral amygdala of the SE-onset group was significantly lower than that in the No-SE group. ***$p < 0.001$ compared to the control group, and *$p < 0.05$ between the no-SE and the SE-onset groups (One-way ANOVA with Tukey HSD post-hoc).

Efficacy of ATS against soman-induced seizures in immature versus adult rats

Testing of anticonvulsant treatments at different time points after nerve agent exposure requires control of the peripheral cholinergic crisis in order to prevent rapid death. For this purpose, most animal models employ administration of ATS within 1 min

after exposure; HI-6 is often administered as well, either as a pretreatment or along with atropine. In order to mimic more closely a real-life scenario, where in the event of a terrorist attack it is unlikely that medical assistance will be administered within the first minute, we have employed administration of ATS and HI-6 at 20 min post-exposure in adult rats (12). We attempted to do the same in the immature rats, in the present study. For these experiments, we injected P21 rats (n = 100) with 1.2 X LD_{50} soman; all of the 100 rats developed seizures, but 67 rats died before the 20 min time-point. In the initial experiments, we injected surviving rats with 2 mg/kg ATS and 125 mg/kg HI-6 at 20 min after soman exposure; we observed that not only the peripheral effects of soman were controlled by ATS and HI-6, but seizures also were terminated. To determine if it was the ATS or the HI-6 that was responsible for the cessation of seizures, we administered 125 mg/kg HI-6 alone to 7 rats, at 20 min after soman injection; this treatment had no effect on seizures (Fig. 5A). However, when we administered 2 mg/kg ATS alone, SE was terminated in all of the P21 rats who received this treatment (n = 10; Fig. 5B). For comparison, twenty four young-adult rats were also exposed to 1.2 X LD_{50} soman. From these rats, 16 developed seizures and none of them died before the 20 min post-exposure time-point. Administration of 2 mg/kg ATS to the 16 rats did not suppress seizures (Fig. 5B), and 4 of these rats died soon after the injection of ATS.

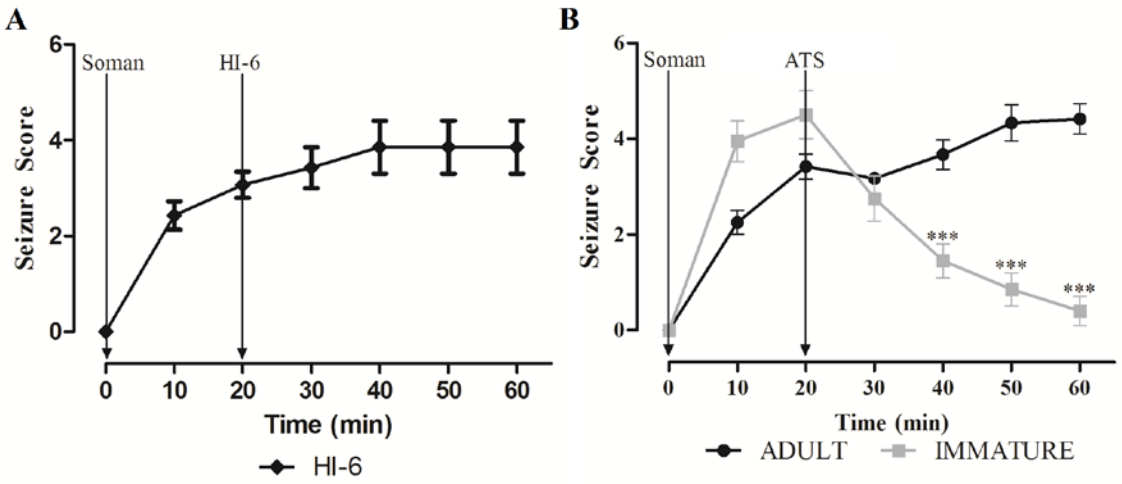

Figure 5. Atropine sulfate (ATS) in immature but not in adult rats arrests generalized seizures induced by soman exposure. Young-adult (n = 12) and P21 (n = 10) rats were exposed to a soman dose corresponding to 1.2 X LD50 (P21 rats: 74.4 µg/kg, young-adult rats: 132 µg/kg). A. Administration of HI-6 to P21 rats, at 20 min after soman injection, had no effect on seizures. B. Administration of 2.0 mg/kg ATS, at 20 min after soman injection, terminated seizures in the P21 rats, but not in the adult rats. ***$p < 0.001$ when seizure severity score is compared between P21 and adult rats at 40, 50, and 60 min after soman exposure (MANOVA, Bonferroni correction).

Efficacy of the GluK1KR antagonists LY293558 or UBP302 against soman-induced seizures in immature rats

Next, we examined if the GluK1R antagonists which are effective in stopping seizures and preventing brain damage in adult rats, even when the anticonvulsants are administered at 1 h or longer after exposure (12; 89), are also effective in the P21 rats. Since at this age, ATS alone at 2 mg/kg terminates soman-induced seizures, in this set of experiments we used a lower concentration of atropine, which was sufficient to control peripheral effects, but did not affect seizures. Thus, P21 rats were injected with 1.2 X LD_{50} soman (74.4 µg/kg) and treated with ATS (0.5 mg/kg) and HI-6 (125 mg/kg) at 1 min post-soman exposure; in this treatment paradigm, the survival rate was 59%. At 1 h post-exposure, rats were administered LY293558 (20 mg/kg; n = 15), or UBP302 (250 mg/kg; n = 18), or the drug vehicle (n = 16). Treatment with LY293558 significantly

suppressed seizures within 20 min, while UBP302 also significantly suppressed seizures but with a slower time course ($p < 0.001$; Fig. 6). In the rats who received only the drug vehicle, SE continued for at least the 2 h of observation.

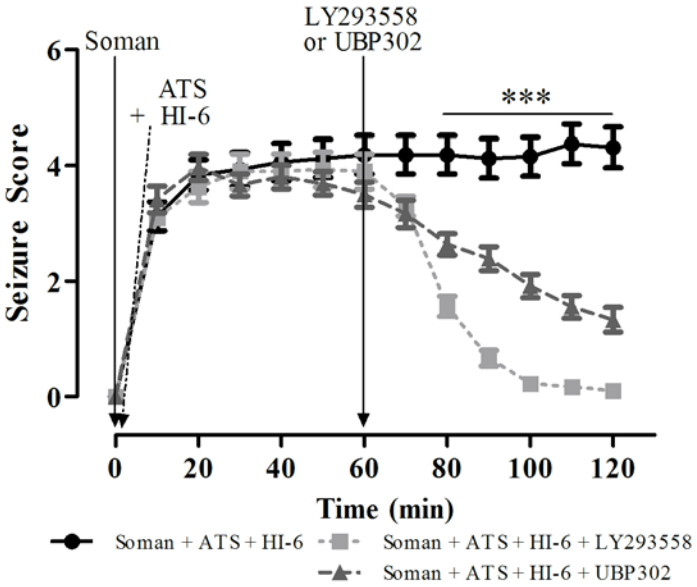

Figure 6. Delayed post-treatment with the GluK1R antagonists LY293558 or UBP302 arrests soman-induced seizures in P21 rats. Rats were exposed to 1.2 X LD50 soman (74.4 μg/kg) and treated with ATS (0.5 mg/kg) and HI-6 (125 mg/kg) at 1 min post-exposure. At 1 hr post-exposure, rats received LY293558 (20 mg/kg; n = 15), or UBP302 (250 mg/kg; n = 18), or the drug vehicle (n = 16). ***$p <$ 0.001 for the difference in seizure score of the LY293558-treated and UBP302-treated groups compared to the vehicle-treated group (MANOVA, Bonferroni post-hoc test).

Immature rats do not undergo neuronal degeneration after soman-induced SE

In adult rats, nerve agent-induced SE causes significant neuronal degeneration in many brain regions (12; 14; 88; 89) and particularly in the amygdala and the hippocampus (14). In the immature rats, the effects of the soman-induced SE on neuronal degeneration was examined at 24 h and 7 days after soman exposure in the group that received 0.5 mg/kg ATS and 125 mg/kg HI-6 at 1 min post-exposure, but no anticonvulsant treatment. There was no evidence for neuronal degeneration at either time

point, in the amygdala or the hippocampus; we also inspected the rest of the brain on the FJC-stained sections, throughout the rostro-caudal extent, but, as in control rats, there were no FJC-stained cells in any brain region. To ensure that the staining procedure worked properly, we also processed sections from adult rats who had been exposed to 1.2XLD$_{50}$ soman, receiving 2 mg/kg ATS and 125 mg/kg HI-6 at 1 min after exposure, but no anticonvulsant treatment; neurodegeneration was pronounced in these rats (Fig. 7).

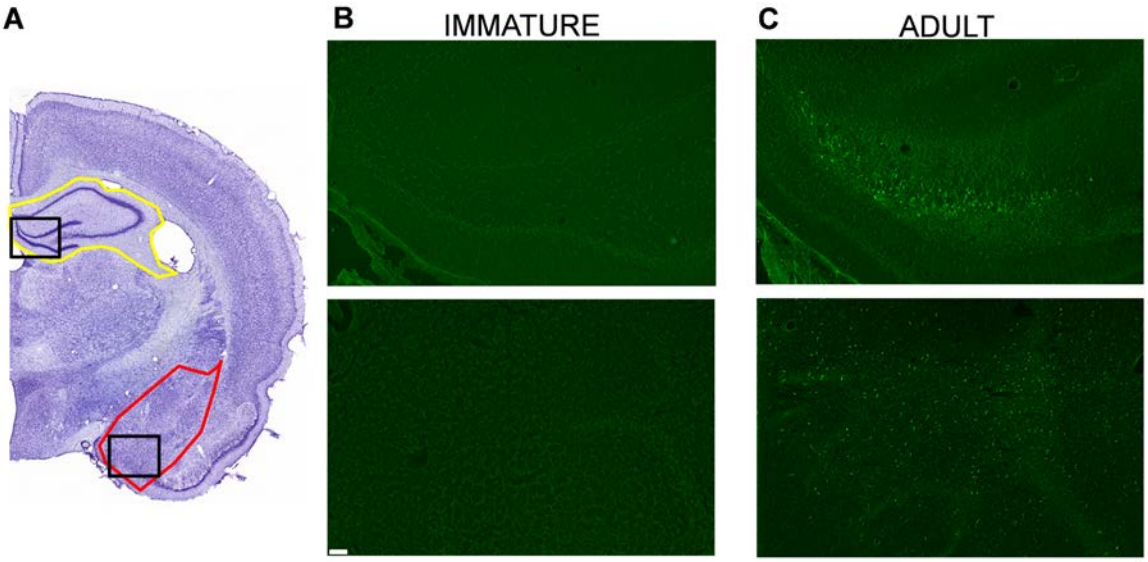

Figure 7. Immature rats do not suffer neuronal degeneration, 1 day and 7 days after soman-induced SE. A. Cresyl violet photomicrographs outline the brain regions (amygdala in red; hippocampus in yellow) from where the FJC photomicrographs (B and C) were taken (the specific areas shown in the photomicrographs are outlined with black rectangles). Immature and adult rats were exposed to the age-specific 1.2X LD50 of soman. In contrast to the adult rats (C), immature rats (B) did not display any degenerating cells. Magnification in A is 200x. Scale bar (for B and C) is 50 μm.

Amygdalar and hippocampal volume is significantly reduced 30 days and 90 days after exposure of immature rats to soman, and this is prevented by LY293558 treatment

Despite the lack of neuronal degeneration after soman-induced SE, volumetric measurements of the amygdala and the hippocampus, 30 and 90 days after soman exposure, indicated that the size of these structures was reduced in the soman-exposed

rats that received only ATS (0.5 mg/kg) and HI-6 at 1 min after exposure, but no anticonvulsant treatment. This type of pathology was not observed in the group that received LY293558 at 1 h after soman exposure (Figs. 8 and 9). Thus, at 30 days post-exposure, the size of the amygdala in the soman-exposed rats was 10.13 ± 0.49 μm^3 (n = 8), while the control size was 11.86 ± 0.27 mm^3 (n = 8, $p < 0.05$); in the soman-exposed rats treated with LY293558, the size of the amygdala (11.72 ± 0.3; n = 8) did not differ from the control ($p = 0.08$; Fig 8D). At 90 days post-exposure, the size of the amygdala in the soman group was 12.10 ± 0.32 mm^3 (n = 8), which was still significantly smaller than the control ($p < 0.05$); in the LY293558-treated group the size of the amygdala (11.98 ± 0.27, n = 8) did not differ from the control ($p = 0.07$; Fig. 8E). The size of the hippocampus at 30 days post-exposure was 48.4 ± 2.2 mm^3 in the soman-exposed group (n = 8) versus 62.5 ± 1.7 mm^3 in the control group (n = 8, $p < 0.05$); in the soman-exposed rats treated with LY293558, the size of the hippocampus (59.8 ± 2.3, n = 8) did not differ from the control ($p = 0.09$; Fig. 9D). At 90 days post-exposure, the hippocampus was still significantly smaller in the soman group (41.2 ± 2.1, n = 8) compared to control ($p < 0.05$); in the LY293558-treated group the size of the hippocampus (62.4 ± 2.6, n = 8) again did not differ from the control ($p = 0.08$; Fig. 9E).

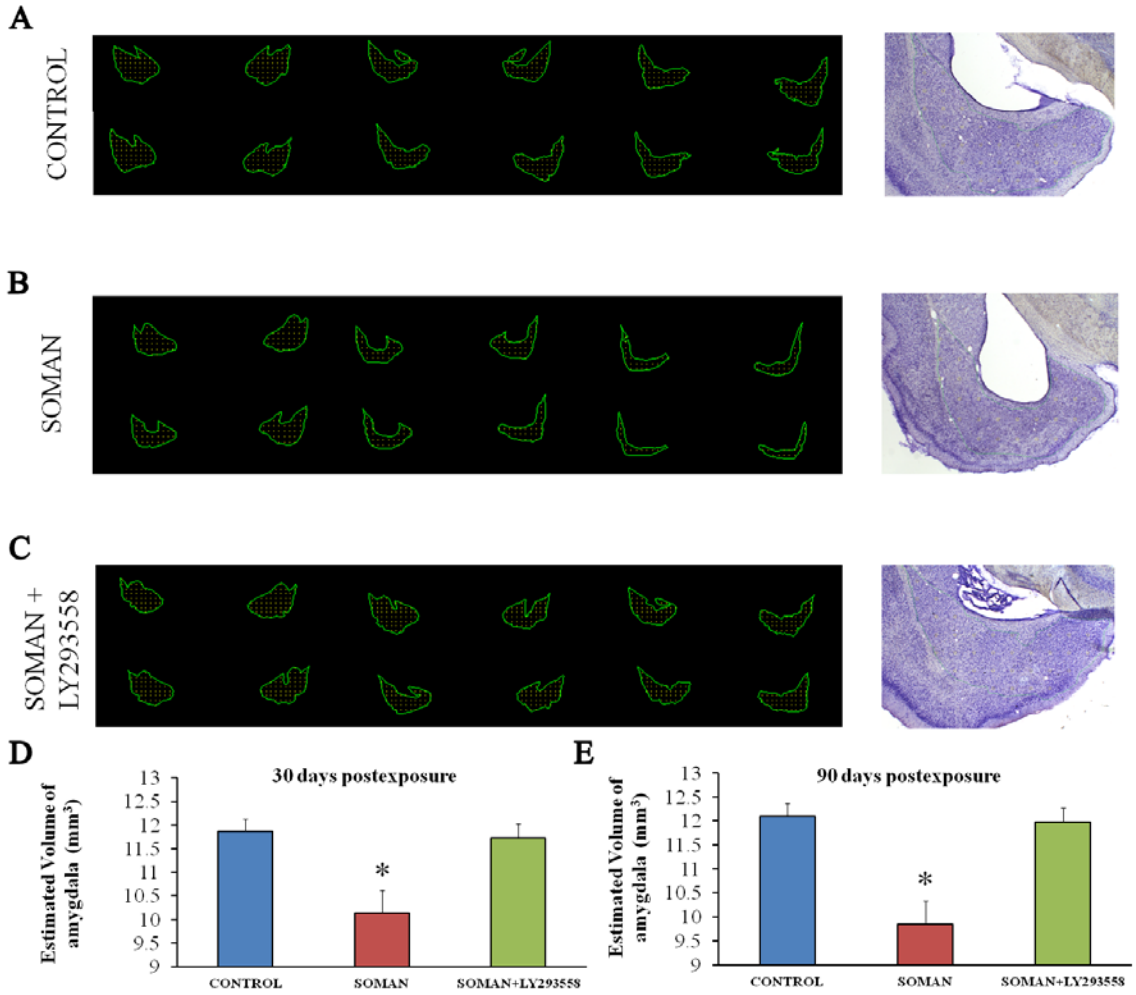

Figure 8. A reduction in amygdalar volume, 30 and 90 days after soman exposure, is prevented by LY293558 treatment. A, B, C. Tracings of the amygdala in series of slices (left) and representative photomicrographs (right) from control animals (A, n = 8), soman-exposed animals that received only ATS (0.5 mg/kg) and HI-6 at 1 min post-exposure (B, n = 8), and soman-exposed animals that received LY293558 (20 mg/kg) at 1 h after soman injection (C, n = 8). D. Group data showing the estimated volume of the amygdala for all three groups, 30 days after the exposure. E. Group data showing the estimated volume of the amygdala for all three groups, 90 days after the exposure. *$p < 0.05$ (ANOVA, LSD post-hoc test).

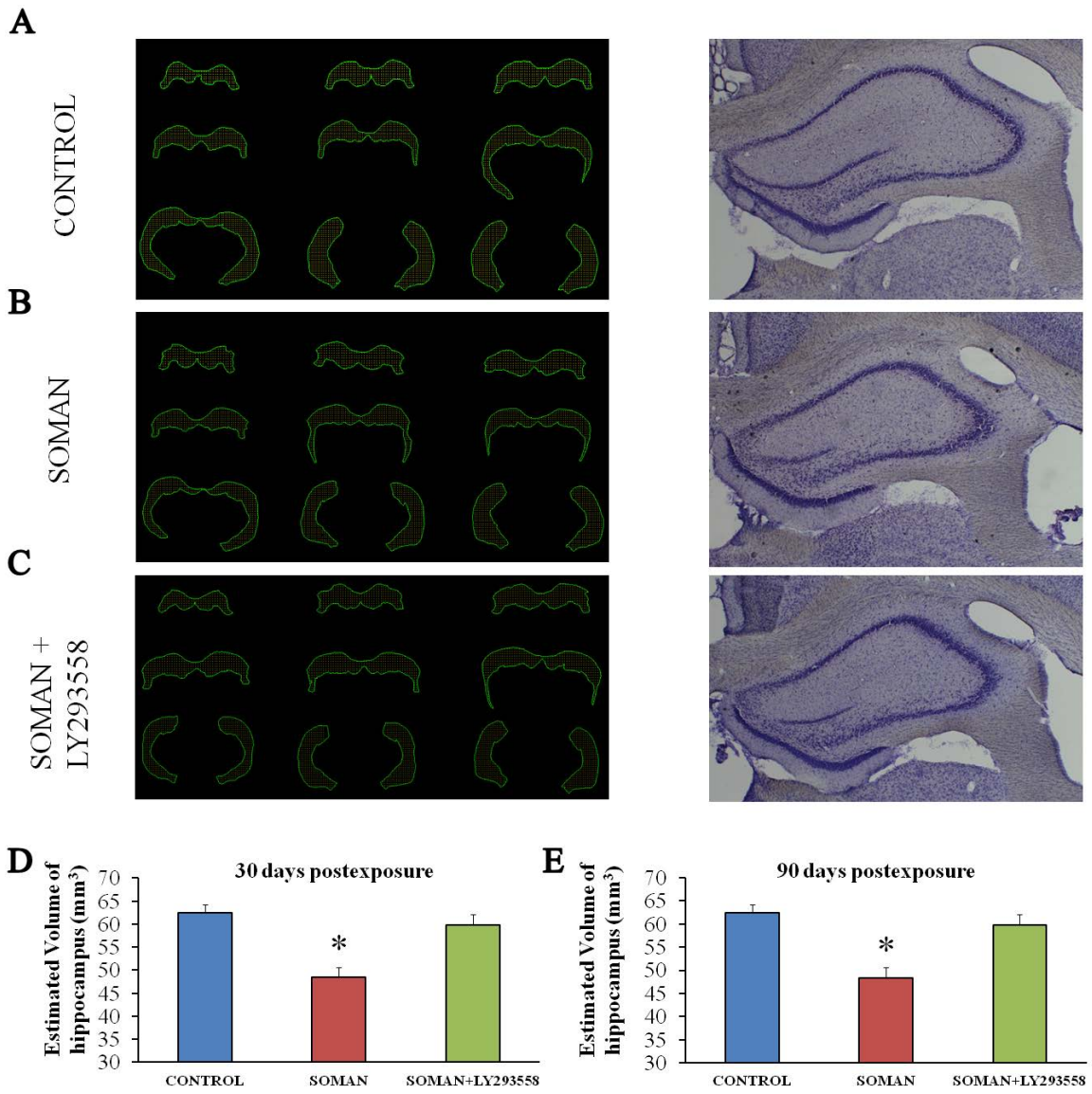

Figure 9. A reduction in hippocampal volume, 30 and 90 days after soman exposure, is prevented by LY293558 treatment. A, B, C: Tracings of the hippocampus in series of slices (left) and representative photomicrographs (right) from control animals (A, n = 8), soman-exposed animals that received only ATS (0.5 mg/kg) and HI-6 at 1 min post-exposure (B, n = 8), and soman-exposed animals that received LY293558 (20 mg/kg) at 1 h after soman injection (C, n = 8). D: Group data showing the estimated volume of the hippocampus for all three groups, 30 days after the exposure. E: Group data showing the estimated volume of the hippocampus for all three groups, 90 days after the exposure. *$p < 0.05$ (ANOVA, LSD post-hoc test).

Soman-exposed immature rats display behavioral deficits 30 days post-exposure, which are prevented by LY293558 treatment

P21 rats that were exposed to soman and received only ATS (0.5 mg/kg) and HI-6 at 1 min after exposure, along with soman-exposed rats that were also treated with LY293558 at 1 h after exposure, as well as control rats, were tested for context- and cue-dependent fear conditioning. Fear conditioning took place at 30 days after exposure, and testing for context-dependent and cue-dependent acquisition of fear took place within the following 4 days (see methods). In the context-dependent test, the total freezing time for the soman-exposed rats was 250 ± 15 s (n = 13), significantly lower than that of the control group (523 ± 24 s, n = 17, p <0.05); for the soman-exposed rats treated with LY293558, the total freezing time (452 ± 28 s, n = 11) did not differ from the control (p = 0.07, Fig.10A). In the cue-dependent fear acquisition test, the freezing time for the soman-exposed rats (214 ± 14 s) was significant lower compared to control (354 ± 20 s, p < 0.05), while for the soman-exposed rats that received LY293558, the freezing time (331 ± 21 s) did not differ from the control (p = 0.08; Fig. 10C). At 90 days post-exposure, there were no differences among the groups (Fig. 10B and D). Thus, the total freezing time in the context-dependent test was 489 ± 20 s for the soman-exposed group, 554 ± 35 s for the control group, and 513 ± 29 s for the soman-exposed rats treated with LY293558 (p = 0.084). The total freezing time in the cue-dependent test was also similar among the groups (p = 0.09). Thus, freezing time was 301 ± 40 s for the soman-exposed rats, 389 ± 25 s for the control rats, and 391 ± 19 s for the soman-exposed, LY293558-treated rats.

The same groups of rats were also tested in the open field. At 30 days after soman exposure the distance traveled in the open field was not significantly different between the soman-exposed rats (2522 ± 246 cm, n = 13), the soman-exposed rats that received LY293558 (2741 ± 254 cm, n = 11) and the controls (2293 ± 158 cm, n = 17). However,

the time spent in the center of the open field was significantly less in the soman-exposed rats that did not receive anticonvulsant treatment (8.6 ± 1.06 % of the total movement time, n = 13, $p = 0.02$) compared to the time spent by the control rats (12.51 ± 1.12 % of the total movement time, n = 17), or the soman-exposed that were treated with LY293558 (11.95 ± 1.08% of the total movement time, n = 11; Fig. 10E). At 90 days after exposure, the distance traveled in the open field was not significantly different between the soman-exposed rats (2851 ± 193 cm, n= 11), the soman-exposed rats that received LY293558 (2698 ± 244 cm, n = 12) and the controls (2752 ± 201 cm, n = 12). The time spent in the center of the open field also did not differ significantly between the soman-exposed rats that did not receive anticonvulsant treatment (11.7 ± 1.25 % of the total movement time, n = 11) and the control rats (13.36 ± 1.03% of the total movement time, n = 12), or the soman-exposed, LY293558-treated rats (13.68 ± 1.08% of the total movement time, n = 12, $p = 0.08$; Fig. 10F).

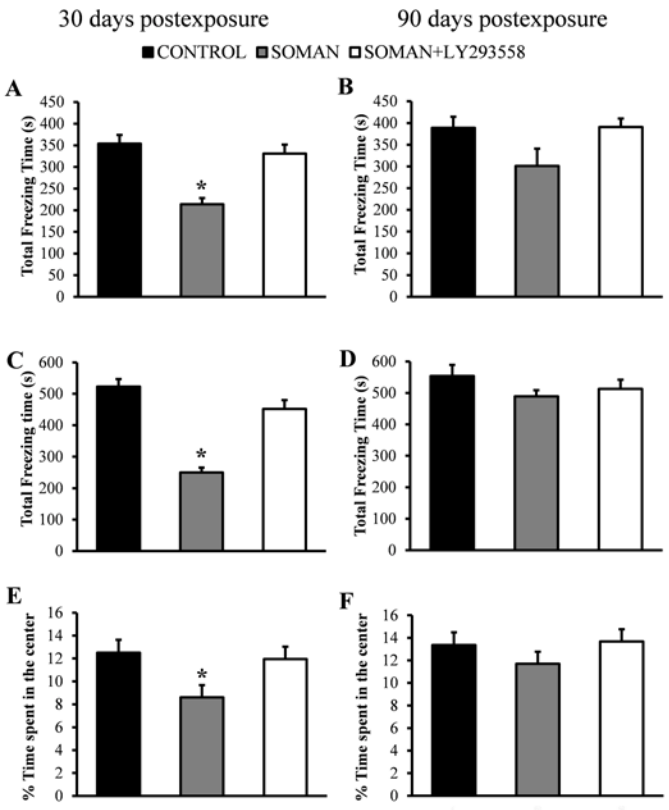

Figure 10. LY293558 treatment prevents behavioral deficits 30 and 90 days after soman exposure. A and B show that total freezing time of the contextual fear-conditioned responses, 30 and 90 days after soman exposure, for the soman-exposed rats who received only ATS (0.5 mg/kg) and HI-6 at 1 min after exposure (n = 13), similarly treated rats who received also LY293558 at 1 h after soman exposure (n = 11), and controls (n = 17). C and D show the total freezing time for the auditory fear-conditioned responses, for the same groups, at 30 and 90 days after exposure. E and F are the results from the open field test, showing the time spent in the center, for the same three groups, at 30 and 90 days after exposure. *$p < 0.05$ (ANOVA, Dunnett post-hoc test).

DISCUSSION

The present study shows that 1) immature rats appear to be more susceptible to the toxicity of nerve agents, as suggested by the LD_{50} of soman for the P21 rats, which was lower than the LD_{50} for the adult rats; 2) immature rats are more prone to generating seizures after nerve agent exposure, as suggested by the time to seizure onset which was significantly shorter in the P21 rats compared to the adults; 3) as in adult rats, reduction of brain AChE activity appears to be the primary mechanism of seizure generation in the

P21 rats, and the BLA plays a key role in that respect; 4) ATS, at a dose that does not affect nerve agent-induced seizures in adult rats, promptly terminates seizures in P21 rats; 5) the GluK1 antagonists LY293558 and UBP302 are effective in terminating soman-induced seizures in P21 rats, even when administered at 1 h after exposure; 6) soman-induced seizures do not cause neuronal degeneration in the brain of P21 rats, but they reduce the volume of the amygdala and the hippocampus, 30 and 90 days after exposure; 7) soman exposure results in fear-learning deficits and increased anxiety at 30 days after exposure; 8) both the brain pathology and the behavioral deficits are prevented if exposed rats are administered LY293558 at 1 h after exposure.

Since nerve agents induce seizures by inhibiting AChE, it seems reasonable to speculate that the faster onset of seizures upon exposure to soman in the P21 rats compared to adults is due to the lower concentration of the enzyme in some brain regions (Fig. 3), which may result in more rapid reduction of AChE activity in the brain. This is not a very plausible explanation, however, for two reasons: a) AChE activity was also dramatically reduced in the prelimbic cortex, the piriform cortex, and the hippocampus of the P21 rats that *did not* develop SE; the only difference of these rats from those who developed SE was that AChE in their BLA was reduced to a lesser extent (Fig. 4). b) AChE activity in the BLA, which appears to play a key role in the induction of seizures in the P21 rats, as in the adult rats (227), did not differ significantly between the two ages in the basal state (Fig. 3). Therefore, the shorter latency to seizure onset in the P21 rats is likely due to reasons that are not related to the baseline concentration of AChE in the brain. It is well recognized that the immature brain has a greater propensity for seizure generation regardless of the triggering stimulus, in both humans and animals (112; 120).

The reasons are not quite clear, but may include the high input resistance of neurons during development and the prevalence of gap junctions–which facilitate bursting and synchronous activity–and the immaturity of the GABAergic and glutamatergic system (30; 120). Contribution of possible differences between P21 and adult rats in the pharmacokinetics of the injected soman must also be considered.

An unexpected finding in the present study was that ATS, at 2 mg/kg, a concentration that has no effect on nerve agent-induced seizures in adult animals (Fig. 5B and (12; 89; 181; 229; 260)), terminated soman-induced seizures in the P21 rats. After nerve agent exposure, seizures are initiated by hyperstimulation of muscarinic receptors, as evidenced by the anti-seizure effects of muscarinic antagonists when administered shortly after exposure (152; 260; 261). In adult rats, ATS, a non-selective muscarinic antagonist, suppresses nerve agent-induced seizures, but with an ED_{50} of more than 50 mg/kg (261). The BBB is weaker early in life (33; 173; 244) and appears to be more susceptible to increased capillary leakiness induced by organophosphorus agents (271); this may explain the anti-seizure efficacy of relatively low concentrations of ATS in the immature rats. However, a weaker BBB in the P21 rats was not sufficient to confer efficacy to HI-6, which had no effect on seizures when administered at 20 min after exposure (Fig. 5A); it is likely though that the inefficacy of HI-6 had to do with the rapid aging of soman-inhibited AChE (168; 265; 282), which renders it non-reactivatable by oximes (24; 168). In the rat whole brain, the activity of choline acetyltransferase, the concentration of ACh, and the number of mAChRs do not mature until after the fourth postnatal week (75). Therefore, in addition to a weaker BBB, differences between the

P21 and the adult rats in the function of the muscarinic cholinergic system may be involved in the differential anticonvulsant response to ATS.

Seizures did not return after the cessation of SE by 2 mg/kg ATS, at least for the two hours that we continued observing the rats. We did not examine, in the present study, whether ATS would also be effective if administered at 1 h after exposure or at more delayed time points. However, from studies in adult rats, it has become clear that muscarinic receptors are involved only in the initiation of seizures after exposure, while it is excessive glutamatergic activity that reinforces and sustains SE (181). Accordingly, soman-induced SE can be terminated by certain glutamate receptor antagonists. Specifically, LY293558, an AMPA/GluK1R antagonist (36; 124), or UBP302, a GluK1R antagonist (190), terminate soman-induced seizures even when administerd at 1 h or 2 h after exposure (13; 89). The efficacy of these two compounds may lie on the fact that GluK1Rs play an important role in the regulation of neuronal excitability of at least two highly seizure-prone regions, the amygdala (15; 16; 18; 42; 237) and the hippocampus (54; 99; 225; 242); both GABAergic and glutamatergic synaptic transmission is modulated by GluK1Rs in different brain regions (124), but the net effect of GluK1R activation appears to be an increase in excitability in both the BLA (17) and the hippocampus (269). During development, there are changes taking place in the distribution (22) and the function of GluK1Rs (249). Although it is unclear how the fuction of GluK1Rs may differ in the brain of a P21 rat from an adult rat, the present study shows that in P21 rats, LY293558 and UBP302 are effective in stopping soman-induced seizures when administered at 1 h after exposure, with UBP302 having a slower time course of action, as we had observed in the adult rats (13).

It is becoming increasingly understood that prolonged seizures early in life may not cause neuronal death/loss, yet, they produce long-term pathological alterations, inhibiting brain growth, modifying neuronal circuits, and leading to lasting behavioral deficits (119; 121; 276). The present study shows that this is also the case when prolonged seizures are induced by soman exposure in P21 rats. There was no irreversible neuronal degeneration at either 24 h or 7 days post-exposure, suggesting that there was no neuronal loss. This is in contrast to the severe neuronal degeneration that is seen in young-adult rats at 24 h and 7 days after soman exposure (12-14; 227; 228). The resistance of immature neurons to seizure-induced degeneration and death is attributed in part to their lower vulnerability to oxidative stress (214) and glutamate toxicity (35; 165; 167). However, despite the absence of neuronal degeneration, the volumes of the amygdala and the hippocampus were significantly smaller in the P21 rats than in control rats, at 30 days and 90 days post-exposure. Considering that prolonged seizures induce neurogenesis in the hippocampus (121; 210) and, at least in some models, in the amygdala as well (212), it may seem surprising that the volume of these structures decreased. However, significant atrophy of temporal lobe structures has also been observed after P12 and P25 rats were subjected to lithium/pilocarpine-induced SE (148). Furthermore, amygdalar and hippocampal atrophy is a common pathology in temporal lobe epilepsy (16; 56; 57), and a smaller amygdala volume was also found in a significant number of the victims of the sarin attack in Tokyo, in 1995 (238). It appears, therefore, that prolonged seizures or chronic recurrent seizures can result in atrophy of temporal lobe structures, and when prolonged seizures occur early in life, atrophy may ensue despite the absence of neuronal loss; in this latter case, perhaps a smaller number or

thickness of synaptic connections contribute to the reduction in the total volume, and/or death of glia cells.

Abnormalities in the amygdala and the hippocampus may also explain the behavioral deficits seen at 30 days after exposure. The amygdala plays a key role in fear-conditioning (127), and the ability for "fear-learning", as reflected in the total freezing time, was impaired in the rats exposed to soman at P21. The amygdala, but the hippocampus as well, also play a central role in anxiety (5; 84; 149), and anxiety-like behavior was increased 30 days after exposure of P21 rats to soman. These behavioral deficits were absent 2 months later, despite that there was no reversal of the amygdalar and hippocampal atrophy. It is possible that during the 2-month-period, which corresponds to more than 8 human years (10; 250), synaptic or biochemical adjustments rectified these behavioral deficits. Others have found persistent cognitive deficits, as revealed by the Morris water-maze test, 3 months after P12 rats and P25 rats experienced lithium/pilocarpine-induced SE (148). Thus, whether or not recovery will occur may depend, in addition to age, on other factors such as the nature of the behavioral deficit. For example, in adult mice exposed to soman-induced SE, increased anxiety-like behavior was still present 90 days after the exposure, but deficits in auditory and contextual fear-conditioned responses recovered during the 30 to 90 day post-exposure period (74).

The present study provides support to the increasing evidence that prolonged seizures early in life may not be benign in long-term, even when they have not produced irreversible neuronal degeneration. The data suggest that children are likely to be more prone to developing seizures upon exposure to nerve agents, but a single injection of

atropine will be sufficient to halt seizures, if administered timely. Control of seizures is necessary in order to prevent long-term brain pathologies and behavioral deficits, and administration of LY293558 is an effective anticonvulsant and neuroprotectant even when administered at 1 h after exposure. Testing of anticonvulsants at delayed time-points after nerve agent exposure in immature animal models requires timely administration of ATS at a low dose, which will alleviate peripheral toxicity and reduce mortality, without preventing or halting seizures.

ACKNOWLEDGMENTS

We thank Dr. Cara H. Olsen for her expert advice on the procedure for the estimation of LD50. This work was supported by the CounterACT Program, National Institutes of Health, Office of the Director and the National Institute of Neurologic Disorders and Stroke [Grant Number 5U01NS058162-07].

The authors have no competing financial interests.

The views expressed in this article are those of the authors and do not reflect the official policy of the Department of Army, Department of Defense, or the U.S. Government.

CHAPTER 3: M_1 Muscarinic Receptors Play a Key Role in Seizure Initiation After Exposure to Paraoxon or Soman: Mechanisms of Their Involvement

Steven L. Miller[1,3], Vassiliki Aroniadou-Anderjaska[1,2,3], Volodymyr I. Pidoplichko[1], Taiza H. Figueiredo[1], James P. Apland[4], Maria F. M. Braga[1,2,3*]

[1]Department of Anatomy, Physiology and Genetics, [2]Department of Psychiatry, and [3]Program in Neuroscience, F. Edward Hébert School of Medicine, Uniformed Services University of the Health Sciences, Bethesda, MD, 20814, USA
[4]Neurotoxicology Branch, U.S. Army Medical Research Institute of Chemical Defense, Aberdeen Proving Ground, Maryland, 21010, USA

*Corresponding Author:
Maria F.M. Braga, D.D.S., Ph.D.
Department of Anatomy, Physiology, and Genetics
F. Edward Hébert School of Medicine,
Uniformed Services University of the Health Sciences
4301 Jones Bridge Road
Bethesda, MD 20814, USA
Phone: (301) 295-3524
Fax: (301) 295-3566
Email: maria.braga@usuhs.edu

ABSTRACT

BACKGROUND AND PURPOSE

Exposure to OP toxins induces seizures and SE. The evidence is clear that seizures are initiated by hyperstimulation of mAChR, subsequent to inhibition of AChE by the OP; this is followed by glutamatergic hyperactivity, which reinforces and sustains seizures. It is unknown, however, which muscarinic receptor subtypes are involved in seizure initiation, or how their stimulation leads to hyperexcitability.

EXPERIMENTAL APPROACH

We tested whether a selective M_1 mAChR antagonist, VU0255035, prevents the development of SE after exposure of rats to POX or soman. In brain slices, we studied the effects of POX on inhibitory and excitatory activity in the BLA, and the involvement of M_1 mAChRs.

KEY RESULTS

Pretreatment of the rats with VU0255035 significantly suppressed the intensity of seizures after POX or soman exposure. In the basolateral amygdala, bath application of POX elicited a barrage of spontaneous inhibitory postsynaptic currents, lasting about 1 min, and followed by an increase in the ratio of the total charge carried by spontaneous glutamatergic postsynaptic currents over GABAergic currents. The effects of POX were prevented by pretreatment of the slices with atropine or VU0255035.

CONCLUSIONS AND IMPLICATIONS: Previous studies have pointed out that the basolateral amygdala plays a key role in seizure initiation after OP exposure. The present study provides an insight into the mechanisms involved. Activation of M_1 receptors tips the balance between GABAergic and glutamatergic activity. The resulting

hyperexcitability provides the background over which seizures commence and propagate to other brain regions.

INTRODUCTION

It is well understood that OPs–used as insecticides or in chemical warfare (nerve agents)–induce seizures by hyperstimulation of mAChRs. Thus, phosphorylation of AChE by these toxins inactivates the enzyme (265), resulting in a built-up of synaptic and extrasynaptic ACh. Although both nAChRs and mAChRs are probably activated by the elevated acetylcholine, it is the activation of mAChRs that raises excitatory activity in neuronal networks and initiates seizures. Evidence for that is provided by studies showing that mAChR antagonists but not nAChR antagonists prevent the induction of seizures if administered before OP exposure (19; 111; 179; 259; 303), and can arrest seizures if administered shortly after exposure (9; 50; 178). mAChR antagonists are ineffective if administered at time points longer than 10 to 20 min after seizure onset (181) because mAChR activation is involved only in the initiation of seizures, and it is the imbalance between GABAergic and glutamatergic activity that reinforces and sustains seizures (77; 125; 181; 303). Little is known, however, about the mechanisms involved in the transition from mAChR hyperstimulation to glutamatergic hyperexcitation, or which mAChR subtypes mediate the triggering of hyperactivity. Uncovering these mechanisms may allow the development of more selective and safer pharmacological means to prevent the development of SE after OP exposure.

There are five subtypes of mAChRs, M_1 to M_5. They all are G-protein coupled; M_2 and M_4 are preferentially coupled to the Gi class of G proteins, while M_1, M_3, and M_5 are coupled to the Gq family (147; 305). Although it is unknown which of these receptor subtypes are primarily involved in seizure initiation after OP exposure, seizures induced by convulsive doses of the mAChR agonist pilocarpine are dependent on

M_1 receptor activation (47; 109; 137; 252). Since both pilocarpine and OPs induce seizures by mAChR hyperstimulation, it is possible that the M_1 receptor also mediates seizure initiation by OPs. As there is now a new, selective M_1 receptor antagonist available (252), in the present study we examined if the M_1 receptors are involved in the generation of seizures by exposure to POX (O,O-diethyl O-*p*-nitrophenyl phosphate), the active metabolite of the insecticide parathion (95), or exposure to the nerve agent soman. To begin to understand how mAChR activation by an OP leads to hyperexcitability of neuronal networks and seizure initiation, we also examined, in brain slices, the effects of POX on spontaneous GABAergic and glutamatergic activity, and whether M_1 receptors mediate these effects. These *in vitro* studies were performed in the BLA, a seizure-prone brain region (16) that plays a key role in the initiation of seizures by nerve agent exposure (179; 227).

METHODS

Animals

Male, Sprague Dawley rats (Charles River Laboratories, Wilmington, MA) were housed in an environmentally controlled room (20 –23°C, 12 hr light/dark cycle, lights on 06:00 A.M.), with food and water available *ad libitum*. For the *in vivo* experiments, adult rats were pair-housed upon arrival. For the *in vitro* electrophysiology experiments, animals were housed with a surrogate mother until they were 21 days-old. After 21 days of age, all rats were pair-housed. The animal care and use programs at the Uniformed Services University of the Health Sciences and the U.S. Army Medical Research Institute of Chemical Defense are accredited by the Association for Assessment and Accreditation of Laboratory Animal Care International. All animal experiments were conducted

following the Guide for the Care and Use of Laboratory Animals, by the Institute of Laboratory Animal Resources, the National Research Council USA, and were approved by the Institutional Animal Care and Use Committees of both of our institutions.

POX and soman exposure

Ten-week-old rats were administered the selective M_1 receptor antagonist VU0255035 (25 $mg.kg^{-1}$, i.p.; Tocris Bioscience, Ellisville, MO) or the vehicle (DMSO, 1 $ml.kg^{-1}$, i.p.; Sigma-Aldrich, St Louis, MO), 15 min before exposure to POX (paraoxon-ethyl; Sigma-Aldrich, St Louis, MO) or soman (pinacoyl methylphosphonofluoridate; obtained from the Edgewood Chemical Biological Center, Aberdeen Proving Ground, Edgewood, MD). For the POX experiments, animals were subcutaneously injected with 4 $mg.kg^{-1}$ POX. In order to control the peripheral cholinergic effects of POX exposure, the rats were intramuscularly injected with 2 $mg.kg^{-1}$ ATS (a non-selective mAChR antagonist that has no effect on seizures at this concentration; Sigma-Aldrich, St Louis, MO) and 50 $mg.kg^{-1}$ 2-PAM (Sigma-Aldrich, St Louis, MO), within 1 min after POX injection; this drug administration protocol replicates the conditions of the DeLorenzo rat survival model of POX intoxication (79). For the soman experiments, animals were subcutaneously injected with 1.8 X LD_{50} soman (198 $\mu g.kg^{-1}$, diluted in cold physiological saline), and within 1 min after soman injection, the rats received 2 mg/kg atropine methylnitrate (i.m.), a non-selective mAChR antagonist that does not cross the blood-brain barrier (Wedgewood Pharmacy, Swedesboro, NJ). Seizures were monitored behaviorally, and their severity was scored for 1 h, using a modified version of the Racine scale (232), as we have described

previously (89). Behavioral seizures above stage 3, correspond to electrographically recorded status epilepticus (76; 89).

Electrophysiology

Rats, 18 to 25 days-old, were anesthetized with isoflurane prior to decapitation for slice preparation. Coronal slices (400 μm thick) containing the amygdala were cut as described previously (17). Recording solution (artificial cerebrospinal fluid, ACSF) consisted of the following (in mM): 125 NaCl, 2.5 KCl, 1.25 NaH_2PO_4, 21 $NaHCO_3$, 2 $CaCl_2$, 1 $MgCl_2$, and 11 D-glucose. All solutions were saturated with 95% O_2, 5% CO_2 to achieve a pH near 7.4. The slice chamber (0.7 ml capacity) had continuously flowing ACSF (~8 ml/min) at a temperature of 31–32°C. The osmolarity of the external solution was adjusted to 325 mOsm with D-glucose. Tight-seal (>1 GΩ), whole-cell recordings from principal neurons in the BLA were performed as described previously (221); BLA principal cells were identified by their pyramidal shape and the presence of the hyperpolarization-activated cationic current (I_h; (17)). Borosilicate glass patch electrodes had a resistance of 3.5-4.5 MΩ when filled with an internal solution of the following composition (in mM): 60 $CsCH_3SO_3$, 60 KCH_3SO_3, 10 EGTA, 10 HEPES, 5 KCl, 5 Mg-ATP, and 0.3 Na_3GTP, pH 7.2, 290 mOsm. The 5 mM KCl allowed the simultaneous recordings of spontaneous inhibitory postsynaptic currents (sIPSCs) and excitatory postsynaptic currents (sEPSCs). Access resistance (15–24 MΩ) was regularly monitored during recordings, and cells were rejected if the resistance changed by >15% during the experiment. Ionic currents were amplified and filtered (1 kHz) using the Axopatch 200B amplifier (Axon Instruments, Foster City, CA) with a four-pole, low-pass Bessel filter, digitally sampled (up to 2 kHz) using the pClamp 10.2 software (Molecular Devices,

Sunnyvale, CA), and further analyzed using the Mini Analysis Program (Synaptosoft, Fort Lee, NJ) and Origin (OriginLab, Northampton, MA). Drugs used for the *in vitro* experiments were paraoxon-ethyl and atropine sulphate, as well as D-AP5, an N-methyl-D-aspartate receptor antagonist (Tocris Bioscience, Ellisville, MO), SCH50911, a $GABA_B$ receptor antagonist (Tocris Bioscience), and LY341495, a metabotropic glutamate group II/III receptor antagonist (Tocris Bioscience).

Statistical Analysis

Seizure scores were analyzed using independent-samples Student's *t*-test. Electrophysiological results were analyzed using paired Student's *t*-tests. Results were considered statistically significant when $P < 0.05$. Data are represented as means ± standard error of the mean. Sample size "n" refers to the number of animals for the *in vivo* experiments and the number of cells for the whole-cell experiments.

RESULTS

Pretreatment with VU0255035 reduced seizure severity following paraoxon exposure

Eighteen rats were randomly divided into two groups: a group that was injected with VU0255035 (25 mg.kg-1, n = 10) and a group injected with the vehicle (DMSO; 1 $ml.kg^{-1}$, n = 8), at 15 min before exposure to paraoxon (4 $mg.kg^{-1}$). All rats developed seizures, but the seizure severity in the VU0255035-pretreated group (average Racine score from 5 min to 60 min after exposure = 3.15 ± 0.03) was significantly lower than the

seizure severity in the vehicle-pretreated animals (average Racine score = 3.57 ± 0.08, $P < 0.01$; Fig. 11A).

Pretreatment with VU0255035 reduced seizure severity following exposure to soman

Eight rats were randomly divided into two groups: a group that was injected with VU0255035 (25 mg.kg-1, n = 4) and a group injected with the vehicle (DMSO; 1 ml.kg^{-1}, n = 4), at 15 min before exposure to soman (198 μg.kg^{-1}). All rats developed seizures, but the seizure severity in the VU0255035-pretreated group (average Racine score = 2.56 ± 0.20) was significantly lower than the seizure severity in the vehicle-pretreated animals (average Racine score = 4.58 ± 0.74, $P < 0.001$; Fig. 11B).

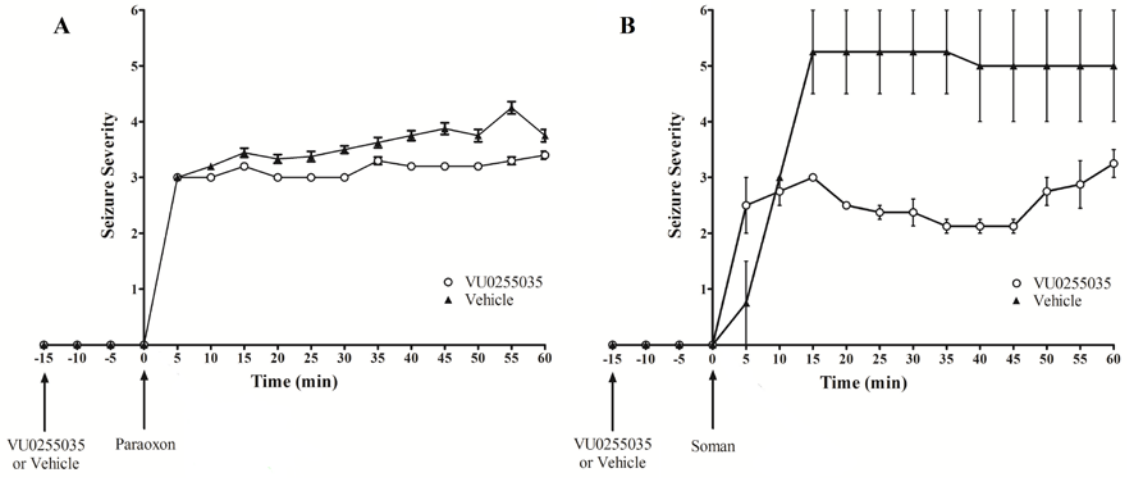

Figure 11. Pretreatment with a selective M_1 receptor antagonist, VU0255035, reduces seizure severity after exposure to paraoxon or soman. Administration of VU0255035, 15 min before exposure to paraoxon (A) or soman (B) reduced the Racine score of seizure severity, averaged over 5 min to 60 min after exposure. For the paraoxon experiments, n = 8 for the vehicle group, and n = 10 for the VU0255035-pretreated group ($P < 0.01$). For the soman experiments, n = 4 for each group (the vehicle-pretreated and the VU0255035-pretreated group; $P < 0.001$).

Effects of POX on spontaneous synaptic activity and the role of M_1 receptors

The *in vivo* experiments suggested that M_1 receptors play a key role in seizure initiation after exposure to POX or soman. To obtain some insight into the mechanisms by which M_1 receptor activation increases the excitability of neuronal networks culminating in seizure generation, we examined the effects of POX on spontaneous inhibitory (GABAergic) and excitatory (glutamatergic) activity in the BLA. Whole-cell simultaneous recordings of sIPSCs and sEPSCs were obtained from principal BLA neurons, at V_h of -58 mV, in the presence of D-AP5 (50 μM), SCH50911 (10 μM), and LY341495 (3 μM); under these conditions, upward currents are mediated by $GABA_A$ receptors (they are blocked by bicuculline), while downward currents are mediated by AMPA/kainate receptors (they are blocked by CNQX; not shown). Bath application of POX, at three different concentrations (0.1, 1, and 10 μM) induced a transient barrage of large-amplitude sIPSCs with a duration of 1.1 ± 0.1 min (n = 21), which was followed by a lasting enhancement of sEPSCs, in 21 out 34 neurons (Fig. 12A). POX took effect (appearance of the barrage of sIPSCs) within 2 to 8 min after application, depending on the concentration (the lower concentration of POX was slower to take effect). To quantify the relative increase of excitatory synaptic activity by POX, we calculated the charge transferred by the excitatory and the inhibitory currents, during a 20 s time-window, in control conditions, and then again after POX had taken effect; the charge transferred, in picoCoulombs, was calculated as the area delimited by the excitatory or inhibitory current and the baseline. The ratio of the charge transferred by sEPSCs to the charge transferred by sIPSCs was increased significantly in the presence of POX. When 0.1 μM POX was applied, the ratio of sEPSC/sIPSC charge-transferred was increased from 0.6 ± 0.1 in control conditions to 1.4 ± 0.3 at 17 min after POX application ($P < 0.05$, n = 7).

When 1 μM POX was applied, this ratio was increased from 0.6 ± 0.1 in control conditions to 0.9 ± 0.1 at 9 min after POX application ($P < 0.05$, n = 4). Finally, when 10 μM POX was applied, the ratio of sEPSC/sIPSC charge-transferred was increased from 0.8 ± 0.1 in control conditions to 1.1 ± 0.1 at 6 min after POX application ($P < 0.01$, n = 10; Fig. 12B).

Figure 12. Paraoxon, at three different concentrations, enhances both spontaneous inhibitory currents (sIPSCs) and spontaneous excitatory currents (sEPSCs), with a greater, lasting effect on the sEPSCs. Whole cell simultaneous recordings of sIPSCs and sEPSCs were obtained from principal cells in the BLA (Vh = -58). (A) The traces shown are representative examples of the effects of paraoxon at 0.1 μM, 1 μM, and 10 μM. Upward currents are GABAergic and downward currents are glutamatergic. (B) The bar graphs show the ratio of the charge transferred by glutamatergic currents over the charge transferred by GABAergic currents, during a 20 s time-window, in control conditions and after bath application of paraoxon (left graph: at 17 min after paraoxon application; middle graph, at 9 min after paraoxon application; right graph, at 6 min after paraoxon application). *$P < 0.05$, **$P < 0.01$.

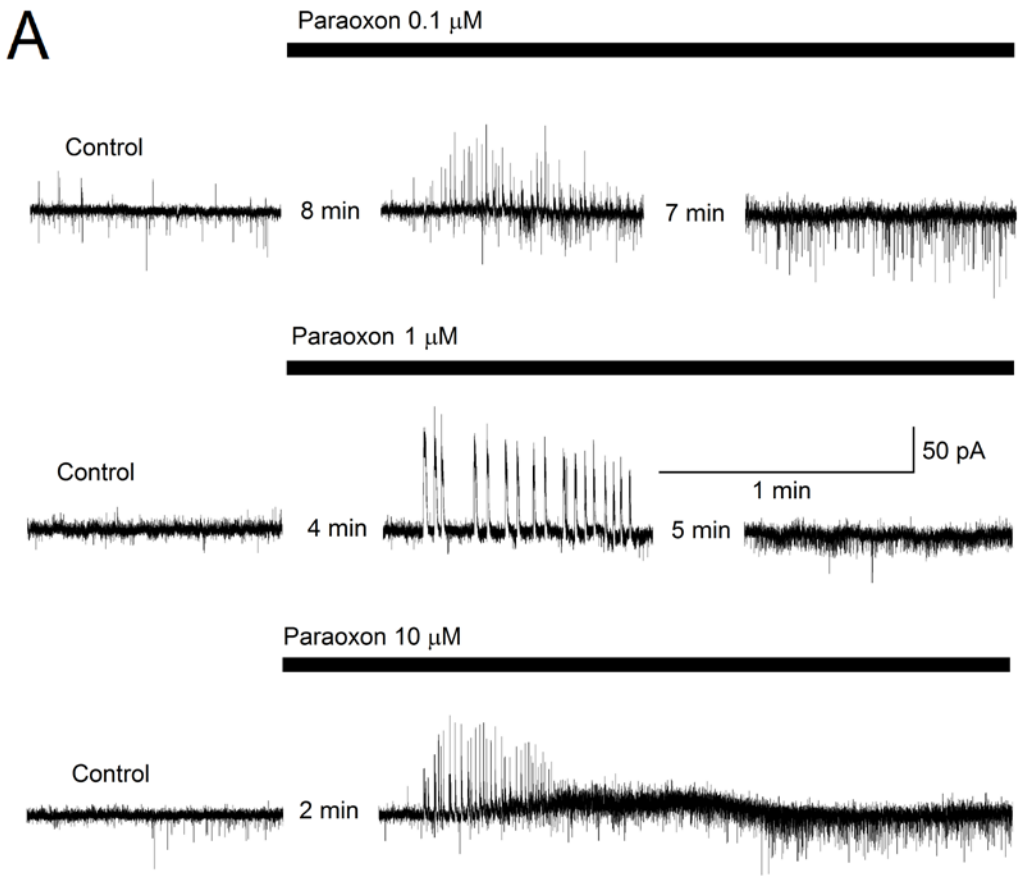
A
Paraoxon 0.1 μM
Control
8 min
7 min
Paraoxon 1 μM
Control
4 min
50 pA
1 min
5 min
Paraoxon 10 μM
Control
2 min

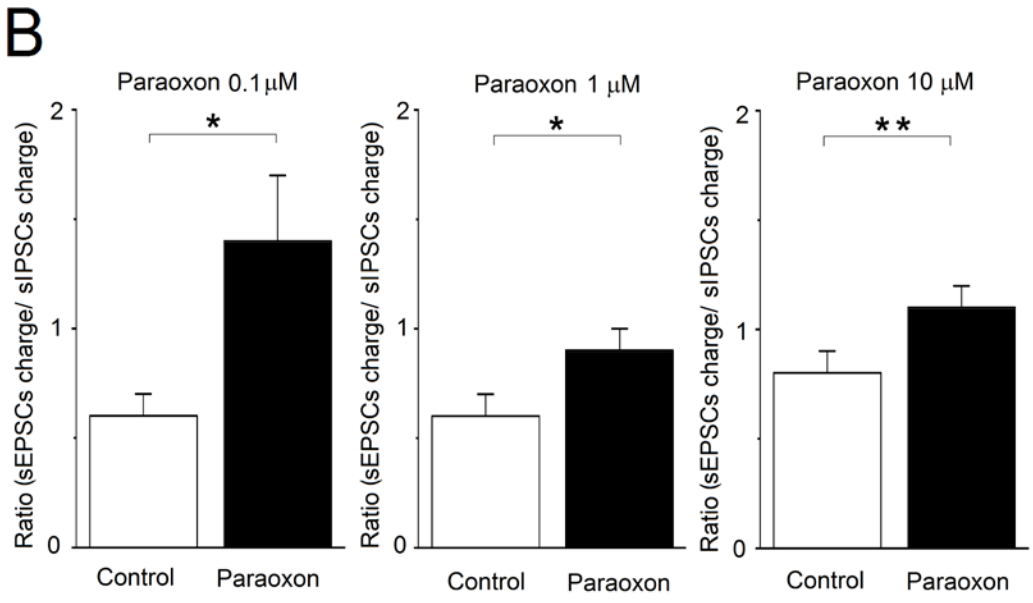
B
Paraoxon 0.1μM
Paraoxon 1 μM
Paraoxon 10 μM
Ratio (sEPSCs charge/ sIPSCs charge)
2
1
0
*
*
**
Control
Paraoxon

Next, we pretreated the slices with atropine (1 μM) or VU0255035 (10 μM), for about 4 min, and then applied 10 μM POX, while recording from principal BLA neurons. The holding potential was again -58 mV, and D-AP5 (50 μM), SCH50911 (10 μM), and LY341495 (3 μM) were present in the slice medium. Examples of simultaneous sIPSC and sEPSC recordings under these pharmacological conditions are shown in Fig. 13A. Figure 13B shows the effects of 10 μM POX separately on sIPSCs and sEPSCs under the three conditions: pretreatment with atropine (left bar graph), pretreatment with VU0255035 (middle bar graph), and when no muscarinic receptor antagonist is present (right bar graph). The total charge transferred by sIPSCs or sEPSCs during a 20 s time-window, 10 min after POX application, was expressed as a percentage of the total charge transferred, during 20 s, in control conditions. When 1 μM atropine was present in the slice medium, the charge transferred by sIPSCs after 10 min in POX was 72 ± 25% of the control (n = 7, $P = 0.203$), while the charge transferred by sEPSCs was 79 ± 23% of the control (n = 7, $P = 0.0441$). When 10 μM VU0255035 was present in the slice medium, the charge transferred by sIPSCs after 10 min in POX was 75 ± 17% of the control (n = 7, $P = 0.1561$), while the charge transferred by sEPSCs was 81 ± 16% of the control (n = 7, $P = 0.3892$). In contrast, in the absence of mAChR antagonists, the charge transferred by sIPSCs was increased by POX to 275 ± 57% of the control (n = 10, $P = 0.0001$), and the charge transferred by sEPSCs was increased by POX to 435 ± 80% of the control (n = 10, $P = 0.00002$). The difference between the increase in sIPSCs and the increase in sEPSCs was statistically significant ($P < 0.001$).

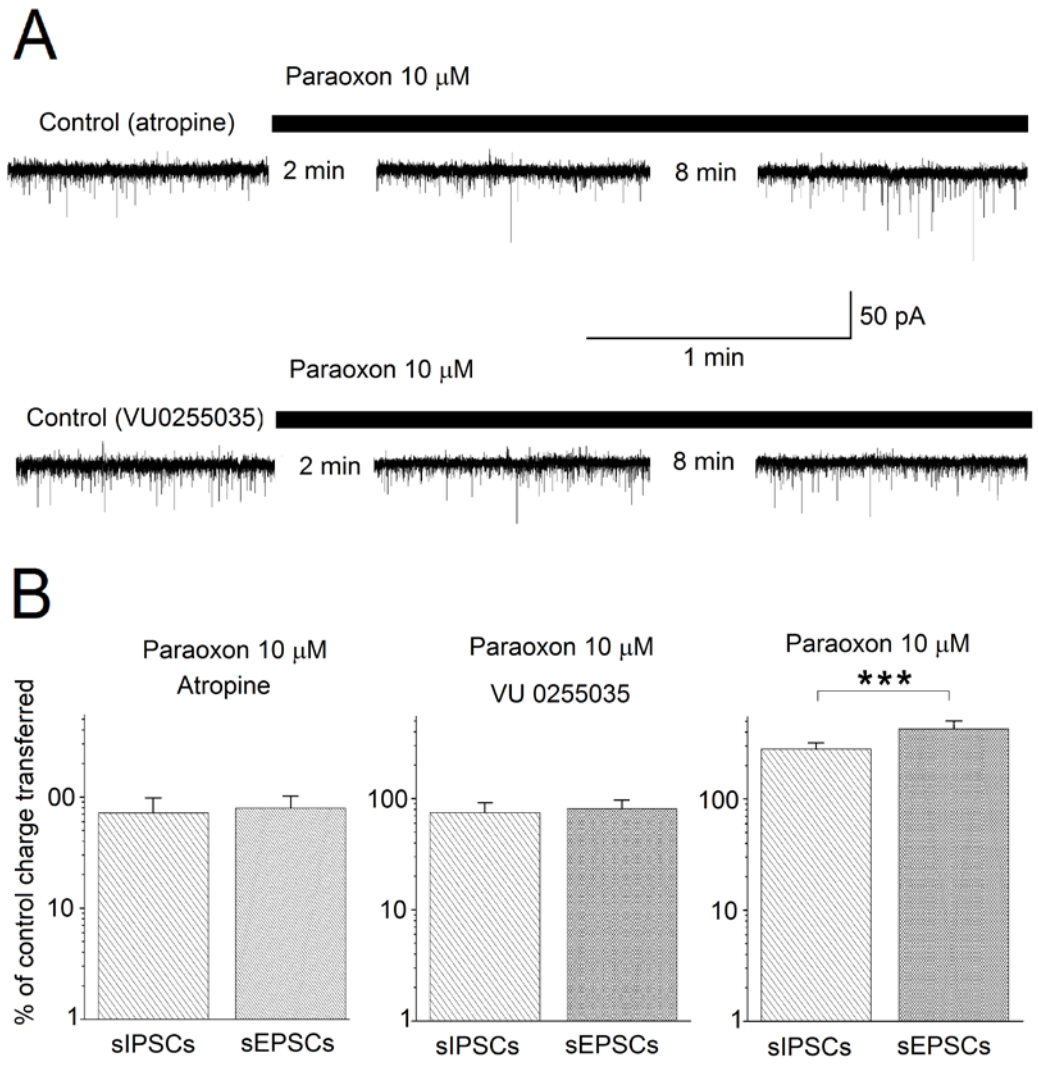

Figure 13. The effects of paraoxon are prevented when slices are pre-exposed to atropine or VU0255035. Whole cell simultaneous recordings of sIPSCs and sEPSCs were obtained from principal cells in the BLA (Vh = -58). (A) Representative traces showing that 10 μM paraoxon had no significant effect when applied in the presence of atropine (1 μM, top row of traces) or VU0255035 (10 μM, second row of traces). (B) Effects of 10 μM paraoxon on sIPSCs and sEPSCs under three conditions: pretreatment with atropine (left bar graph), pretreatment with VU0255035 (middle bar graph), and in the absence of any muscarinic receptor antagonist (right bar graph). The total charge transferred by sIPSCs or sEPSCs during a 20 s time-window, 10 min after paraoxon application, was expressed as a percentage of the total charge transferred, during 20 s, in control conditions. Only when there was no atropine or VU0255035 in the slice medium, the total charge transferred by sIPSCs and sEPSCs was increased by paraoxon, and the difference between the increase in sIPSCs and the increase in sEPSCs was statistically significant (***$P < 0.001$).

DISCUSSION AND CONCLUSIONS

The present study demonstrated that pretreatment with a selective M_1 receptor antagonist interfered with seizure initiation and significantly decreased seizure severity after exposure to POX or soman. The *in vitro* experiments suggested that one of the mechanisms via which M_1 receptors are involved in seizure initiation by OP exposure is by mediating a derangement in the balance between GABAergic and glutamatergic activity in the BLA, favoring glutamatergic hyperactivity.

The BLA plays a key role in seizure initiation after OP exposure (15). Thus, when McDonough *et al.* (179) microinjected nerve agents into different brain regions, they observed that convulsions were elicited only when the nerve agent was injected into the BLA. Recently, Prager *et al.* (227) found that in the small proportion of rats that do not develop seizures when exposed to high doses of soman, the activity of acetylcholinesterase (AChE) is reduced in the hippocampus and the piriform cortex to a similar extent as in the rats that develop seizures, but to a significantly lesser extent in the BLA; this suggests a crucial role of AChE reduction in the BLA for seizure initiation. The importance of the amygdala in nerve agent-induced seizure generation is also highlighted by the findings that the amygdala displays the earliest increase in extracellular glutamate after exposure to soman (151), and generates ictal-like discharges after *in vitro* application of soman (11). It has remained unclear, however, what are the synaptic events in the BLA that are triggered by AChE inhibition and lead to glutamatergic hyperactivity.

The BLA receives a very dense cholinergic innervation from the basal forebrain (31; 51; 140; 187; 192; 197), and has a higher basal AChE activity in comparison to other

brain regions in both adult (31; 227; 228) and 21-day old rats (Miller et al., unpublished). Cholinergic nerve terminals synapse on both pyramidal cells and interneurons (51; 192; 201), targeting nicotinic and/or muscarinic acetylcholine receptors, which are abundantly present in the amygdala (117; 171; 192; 248; 281; 293; 319). When acetylcholine levels rise subsequent to inhibition of AChE by an OP (150), both nicotinic and muscarinic receptors can be expected to be activated. The lack of contribution of nicotinic receptors to seizure initiation by OP exposure may relate to the increase of inhibitory rather than excitatory activity when these receptors are activated in the BLA (224; 319), or to the rapid desensitization of nicotinic receptors (98) in the persistent presence of elevated acetylcholine.

From the mAChRs, both the M_1 and M_2 subtypes are present in the rat BLA (71; 171; 172; 275), as well as the M_3 and/or M_4 receptors (267), but the M_1 receptors predominate (44). Immunocytochemistry along with electron microscopy have revealed that M_1 receptors in the rat BLA are located on somata, dendritic shafts, and, to a lesser extent, spines of pyramidal neurons, as well as on aspiny dendrites with morphological features typical of interneurons (193). In addition, M_1 immunoreactivity was found on presynaptic terminals most of which formed asymmetrical synapses with dendritic spines, but some of which formed symmetrical synapses with neuronal somata and dendritic shafts (193). It appears, therefore, that M_1 receptors in the rat BLA are in a position to affect the activity of both glutamatergic and GABAergic neurons, by postsynaptic or presynaptic mechanisms. Knowledge of their function has been hampered by the lack of selective M_1 agonists and antagonists. The availability of the selective M_1 antagonist VU0255035 (252) has allowed us, in the present study, to discover that these receptors

mediate the increase of glutamatergic activity in the BLA upon exposure to POX. The first event observed when POX took effect was a dramatic but short-lasting increase of GABAergic inhibitory activity, which did not occur in the presence of atropine or VU0255035. Whether this was due to direct depolarization–by the elevated acetylcholine–of GABAergic interneurons, facilitation of GABA release from GABAergic presynaptic terminals, or depolarization of glutamatergic neurons or terminals synapsing onto inhibitory interneurons cannot be ascertained by the present study; presynaptic facilitation of GABA release may be the least likely of the three possibilities, as it has been previously suggested that in the rat lateral amygdala M_1 receptors mediate inhibition of GABA release (280). GABAergic activity subsided within about 1 min, which could imply either that the drive of interneuronal depolarization was reduced, or the availability of presynaptic GABA-containing vesicles was decreased. Negative feedback inhibition via $GABA_B$ autoreceptors is not a possibility, since recordings were performed in the presence of a $GABA_B$ antagonist. We should note here that we also performed some experiments in the absence of $GABA_B$, NMDA, and metabotropic glutamate receptor antagonists, and the sequence of events upon application of POX was the same as in the presence of the antagonists.

After the initial barrage of sIPSCs subsided, inhibitory activity remained elevated relative to the baseline, while glutamatergic activity was also increased, significantly more than the GABAergic; again, these effects were not seen in neurons pretreated with atropine or VU0255035. The increase in sEPSCs could be the result of M_1 receptor-mediated depolarization of BLA principal neurons; such a depolarizing effect of M_1 activation could be due to inhibition of the voltage-dependent K^+ current (Im) (307; 308),

and/or increase of the mixed Na^+/K^+ current (Ih) and the Ca^{++}-dependent nonspecific cation current (91). In addition, M_1 receptors on glutamatergic terminals may facilitate glutamate release; in granule cells of the hippocampus, the frequency and amplitude of sEPSCs are increased by application of POX via a presynaptic mechanism, and this effect is blocked by pre-application of atropine (143).

It is possible, therefore, that the M_1 receptor-mediated enhancement of glutamatergic activity over that of GABAergic activity in the BLA network, upon OP exposure, creates a background of hyperexcitability. Over this background, seizures will be triggered when the ratio of glutamatergic over GABAergic activity becomes sufficiently high to reach the seizure threshold for the network, and from the BLA, seizures will propagate to other brain regions.

ACKNOWLEDMENTS

This work was supported by the CounterACT Program, National Institutes of Health, Office of the Director and the National Institute of Neurologic Disorders and Stroke [Grant Number 5U01NS058162-07].

CONFLICT OF INTEREST

None.

The views expressed in this article are those of the authors and do not reflect the official policy of the Department of Army, Department of Defense, or the U.S. Government.

CHAPTER 4: Discussion

Development of animal models is critical for testing antidotes against nerve agent intoxication. The FDA has a special rule, referred to as the "Animal Efficacy Rule", for approving medications for the treatment of chemical, biological, radiological or nuclear threats. Organizations seeking approval for the treatment of these threats must satisfy the requirements for this special rule if normal approval mechanisms, requiring human trials, are not ethical or feasible (270). For example, attacks employing nerve agents do not occur with high enough frequency to test antidotes against them; additionally, it would not be ethical to intentionally poison patients with nerve agents simply to test putative antidotes. However, as the sarin attacks in Syria (81) demonstrate there is still a critical need for the development of treatments for nerve agent intoxication, and especially nerve agent-induced seizures in the event that these lethal chemicals are employed in the future.

One of the main primary objectives of this dissertation was to develop a rodent model relevant to children exposed to nerve agents that reflects the acute and long-term symptomatology associated with nerve agent exposure and facilitate the testing of potential therapies to nerve agent-induced seizures. In line with these goals, this dissertation characterized the following aspects of soman exposure in immature male rats: the median lethal dose, the time to seizure onset, AChE activity in a variety of brain structures, and the efficacy of conventional and novel therapies against soman-induced seizures, as well as the efficacy of the conventional therapy in protecting against the long-term behavioral and morphological alterations associated with soman exposure.

A second objective of this research is to understand the cellular and molecular mechanism by which OPs induce, maintain, and reinforce seizure activity. Understanding

these mechanisms will help with the identification of novel molecular targets for the development of more efficacious therapies for seizures induced by these compounds, and could provide new treatments for patients suffering from temporal lobe epilepsy (77). Neuropharmacological models have proposed that mAChRs are largely responsible for seizure onset following OP intoxication but it has been unclear which mAChR subtype is responsible for the generation of seizure activity (181). Additionally, it has yet to be elucidated as to how mAChR hyperstimulation can lead to seizure activity following OP intoxication. As such, we identified the mAChR subtype that plays a critical role in seizure induction following OP intoxication and the electrophysiological mechanism underlying its activity.

DEVELOPMENT OF A RAT MODEL FOR TESTING ANTICONVULSANTS AGAINST NERVE AGENT-INDUCED SEIZURES AND ITS RELEVANCE TO THE PEDIATRIC POPULATION

To date, only one study has investigated nerve agent exposure in immature animals. Sterri and Colleagues (279) found the median lethal dose of soman to be 50 μg/kg (s.c.) for P21 rats. In our model, we calculated the median lethal dose for P21 male rats to be 62.02 μg/kg. This difference may result from the reduced toxicity of soman in female compared to male rats as Sterri and Colleagues used a mixed group of male and female rats for their median lethal dose calculation. The resistance of female rats to the toxic effects and mortality induced by soman exposure they observed is consistent with our work. We have found much greater doses are required to elicit seizures or induce mortality following soman exposure in female rats (unpublished data) and the findings of Sterri and Colleagues when groups of only female rats were used at different ages (279). An LD_{50} of 62.02 μg/kg for P21 male rats is nearly half that of young adult male rats, only one week older, with an LD_{50} of 110 μg/kg (126) illustrating the higher sensitivity of

immature rats to the toxicity of nerve agents. Consistent with clinical data on children (113; 119; 120) immature rats were also more susceptible to generating seizures following exposure to soman. We hypothesized this extremely rapid, generalized seizure onset following soman exposure was possibly due to a developmental difference in AChE activity within the BLA given its role in seizure induction following OP exposure (227). However, we found no difference in AChE activity of the BLA in naïve immature and adult male rats. Because it is unlikely this rapid seizure onset is due to the levels of AChE activity in immature rats, we performed a semi-quantitative analysis of publically available *in situ* hybridization data from mice of the different mAChR subtypes throughout development (See Appendix 1) (21; 157). Of note, the M_2 mAChR subtype has not reached adult intensity or density of expression within the BLA as late as P28 in mice. A reduction, compared to adult levels, in the expression of M_2 mAChRs may prevent an increase in g-protein coupled potassium conductance that is typically associated with M_2 stimulation (45), thereby increasing susceptibility to seizure induction. Additionally, binding of [^{3}H]3-quinuclidinyl benzilate, a nonspecific mAChR antagonist, in rat brain suggests that the total mAChR content has not reached adult levels in a P21 rat and may also explain the rapid seizure onset (75). An incomplete transition of the excitatory to an inhibitory function of GABA early in life and the subsequent rapid development of excitatory synapses may also make immature animals and children more susceptible to seizure induction (30).

Following exposure to 1.2 X LD_{50} soman, 2.0 mg/kg ATS was found to be a highly effective anticonvulsant against generalized seizures when administered at 20 minutes post-exposure. This was an unexpected finding as this dose of ATS and the time

at which ATS is administered usually has no anticonvulsant efficacy in adult animals against nerve agent-induced seizures (12; 89; 181; 229; 260). A variety of factors may help explain the age-dependent efficacy of ATS as an effective anticonvulsant. Ongoing SE has been found to increase the permeability of the BBB in immature and adult rats (208); and this permeability is also enhanced by OP exposure (4; 19; 52; 106; 208), even at subconvulsive doses (208). While OP exposure itself may increase BBB permeability, thereby increasing the OP content in the central compartment, this is also true for potential therapies, and this age-dependent increase in BBB permeability following OP exposure could explain the increase in seizure susceptibility but also in the efficacy of potential therapies in early development. Further, the reduced total mAChR content in the developing brain may also explain the rapid seizure onset since it is likely that less ACh would be required to elicit seizure activity following AChE inhibition. Regardless of the explanation for the increased efficacy of ATS, our findings suggest that it might be a highly effective anticonvulsant for children if administered rapidly after seizure onset.

We also investigated the efficacy of the GluK1KR antagonist LY293558 in arresting soman-induced seizures even when treatment is delayed to 1 h post-exposure in immature male rats. We performed these experiments to determine whether these compounds would exert the same efficacy that we have observed in adult rats against soman-induced seizures. LY293558 treatment, when delayed to 1 hr post-soman exposure, rapidly arrested ongoing SE and prevented long-term behavioral, pathological or pathophysiological changes that develop as a result of soman exposure (12; 89; 229). This potent efficacy as an anticonvulsant against nerve agent-induced SE is likely due to

the role of glutamate receptors in maintaining and reinforcing seizure activity at delayed timepoints post-exposure (181).

Ongoing seizure activity is thought to result in excitotoxic effects and subsequent cell-death through a variety of downstream mechanisms. Initially, in adult animals, cell loss occurs over a short time-scale via necrosis, likely due to the large influx of calcium through NMDA receptors during ongoing SE activity (108; 181). Delayed neuronal degeneration also occurs and may be observed for months post-exposure and is likely caused by edema, inflammation and apoptosis (62). This cell death is largely thought to be responsible for the long-term side effects associated with seizures induced by OPs (62; 67; 70; 74). However, it is unclear what mechanism might underlie the increase in anxiety-like behavior and impaired fear-learning 1 month following soman-induced seizures in immature rats as we observed no neuronal degeneration.

Numerous studies suggest that immature animals are resistant to the cell loss that is typically observed following seizure induction in adult animals (30; 113). The literature on this topic, as to what age seizures are associated with neuropathology, is complex and strongly dependent on the method employed to induce seizures, the sex, age, species and genetic profile of the organism (114). A variety of features of the immature brain may be neuroprotective following seizures. Superoxide radicals increase dramatically following seizure induction and may contribute, in part, to neuronal death in adult animals but no superoxide radical increases are observed following seizures in immature animals (159; 214). In P30 or P45 Sprague-Dawley rats, seizures induced by kainic acid increased the inactivation of mitochondrial aconitase, a metric of increased oxidative stress in mitochondria and in oxidative DNA damage (214). However, the

authors of this study did not find this increase in aconitase inactivation when seizures were induced in P12 or P21 rats, suggesting that immature brains are resistant to oxidative stress associated with seizure activity (214). Excessive glutamate-receptor stimulation is thought to be responsible for part of the signaling cascades that lead to cell death during episodes of SE in adult animals (165; 181). Direct microinjection of equal amounts of glutamate into the CA1 of P10, P20, P30 and P60 rats results in either minimal or no cell loss 7 d post-injection but the lesion size increased beyond this age (165). Brain-derived neurotrophic factor (BDNF) regulates the differentiation, growth and survival of neurons throughout development (6; 29; 122; 156; 317) and has been found to be neuroprotective against a variety of insults including excitotoxic injury in the adult (63). Seizures can modulate the expression of neurotrophins such as BDNF. Seizures induced by either kainic acid or lithium-pilocarpine in P7 or P12 rats increase BDNF in a variety of cortical and limbic structures and may play a role in the resistance to seizure-induced cell loss observed at this age (141). When the increase in expression of BDNF was blocked prior to seizure induction by kainic acid in P20 rats, neuronal loss was observed within hippocampus (283). When BDNF expression was not blocked, kainic acid injection resulted in a twofold increase in BDNF expression and no neuronal loss was observed (283), strongly suggesting a neuroprotective role for this neurotrophin early in development. While we did not study this in our model, a variety of these factors may explain the lack of neurodegeneration following soman-induced seizures in P21 rats.

Despite the lack of neurodegeneration observed in our model, the volumes of both the amygdala and hippocampus were significantly reduced at 30 and 90 d post-soman exposure. In structural MRI studies, atrophy of amygdala and hippocampus is a common

finding in temporal lobe epilepsy (TLE) patients, and may correlate with a history of febrile seizures during childhood (32; 55; 57-59; 104; 139; 274). P12 and P25 rats have also been observed to have reductions in the volume of temporal structures at timepoints as long as 5 or 7 months following SE induction by lithium-pilocarpine (148). This finding may also be important in the pathogenesis of the symptoms related to OP exposure as a reduction in the volume of the amygdala was observed in victims exposed to sarin during the Tokyo subway attack (238). Notably, this reduction in volume lasted over a decade (238). Though it is unclear what mechanism is responsible for the volumetric reductions observed in our study, long-term behavioral impairments are commonly observed following early life seizures and must be due to a mechanism unrelated to seizure-induced cell loss.

Given the role of the amygdala and hippocampus in regulating anxiety (5; 84; 149), and their role in cue- and context-dependent fear conditioning, respectively (127; 138; 219); it is expected that pathological damage to these structures would disrupt fear learning and the regulation of anxiety. 1 month post-soman exposure, rats displayed an increase in anxiety-like behavior and were unable to undergo fear learning. Though the volumes of both amygdala and hippocampus were still reduced 3 months post-soman exposure, fear-learning returned to control conditions as did anxiety-like behavior. This suggests that between 1 and 3 months post-soman exposure, networks responsible for mediating anxiety-like behavior and fear learning compensated for the initial damage induced by SE at P21. Recovery from behavioral impairment was also observed in the patients exposed to sarin in the Tokyo subway attacks (238; 315); patients that presented with a reduction in amygdalar volume over a decade following the attack, which had a

history of PTSD associated with sarin exposure, no longer presented with PTSD at the time of the volumetric analysis but amygdala volume was persistently reduced (238).

Despite the suggestion from the clinical literature that seizures in children are relatively benign, data from these studies suggest that nerve agent-induced seizures can result in profound, long-term alterations in brain pathology and behavior. Importantly for mass casualty scenarios, ATS may be very efficacious in arresting nerve agent-induced seizures in children if treatment is delivered soon after seizure onset. In the event that first responders cannot address the symptoms resulting from nerve agent exposure, delayed treatment following seizure onset with LY293558 appears to be effective in rapidly arresting SE induced by nerve agent exposure in the developing brain. This treatment is also promising as it was capable of preventing long-term alterations in brain pathology or behavioral impairments typically associated with nerve agent exposure. This study establishes a model of nerve agent exposure that displays all of the symptoms of severe poisoning, clinically relevant long-term symptoms, and has identified a potential anticonvulsant for nerve-agent induced seizures that is efficacious even when treatment is delayed; but also allows for the identification of novel therapies for the complex variety of symptoms that present with OP poisoning.

THE ROLE OF THE M1 MUSCARINIC RECEPTOR IN SEIZURES INDUCED BY ORGANOPHOSPHATES

Understanding the cellular and molecular mechanisms of seizure induction following OP intoxication will aide in the development of novel treatments that will reduce or eliminate seizure activity after an OP exposure. Numerous studies indicate that the BLA plays a key role in facilitating seizure induction following OP poisoning (15). Moreover, the amygdala is often identified as a seizurogenic structure in TLE and is

routinely removed in an effort to reduce seizures (107; 289). In the case of nerve agents, a variety of studies have suggested its causal role in seizure initiation. When soman or VX is directly injected into the BLA, motor convulsions are elicited that closely resemble nerve agent exposure via systemic injection (179). Following systemic injection, glutamate levels also rapidly rise in the amygdala (151), before other structures, and sustains the most extensive neuropathology (15), perhaps due to an increase in the duration of exposure to the excitotoxic effects of glutamate. Recent data from our group in adult rats (227) and immature rats (Miller et al., unpublished) also suggest a role of the BLA in seizure induction as it appears that unless almost all of the total pool of AChE activity is specifically inhibited there, seizure initiation does not occur. McDonough and Shih (181) have suggested that following AChE inhibition, seizure initiation is mediated via mAChRs but it is unclear how this may occur.

In this study we found that application of the OP POX to BLA slices initially resulted in a relative increase in GABAergic inhibitory over glutamergic excitatory activity. This dramatic increase in $GABA_A$ receptor mediated inhibition subsided rapidly, although there was a persistent increase in sIPSCs following POX application. This may seem counterintuitive if OP exposure is going to initiate seizures. However, in addition to the significant increase of sIPSCs, an increase in AMPA receptor mediated sEPSCs was also observed and prevailed as the dominating driving force to BLA activity as indicated by a greater sEPSC to sIPSC ratio. This effect of POX on sIPSCs and sEPSCs was completely blocked by atropine and VU0255035. Indeed, the blockade of the increase in $GABA_A$ receptor mediated sIPSCs or AMPA receptor mediated sEPSCs by POX when slices were pretreated with either atropine or VU0255035 strongly implicates the

mAChRs, but more specifically, the M_1 mAChR subtype in facilitating a relative increase in glutamatergic activity within the BLA following OP exposure. If M_1 mAChR hyperstimulation is required for seizure induction, pretreatment with VU0255035 *in vivo* may block or suppress the severity of seizures induced by OP exposure. In agreement with this hypothesis, we found that when adult rats were pretreated with VU0255035 the severity of the seizures induced by either POX or soman was reduced compared to vehicle pretreated controls. While VU0255035 pretreatment may be thought to possibly block seizure induction, we do not find our data too surprising as this compound is a competitive antagonist (252) and synaptic ACh levels will continue to rise due to the irreversible inhibition of AChE; eventually overcoming the M_1 mAChR antagonism. Though our findings strongly implicate the role of the M_1 mAChR in seizure induction, it is unclear how hyperstimulation of this receptor could lead to a prevalence of glutamatergic excitatory activity within the BLA.

Stimulation of postsynaptic mAChRs in the BLA may facilitate enhanced excitatory transmission through the blockade of the voltage-dependent Im current (307). mAChR stimulation in the BLA or hippocampus increases Ih (307) or the Ca^{++}-dependent nonspecific cation current (91), respectively. Presynaptic mAChRs also been increase the release of glutamate at synaptic terminals and the combination of all of these events may drive the BLA network into a more excitable state, eventually reaching a level that induces seizure activity. The strong role of mAChRs in generating seizures following OP intoxication suggests the importance of mAChR antagonists, ideally selective for the M_1 mAChR, with higher availability to the central compartment. This is especially true for the early phase of seizure activity, which is predominantly mediated by

mAChR hyperactivity (181). In addition to GluK1KR antagonists, including M_1 mAChR antagonists in the delayed treatment of OP-induced seizure may be important as an adjunct therapy. Due to the irreversible inhibition of AChE, synaptic concentrations of ACh are likely to be maintained at high levels until AChE is resynthesized and result in further M_1 mAChR stimulation; promoting further hyperexcitability. Indeed, our group has found that the drug caramiphen, which has antagonistic properties to the M_1 mAChR and the NMDA receptor, is an effective anticonvulsant against soman-induced seizures in rats, even when seizures are delayed to 1 hour post-exposure (88). These data highlight the importance of this receptor for OP-induced seizures and their potential role as target for treatment.

CONCLUSIONS AND FUTURE DIRECTIONS

OP intoxication constitutes a significant threat to public health and has become one of the most widely studied class of compounds in toxicological research. While a dearth of data exists on OPs, an understanding as to how the irreversible inhibition of AChE can lead to seizures and an associated set of long-term behavioral impairments is lacking, especially for children. This investigation has yielded a rat model of nerve agent exposure to facilitate testing of novel anticonvulsants for the pediatric population. We found that immature rats are much more sensitive than adult rats to the toxic effects of soman exposure, which produce a long-lasting reduction in the volumes of the amygdala and hippocampus, lasting up to 3 months post-exposure. This volumetric reduction in the amydala and hippocampus may underlie the observed increase in anxiety-like behavior and the inability to undergo fear-learning at 1 months post-exposure. The explanation for normal behavior at 3 months post-soman exposure is unclear, given the persistent

reduction in amygdala and hippocampus, and requires further investigation. Although immature rats were highly sensitive to the toxic and lethal effects of soman exposure, they were also very amenable to anticonvulsant therapy. ATS, if administered within 20 minutes post-soman exposure was capable of arresting ongoing seizure activity induced by soman. LY293558 was also effective in arresting seizures induced by soman, similar to our previous data in adult rats (12; 89), even if administered 1 hour post-soman exposure. Additionally, this compound blocked the volumetric reduction in the amygdala and hippocampus, and prevented the behavioral impairments associated with soman exposure. This strongly suggests the role of GluK1KR antagonists as an excellent treatment for arresting seizures induced by OPs and protecting against the long-term side effects associated with OP exposure.

Further understanding was provided in these studies as to the mechanisms responsible for seizure induction following OP intoxication. We found that POX exposure to the BLA facilitates a net shift in network activity towards glutamatergic excitatory activity, which is mediated by mAChRs, and specifically, the M_1 mAChR. Blockade of the M_1 mAChR *in vivo* prior to POX or soman exposure significantly suppressed the seizure severity and strongly indicates their importance for seizure induction following OP poisoning.

Appendix 1: Semi-Quantitative Analysis of the Expression of mAChR Subtypes Throughout Development in Mouse Basolateral Amygdala

Using a semi-quantitative scale, mAChR expression was evaluated from sagittal sections of the BLA throughout development (Figure 14). An analysis of the density and intensity of gene expression was performed as described in the Allen Institute's white paper for *in situ* hybridization on their website (3).

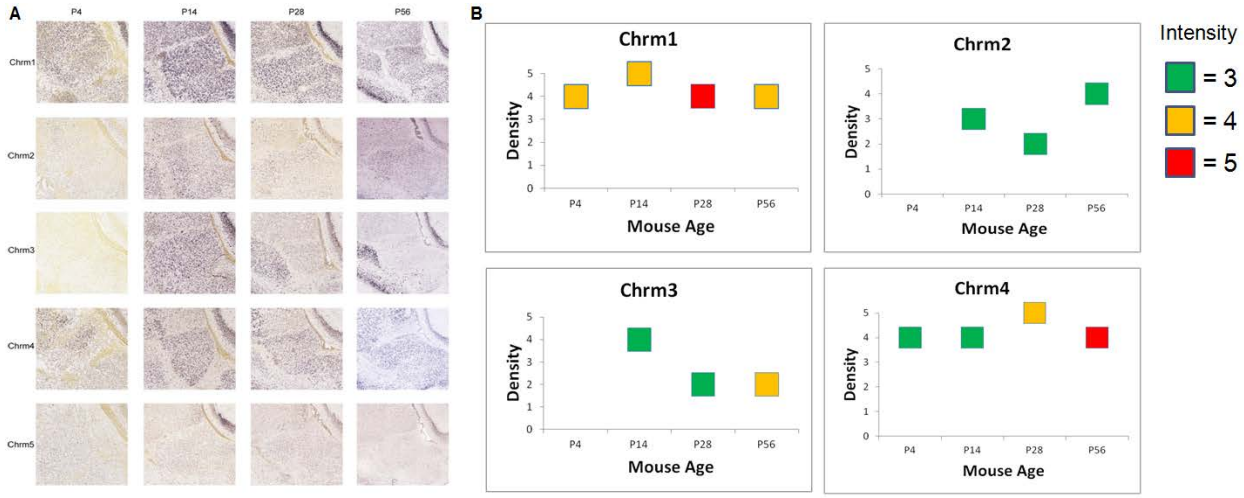

Figure 14. Semi-quantitative analysis of mouse mAChR gene expression. Density and intensity was analyzed using the semi-quantitative scale published on the website for the Allen Institute for Brain Science (3). A - Representative images of sagittal sections of mouse BLA for each age and gene analyzed in the analysis. B - Quantification of the density and intensity for each age and gene in the analysis. Chrm5 was not detected in the analysis. "Chrm" designation indicates mouse gene names (e.g. Chrm1 refers to mAChR subtype 1).

Appendix 2: ASIC1a Activation Enhances Inhibition in the Basolateral Amygdala and Reduces Anxiety

Volodymyr I. Pidoplichko[1], Vassiliki Aroniadou-Anderjaska[1,2,3], Eric M. Prager[1,3], Taiza H. Figueiredo[1], Camila P. Almeida-Suhett[1,3], Steven L. Miller[1,3], and Maria F. M. Braga[1,2,3]

[1]Department of Anatomy, Physiology, and Genetics, [2]Department of Psychiatry, and [3]Program in Neuroscience, F. Edward Edward Hébert School of Medicine, Uniformed Services University of the Health Sciences, Bethesda, Maryland 20814

*Corresponding Author:
Maria F.M. Braga, D.D.S., Ph.D.
Department of Anatomy, Physiology, and Genetics
F. Edward Hébert School of Medicine
Uniformed Services University of the Health Sciences
4301 Jones Bridge Road
Bethesda, MD 20814
Phone: (301) 295-3524

ABSTRACT

The discovery that even small changes in extracellular acidity can alter the excitability of neuronal networks via activation of acid-sensing ion channels (ASICs) could have therapeutic application in a host of neurological and psychiatric illnesses. Blockade of ASIC1a has been recently proposed as a potential treatment for anxiety, as these channels appear to mediate fear and anxiety in response to certain stimuli. The basolateral nucleus of the amygdala (BLA) is a key brain region in the generation and expression of fear. To provide a direct assessment of the role of ASIC1a in the regulation of BLA excitability we recorded from interneurons and principal neurons in the rat BLA. We found that ASIC1a activation favors the increase of GABAergic inhibition. Accordingly, *in vivo* activation or blockade of ASIC1a in the BLA suppressed or increased, respectively, anxiety-like behavior. These findings suggest an inhibitory and anxiolytic function of ASIC1a in the rat BLA.

INTRODUCTION

Reduction of extracellular pH in the central and peripheral nervous system can alter neuronal activity and network excitability via activation of specific cation channels that are gated by H^+. This has raised great interest, as manipulation of these channels may be useful in the treatment of many neurological or mental illnesses that involve derangements in neuronal excitability. The existence of an inward current activated by lowering extracellular pH and carried by Na^+ and K^+ was first reported in rat spinal ganglia and trigeminal nerve ganglion by Krishtal and Pidoplichko, in 1980 (146). A cation channel with these biophysical properties was later cloned from cDNA isolated from rat brain, and was named ASIC for acid-sensing ionic channel (299). There are three

types of ASICs: ASIC1, ASIC2, and ASIC3 (300). The three proton-gated channels are members of the degenerin/epithelial Na^+ channel family, but have different biophysical properties and regional distribution (300). The ASIC1 has two splice variants: ASIC1a and ASIC1b. The ASIC1a is permeable to Ca^{++} (103; 316) and is widely expressed in the brain, with the highest expression levels found in the amygdala, the main olfactory bulb, cerebral cortex, hippocampus, habenula, and cerebellum (34; 299). The ASIC1b is expressed only in sensory neurons (61) and is not permeable to Ca^{++} (28). Native ASIC1a channels appear to be homomeric trimers, but they may also be heteromeric trimers combining with the ASIC2a or ASIC2b subunits (27; 254), which are splice variants of the ASIC2.

It is unclear whether activation of ASIC1a enhances or suppresses the activity and excitability of the neuronal networks where the channel is expressed. ASIC1a activation evokes larger currents in freshly dissociated hippocampal interneurons than in CA1 pyramidal cells (38; 321), suggesting that these channels may preferentially mediate increases in inhibitory activity. Accordingly, low pH suppressed epileptiform activity in mouse hippocampal slices, an effect that was apparently mediated by ASIC1a activation, since epileptiform activity in hippocampal slices from ASIC1a-null mice was not affected by acidification (321). Further evidence suggesting an inhibitory role of ASIC1a activation is that the intensity and duration of chemoconvulsant-induced seizures is greater in ASIC1a-null mice than in wild-type mice, and the inhibition of seizures by CO_2 inhalation-induced acidosis is observed in wild type mice but not in ASIC1a-null mice (321).

Behavioral studies, however, seem to suggest that, at least in the amygdala, a brain region that plays a central role in emotional behavior (217) and associated disorders – such as anxiety disorders including post-traumatic stress syndrome (86; 236; 253; 278) – the function of the ASIC1a is to promote rather than suppress hyperexcitability. Thus, intra-cerebroventricular administration of an ASIC1a antagonist, or genetic elimination of ASIC1a reduced fear/anxiety (73) and had antidepressant (72) and anxiolytic effects (82). Similarly, genetically eliminating or pharmacologically inhibiting ASIC1a, markedly reduced the fear evoked by CO_2 inhalation (320). Anxiety, fear, and, in most cases, depression are associated with hyperexcitability and hyperactivity of the amygdala (236; 253; 306). Therefore, the implication of studies showing reduced fear and anxiety when ASIC1a channels are blocked or genetically eliminated (72; 73; 82; 320) is that, in the amygdala, the function of ASIC1a is to promote hyperactivity. Accordingly, localized ASIC1a expression in the amygdala of ASIC1a- null mice prevented the deficit in CO_2-induced fear (320), and intra-amygdala infusion of an ASIC1a antagonist increased the levels of GABA but not glutamate (82). These observations have led to the suggestion that antagonism of ASIC1a must receive consideration as a potential treatment for anxiety (73; 82) and depression (72). However, so far there has been no direct evidence that ASIC1a antagonism suppresses amygdalar excitability.

In the present study, we attempted to determine the role that ASIC1a channels play in the regulation of amygdalar excitability. We recorded from neurons in the basolateral nucleus of the amygdala (BLA), the region that is most closely associated with the generation and expression of fear and anxiety (94; 253; 295). We found that functional ASIC1a channels are present on both interneurons and principal cells in the

BLA, and their activation increases glutamatergic and GABAergic activity in the network. However, the increase in GABAergic activity predominates, suppressing overall excitability. Furthermore, these channels are active in the basal state, enhancing GABAergic inhibition. Consistent with the electrophysiological results, behavioral tests suggested that, in contrast to the findings in mice (73; 82), ASIC1a activation in the rat BLA has anxiolytic effects, while ASIC1a blockade augments anxiety-like behavior.

METHODS

Electrophysiological Experiments.

Male, Sprague-Dawley rats (25 to 40 days old) were anesthetized with isoflurane before decapitation. Coronal brain slices (400 μm thick) containing the amygdala were cut with a vibratome (Leica VT 1200 S; Leica Microsystems, Buffalo Grove, IL), in ice-cold solution consisting of (in mM): 115 sucrose, 70 NMDG, 1 KCl, 2 $CaCl_2$, 4 $MgCl_2$, 1.25 NaH_2PO_4, 30 $NaHCO_3$, 25 D-glucose. The slices were transferred to a holding chamber, at room temperature, in a bath solution (artificial cerebrospinal fluid, ACSF) containing (in mM): 125 NaCl, 2.5 KCl, 1.25 NaH_2PO_4, 21 $NaHCO_3$, 2 $CaCl_2$, 1 $MgCl_2$, and 11 D-glucose. Recording solution was the same as the holding bath solution. For field potential recordings the bath/recording solution was same as above, except for the concentration of $MgCl_2$ (1.5 mM) and KCl (3 mM). All solutions were saturated with 95% O_2, 5% CO_2 to achieve a pH near 7.4. For whole-cell recordings, the slice chamber (0.7 mL capacity) had continuously flowing ACSF (~8 mL/min) at temperature 31~32°C, except for a few experiments where the bath temperature was reduced to 27°C, as indicated in the results. The osmolarity of the external solution was

adjusted to 325 mOsm with D-glucose. Field potential recordings were obtained in an interface-type chamber, maintained at ~32°C, with a flow rate of the ACSF at 1.5 ml/min.

For whole-cell recordings, neurons were visualized under infrared light using Nomarski optics of an upright microscope (Zeiss Axioskop 2, Thronwood, NY) through a 40x water immersion objective, equipped with a CCD-100 camera (Dage-MTI, Michigan City, IN). The patch electrodes had resistances of 3.5–4.5 MΩ when filled with the internal solution (in mM): 60 $CsCH_3SO_3$, 60 KCH_3SO_3, 10 KCl, 10 EGTA, 10 HEPES, 5 Mg-ATP, 0.3 Na_3GTP (pH 7.2), 290 mOsm. When recordings were obtained in the absence of CNQX, the internal chloride concentration was 1 mM, and osmolarity was adjusted with potassium gluconate. Tight-seal (over 1 GΩ) whole-cell recordings were obtained from the cell body of interneurons and pyramidal-shaped neurons in the BLA region. Access resistance (5–24 MΩ) was regularly monitored during recordings, and cells were rejected if the resistance changed by more than 15% during the experiment. Agonists or antagonists of ASIC1a were applied either to the bath or by pressure injection. Pressure application was performed using a push–pull experimental arrangement (222). Pressure was applied to the pipette via a Picospritzer (General Valve Division, Parker Hannifin Corp., Fairfield, NJ), set at about 100 kPa (14 psi). A motorizer (Newport, Fountain Valley, CA) was coupled with the approach/withdrawal (push–pull) actuator of a micromanipulator (Burleigh PCS-5000 series; EXFO Photonic Solution Inc., Mississauga, Ontario, Canada). Motorizer movement and duration of application pulses were controlled with a Master-8 digital stimulator (AMPI; Jerusalem, Israel). Ionic currents and action potentials were amplified and filtered (1 kHz) using the Axopatch 200B amplifier (Axon Instruments, Foster City, CA) with a four-pole, low-pass Bessel

filter, were digitally sampled (up to 2 kHz) using the pClamp 10.2 software (Molecular Devices, Sunnyvale, CA), and further analyzed using the Mini Analysis program (Synaptosoft Inc., Fort Lee, NJ) and Origin (OriginLab Corporation, Northampton, MA).

Field potentials were evoked by single-pulse stimulation of the external capsule at 0.05 Hz. Recording glass pipettes were filled with ACSF, and had a resistance of approximately 5 MΩ. Stimulation was applied with a bipolar concentric stimulating electrode made of tungsten (World Precision Instruments, Sarasota, FL). Signals were digitized using the pClamp 10.2 software (Molecular Devices, Union City, CA), analyzed using Clampfit 10.2, and final presentation was prepared using Origin (OriginLab Corporation, Northampton, MA) or Graphpad Prism (GraphPad Software, La Jolla, CA). In some experiments, the charge transferred by postsynaptic currents was calculated, using the Mini60 software by Synaptosoft (Synaptosoft Inc., Fort Lee, NJ).

Drugs used were as follows: CNQX, an AMPA/kainate receptor antagonist, bicuculline methiodide, a $GABA_A$ receptor antagonist, and ammonium chloride, an activator of ASIC1a (223) (from Sigma-Aldrich, St. Louis, MO); D-AP5, an NMDA receptor antagonist, SCH50911, a $GABA_B$ receptor antagonist, and flurbiprofen, an ASIC1a antagonist (298) (from Tocris, Ellisville, MO); tarantula venom psalmotoxin (PcTX1, 100 μl lyophilized milked venom, from Spider Pharm Inc., Yarnell, AZ), an ASIC1a antagonist (27; 80; 85); synthetic psalmotoxin 1 (Peptides International, Louisville, KY), an ASIC1a antagonist. Low pH solutions for bath application were prepared as described by Ziemann et al. (321), except that sodium bicarbonate content was lowered to 5 mM to yield a pH of 6.6. Solutions with pH 5.0 for pressure-application were buffered with HEPES. Osmolarity was adjusted by adding sodium gluconate.

Behavioral experiments

Subjects

Male, Sprague-Dawley rats (200 ~ 220 g) were individually housed in an environmentally controlled room (20–23°C, 12-h light/12-h dark cycle, lights on 06:00 pm), with food and water available ad libitum. All experimental procedures adhered to the National Institutes of Health Guide for the Care and Use of Laboratory Animals, and were approved by the Institutional Animal Care and Use Committee (IACUC) of the Uniformed Services University of the Health Sciences.

Surgical procedure

Forty rats were anesthetized with 2-5% isoflurane, using a KSC Anesthesia System (Kent Scientific, Torrington, CT). Each rat was mounted on a stereotaxic frame (David Kopf Instruments, Kent, UK), and a midline incision was made over the skull. The skull was scraped clean, four holes were then drilled into the skull, and self-tapping stainless-steel screws were inserted to help anchor the guide cannulae (Plastics One Inc., Roanoke, VA). Next, two additional sites were drilled, and stainless steel guide cannulae (26 gauge, Plastic One Inc) of 8.0 mm length were implanted at the following coordinates: 2.8 mm anteroposterior to the bregma, 4.6 mm lateral to the midline, and 8.0 mm in depth (based on Paxinos and Watson, 2005). Dental cement (A-M Systems, Sequim, WA) was used to affix the guide cannulae and to stabilize the assembly by adhering to the four stainless steel screws.

Microinjection procedure

Beginning on the seventh day following surgery, each rat was extensively handled by the experimenter for 3 days. During the following 3 days, the rats were gently restrained by hand, and injection tubing (Plastics One Inc., Roanoke, VA) was screwed in the animals' head, while an electric pump was turned on, in order to habituate the rats to the handling and noises associated with the microinjection procedure. On experimental days, 33 gauge injector-cannulae were inserted into the guide cannulae. The injectors were 9 mm length to extend 1 mm beyond the end of the guide cannulae. Drug solutions were bilaterally infused for 2 min, at a rate of 0.5 µl/min, with the use of a microinfusion pump (Harvard Apparatus, Holliston, MA); 1 µl total volume was delivered in the BLA of each hemisphere. Injectors were left in place for 1 min after the end of the infusion. In the open field test (see next paragraph), each rat was tested only with a single dose of one of three drugs (ammonium chloride, synthetic psalmotoxin, tarantula venom psalmotoxin; all dissolved in ACSF) and a single dose of the vehicle (ACSF); the two tests were separated by one week, and the order of testing was randomized.

Open Field test

Behavioral tests took place during the dark phase of the rats' light/dark cycle. Anxiety-like behavior was assessed using an open field apparatus (40 X 40 X 30 cm clear Plexiglas arena). The animals were acclimated to the apparatus in one session. On test days, the rats were placed in the center of the open field, 5 min after drug or vehicle injection. Activity was measured and recorded for 5 min, using an Accuscan Electronics infrared photocell system (Accuscan Instruments Inc., Columbus, OH). Data were automatically collected and transmitted to a computer equipped with "Fusion" software (Accuscan Electronics). Locomotion (distance traveled in cm), total movement time, and

time spent in the center of the open field were analyzed. Anxiety behavior was measured as the ratio of the time spent in the center over the total movement time, expressed as a percentage of the total movement time.

Light-Dark Box test

Anxiety-like behavior was also assessed using a light/dark box apparatus, which consisted of an activity arena that was fitted with a light/dark box insert (Accuscan Instruments Inc.). The light and dark compartments measured 20 X 40 X 30 cm each. About 5 min after drug or vehicle microinjection, rats were placed in the light compartment facing the dark compartment, and their activity was recorded for 5 minutes, using an Accuscan Electronics infrared photocell system. Anxiety behavior was assessed by the latency to enter the dark compartment and the time spent in the light compartment.

Histology

After completion of the behavioral tests, rats were deeply anesthetized with isoflurane using a KSC Anesthesia System (Kent Scientific, Torrington, CT) and decapitated. The brains were removed and stored in 4% paraformaldehyde for at least 7 days before being sectioned on a freezing microtome (40 µm sections). Brain sections were mounted onto slides, and stained with cresyl violet according to standard procedures. The location of the guide cannulae was determined using a light microscope. Only rats with confirmed cannulae position in the BLA were used in the results analysis.

Statistical Analysis

The results from the electrophysiological and behavioral experiments were tested for statistical significance using the two-sample- or the paired t-test. Differences were

considered significant when $P < 0.05$. Data are presented as Mean ± standard error. Sample size "n" refers to the number of neurons for the whole-cell experiments, the number of slices for the field potential recordings, and the number of animals for the behavioral experiments.

RESULTS

ASIC1a channels are present on both interneurons and principal cells

Our first aim was to determine whether interneurons and principal neurons in the BLA carry functional ASIC1a channels. We distinguished interneurons from principal cells based on size and shape (larger size and pyramidal shape for principal cells), as well as on their electrophysiological characteristics. The majority of BLA interneurons fire fast, non-accommodating action potentials in response to depolarizing current pulses, while principal cells fire longer duration action potentials displaying various patterns of accommodation (241; 273). In addition, the majority of interneurons demonstrate linear change in leakage current in response to hyperpolarizing voltage steps, in contrast to the principal BLA neurons, which display a hyperpolarization-activated cationic current (I_h) (17; 213; 308). Figure 1a and 2a show the characteristic responses of interneurons and principal cells, respectively, to 1 s -long hyperpolarizing steps (10 mV increments) from the holding potential of -70 mV (left panel), as well as to 500 ms-long current injections in the current-clamp mode (right panel).

ASIC1a is also gated by ammonium (220; 223). Therefore, to determine whether ASIC1a channels are present on BLA interneurons, we pressure-applied acidified ACSF (pH 5), or ACSF containing 40 mM ammonium chloride, while recording from interneurons (n = 9) at a holding potential (V_h) of -70 mV, and in the presence of CNQX

(10 μM), D-AP5 (50 μM), and bicuculline (20 μM). Both low pH and ammonium induced inward currents that were dramatically enhanced when the temperature of the bathing solution was reduced from 32° to 27°C (Fig. 15b), which is consistent with the paradoxical temperature dependency of ASIC1a channels (20). The evoked currents were reversibly blocked by the ASIC1a antagonist flurbiprofen (Fig. 15c). In the current clamp mode, bath application of 5 mM ammonium induced high-frequency firing of the recorded interneurons (n=4, Fig. 15d). These data indicate that ASIC1a channels are present on BLA interneurons, and their activation produces strong depolarization.

Figure 15. ASIC1a channels are present on BLA interneurons. (a) Typical linear currents (I_h is absent) recorded from interneurons in response to hyperpolarizing voltage steps in voltage-clamp (v-clamp) mode (left), and an example of fast, non-accommodating spiking of interneurons in response to current injection in the current-clamp (c-clamp) mode (right). (b) Brief (200 ms) pressure application of acidified solution (left), or 40 mM ammonium (right) induced inward currents in interneurons, which were increased by lowering the bath temperature. (c) Currents evoked in interneurons by acidified solution or 40 mM ammonium were blocked by 2 mM flurbiprofen. (d) In the current clamp mode, bath application of 5 mM ammonium induced high-frequency firing of interneurons. In (b) and (c), holding potential is -70 mV. In (b), (c), and (d), recordings are in the presence of CNQX (10 μM), D-AP5 (50 μM), bicuculline (20 μM), and SCH50911 (10 μM).

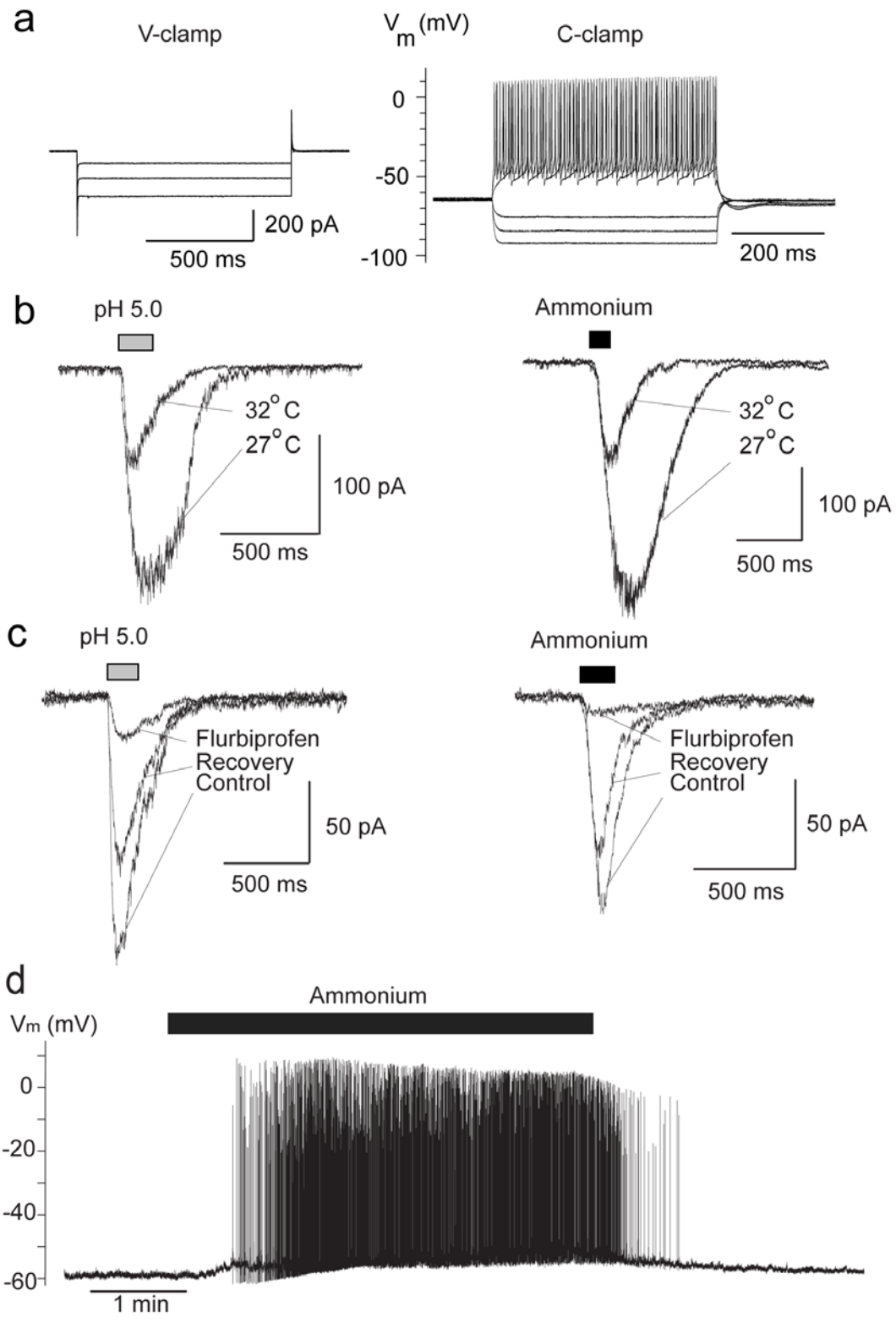
a
V-clamp
V_m (mV)
C-clamp
0
-50
-100
200 pA
500 ms
200 ms
b
pH 5.0
Ammonium
32° C
27° C
100 pA
500 ms
c
pH 5.0
Ammonium
Flurbiprofen
Recovery
Control
50 pA
500 ms
d
Ammonium
Vm (mV)
0
-20
-40
-60
1 min

Next, we examined if principal neurons in the BLA also carry ASIC1a channels. Pressure application of either acidified ACSF of pH 5.0 (n = 27), or ACSF containing 40 mM ammonium (n = 24) induced inward currents in principal cells, which were enhanced when the temperature of the bathing solution was reduced from 32^{o} to 27^{o}C (Fig. 16b), and were reversibly blocked by flurbiprofen (Fig. 16c). In the current clamp mode, bath application of ammonium (5 mM) induced repetitive bursts of action potentials (n = 5, Fig. 16d). Thus, BLA principal neurons also express functional ASIC1a channels.

Figure 16**.** ASIC1a channels are present on BLA principal neurons. (a) Currents recorded from principal neurons in response to hyperpolarizing voltage steps in voltage-clamp (v-clamp) mode (left; notice the presence of I_h), and an example of accommodating firing in response to current injection in the current-clamp (c-clamp) mode (right). (b) Pressure application (200 ms) of acidified solution (left), or 40 mM ammonium (right) induced inward currents in principal cells, which were increased by lowering the bath temperature. (c) Currents evoked in principal cells by acidified solution or 40 mM ammonium were blocked by 2 mM flurbiprofen. (d) In the current clamp mode, bath application of 5 mM ammonium induced bursts of action potentials. In (b) and (c), holding potential is -70 mV. In (b), (c), and (d), recordings are in the presence of CNQX (10 μM), D-AP5 (50 μM), bicuculline (20 μM), and SCH50911 (10 μM).

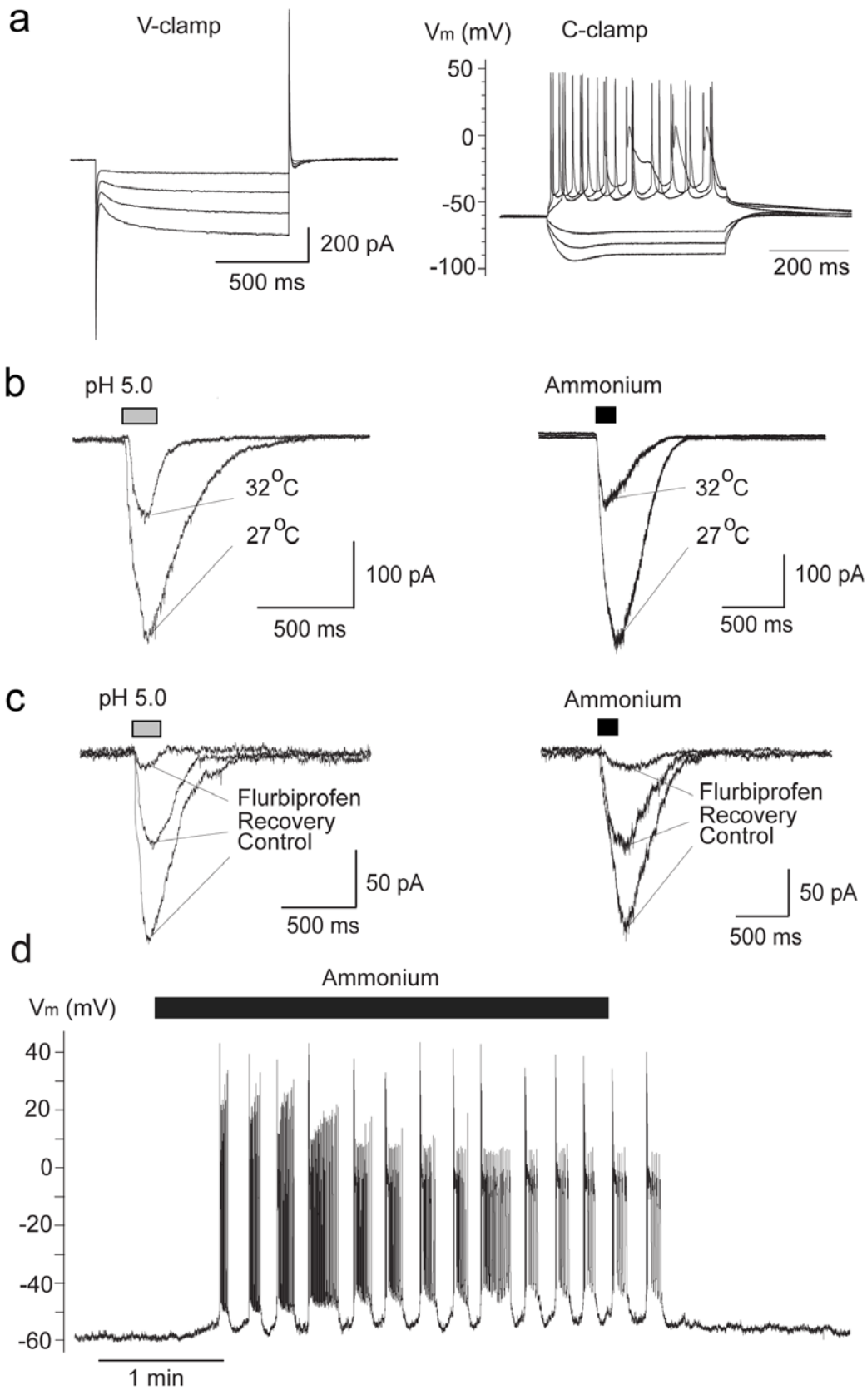
a
V-clamp
200 pA
500 ms
Vm (mV)
C-clamp
50
0
-50
-100
200 ms
b
pH 5.0
32°C
27°C
100 pA
500 ms
Ammonium
32°C
27°C
100 pA
500 ms
c
pH 5.0
Flurbiprofen
Recovery
Control
50 pA
500 ms
Ammonium
Flurbiprofen
Recovery
Control
50 pA
500 ms
d
Ammonium
Vm (mV)
40
20
0
-20
-40
-60
1 min

The effects of ASIC1a activation or blockade on spontaneous inhibitory activity

The presence of ASIC1a on interneurons - presumed to be GABAergic - predicts that activation of these channels will increase GABAergic activity in the BLA network. Indeed, bath application of 5 mM ammonium, in the presence of CNQX (10 μM), D-AP-5 (50 μM), and SCH50911 (10 μM), increased the frequency of spontaneous inhibitory postsynaptic currents (sIPSCs) recorded from principal neurons, from 25 ± 2 Hz to 36 ± 3 Hz (n = 11, $P = 0.0006$; Fig. 17a,b,c). Similarly, perfusion of the slices with acidified ASCF (pH 6.6) increased the frequency of sIPSCs from 17 ± 2 Hz to 24 ± 1 Hz (n = 8, $P = 0.00008$; Fig. 17d,e,f).

Figure 17. Activation of ASIC1a increases spontaneous inhibitory activity. Recordings were obtained from BLA principal cells in the presence of CNQX (10 μM), D-AP5 (50 μM), and SCH50911 (10 μM), at V_h = +30 mV. (a) Spontaneous inhibitory postsynaptic currents (sIPSCs) before, during, and after bath application of 5 mM ammonium. (b) Amplitude-frequency histogram of sIPSCs before and after bath application of 5 mM ammonium (n =11); bin width is 5 pA. (c) Group data of the frequency of sIPSCs in control medium, in 5 mM ammonium, and after washing out of ammonium (n = 11). (d) sIPSCs before, during, and after application of acidified ACSF. (e) Amplitude-frequency histogram of sIPSCs in control medium and in pH 6.65 (n = 8); bin width is 5 pA. (f) Group data of the frequency of sIPSCs in control medium, in low pH, and after return to control medium (n = 8). ***$P < 0.001$.

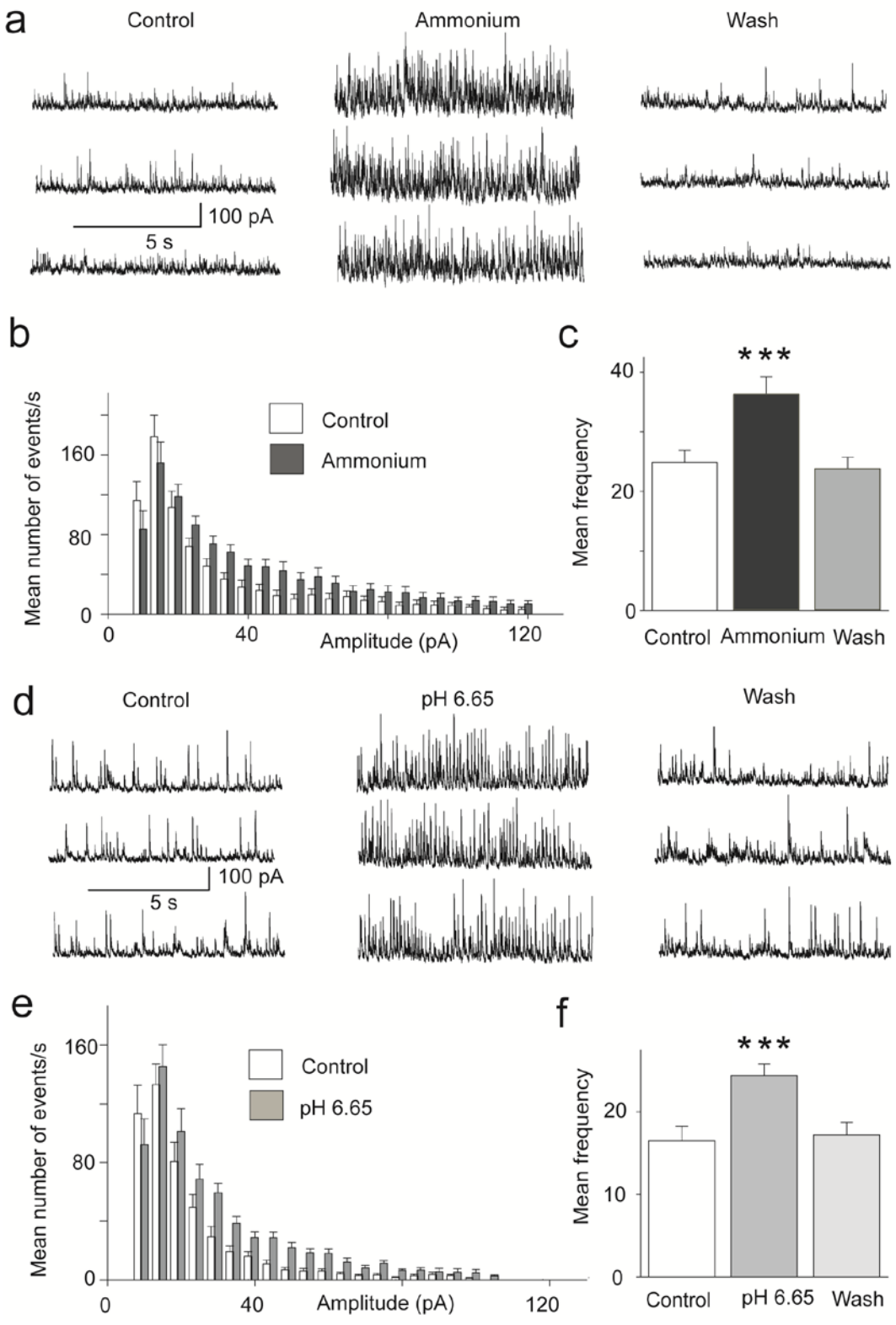
a
Control
Ammonium
Wash
100 pA
5 s
b
Mean number of events/s
Control
Ammonium
160
80
0
0
40
120
Amplitude (pA)
c
***
40
20
0
Mean frequency
Control
Ammonium
Wash
d
Control
pH 6.65
Wash
100 pA
5 s
e
Mean number of events/s
Control
pH 6.65
160
80
0
0
40
120
Amplitude (pA)
f
***
20
10
0
Mean frequency
Control
pH 6.65
Wash

Since ASIC1a activation enhances sIPSCs, we asked if these channels are also active in the basal state, contributing to the tonic level of inhibition ("background" inhibition due to spontaneous GABA release) in the BLA. To answer this question, we recorded sIPSCs from principal BLA neurons, and then applied either flurbiprofen, or the tarantula venom, psalmotoxin (PcTx1), which specifically blocks homomeric ASIC1a channels (27; 80; 85). Both compounds significantly decreased the frequency and amplitude of sIPSCs; flurbiprofen decreased the frequency of sIPSCs from 26 ± 2 Hz to 7 ± 2 Hz (n = 7, $P = 0.00001$; Fig. 18a,b,c), whereas PcTX1 decreased sIPSCs from 38 ± 2 Hz to 24 ± 3 Hz (n = 4, $P = 0.005$; Fig. 18d,e,f). To be certain that flurbiprofen or PcTX1 did not have a direct suppressive effect on GABAergic synaptic transmission, we also evoked GABA currents by pressure application of GABA on the recorded principal neurons. Neither flurbiprofen nor PcTX1 had any significant effect on the GABA-evoked currents at the time that these drugs suppressed sIPSCs (Fig. 18a,d). These data suggest that ASIC1a channels are active during basal synaptic activity and contribute significantly to the generation of sIPSCs. We should note here that we also attempted to antagonize the activity of ASIC1a with amiloride (298; 299) or nafamostat mesylate (290), but found that these compounds directly affect GABAergic transmission; currents evoked by pressure application of GABA were reduced by about 40% and 90% by amiloride and nafamostat mesylate, respectively (see Supplementary Figure 1).

Figure 18. Antagonism of ASIC1a reduces spontaneous inhibitory activity. Recordings were obtained from BLA principal cells in the presence of CNQX (10 μM), D-AP5 (50 μM), and SCH50911 (10 μM), at V_h = +30 mV. (a) sIPSCs in control medium, in the presence of bath-applied flurbiprofen (2 mM), and after a 10 min-wash. Flurbiprofen suppressed sIPSCs, with no significant effect on the amplitude of GABAA-mediated currents evoked by pressure-applied GABA (arrowheads; 400 mM GABA, 200 ms). The lower traces show, in an expanded view, the last 5 s of the upper traces. (b) Amplitude-frequency histograms for

sIPSCs in control medium and in the presence of 2 mM flurbiprofen, for the cell shown in (a) (bin size, 10 pA). (c) Group data of the frequency of sIPSCs in control medium and in the presence of 2 mM flurbiprofen (n = 7, ***P < 0.001). (d) sIPSCs before, during, and after bath-applied PcTx1 venom (1:1000 dilution of the 100 μl lyophilized, milked venom). PcTx1 suppressed sIPSCs, with no significant effect on the amplitude of GABAA-mediated currents evoked by pressure-applied GABA. The lower traces show, in an expanded view, the last 5 s of the upper traces. (e) Amplitude-frequency histograms for sIPSCs in control medium and in the presence of PcTx1, for the cell shown in (d) (bin size, 10 pA). (f) Group data of the frequency of sIPSCs in control medium and in the presence of PcTx1 (n = 4, **P < 0.01).

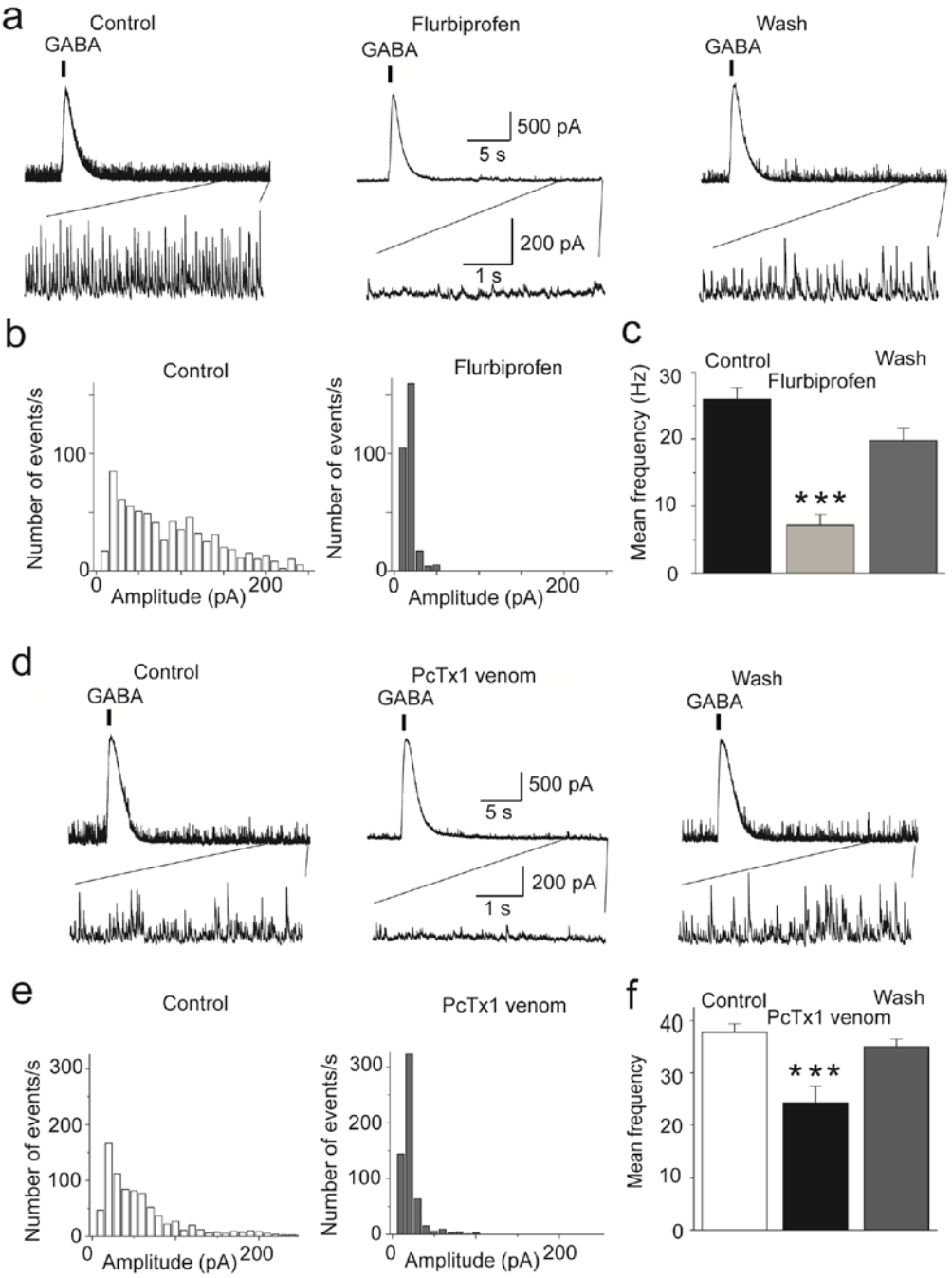
a
Control
GABA
Flurbiprofen
GABA
500 pA
5 s
200 pA
1 s
Wash
GABA
b
Control
Number of events/s
100
0
0
Amplitude (pA)
200
Flurbiprofen
Number of events/s
100
0
0
Amplitude (pA)
200
c
Control
Flurbiprofen
Wash
Mean frequency (Hz)
30
20
10
0
***
d
Control
GABA
PcTx1 venom
GABA
500 pA
5 s
200 pA
1 s
Wash
GABA
e
Control
Number of events/s
300
200
100
0
0
Amplitude (pA)
200
PcTx1 venom
Number of events/s
300
200
100
0
0
Amplitude (pA)
200
f
Control
PcTx1 venom
Wash
Mean frequency
40
30
20
10
0
***

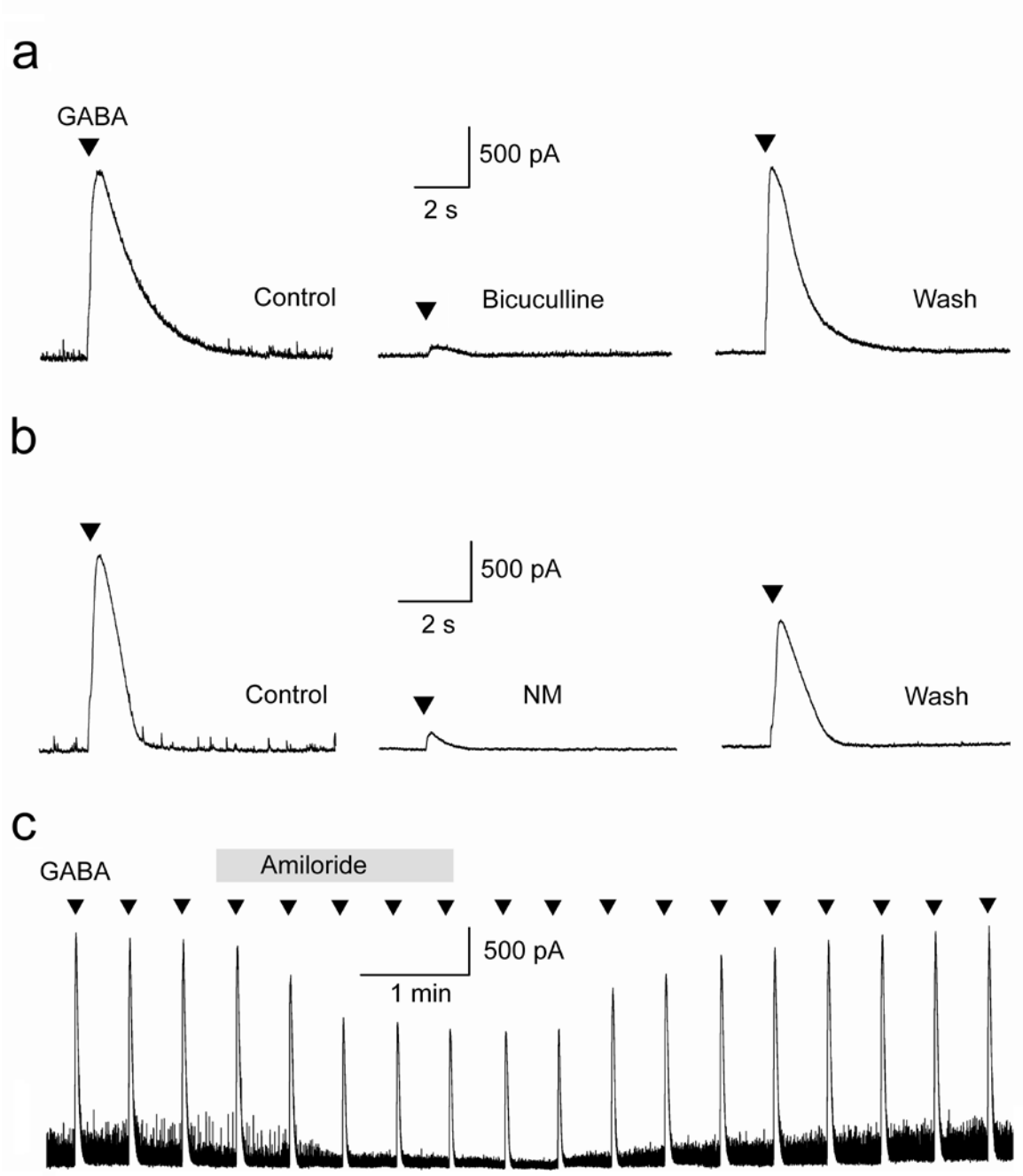

Supplementary Figure 1: The non-specific ASIC1a antagonists Nafamostat mesylate (NM) and amiloride reduce $GABA_A$ receptor-mediated currents. The recordings shown are from principal BLA neurons in the presence of 10 μM CNQX, 50 μM D-AP5, and 10 μM SCH50911 (V_h = +30 mV). (a) Currents evoked by pressure-applied GABA (400 mM, 200 ms) were blocked by bicuculline (40 μM). (b) NM (200 μM) nearly blocked GABA-evoked currents. (c) Amiloride also reduced the GABAA receptor-mediated currents.

ASIC1a activation increases glutamatergic excitation of interneurons

Considering that in addition to GABAergic cells, principal BLA neurons also have functional ASIC1a channels, we examined if under acidic conditions, interneurons are not depolarized only directly by activation of ASIC1a, but also due to glutamatergic excitation secondarily to ASIC1a-mediated depolarization of principal cells. When we recorded spontaneous excitatory postsynaptic currents (sEPSCs) from BLA interneurons, application of acidified solution increased the frequency of sEPSCs from 19 ± 3 Hz to 25 ± 3 Hz (n = 4, P = 0.01023, Fig. 19a). When we recorded currents evoked by pressure application of acidified solution in the absence of CNQX, sEPSCs were present, overlapping with the evoked currents (n = 3, Fig. 19b). The frequency of sEPSCs recorded from interneurons was also increased by pressure application of ammonium (n = 4, Fig. 19c). To determine if in the basal state, ASIC1a activity on principal cells contributes to glutamatergic excitation of interneurons, we recorded sEPSCs from interneurons, and then applied flurbiprofen; the frequency of sEPSCs was reduced by flurbiprofen from 20 ± 3 Hz to 5 ± 1 Hz (n = 4, P = 0.00528, Fig. 19d). Thus, activation of ASIC1a channels depolarizes interneurons not only directly, but also indirectly due to glutamate release from principal cells, and this mechanism is in effect also in the basal state.

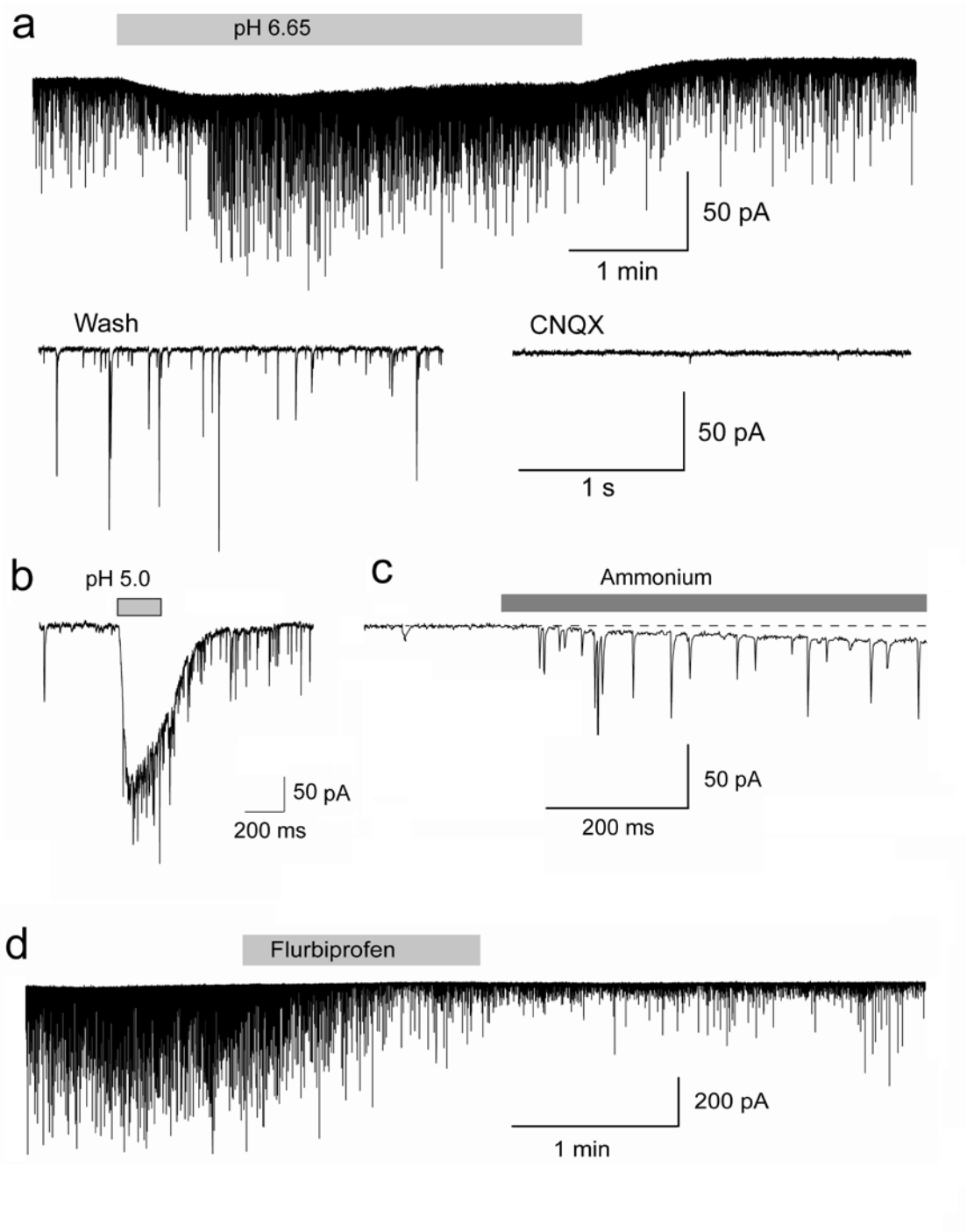

Figure 19. Activation of ASIC1a increases the excitatory drive of interneurons. Recordings are from interneurons at V_h -58 mV and in the presence of D-AP5 (50 μM) and SCH50911 (10 μM). (a) Lowering the pH of the bath increased the frequency of sEPSCs. The lower current traces in (a) are from the same cell as in the upper trace, at an expanded view. CNQX (10 μM) blocked the recorded currents. (b) Currents evoked by pressure application (arrowhead, 200 ms) of acidified ACSF in the absence of CNQX, displayed "riding" EPSCs. (c)

Pressure application of ammonium (40 mM, 500 ms) increased the frequency of sEPSCs. (d) Bath application of flurbiprofen (1 mM) decreased the frequency of sEPSCs.

The net effect of ASIC1a activation on BLA excitability

The results described above demonstrate that activation of ASIC1a increases inhibitory activity in the BLA due to direct and indirect (via synaptic glutamatergic excitation) depolarization of interneurons. However, ASIC1a activation can be expected to also increase excitatory activity, since principal neurons also carry these channels. The question, therefore, arises as to what would be the net effect of ASIC1a activation on the overall level of activity and excitability of the BLA. To answer this question, first we examined the effect of ASIC1a activation on sIPSCs and sEPSCs recorded simultaneously from principal cells. To quantify these effects we calculated the total charge transferred. The charge, in pico Coulombs, was calculated as the area delimited by the inhibitory or excitatory current and the baseline. Current areas were analyzed for a time window of 5s. Bath application of ammonium (5mM) increased the charge transferred by sIPSCs from 1.4 ± 0.2 pC to 38 ± 4 pC (n = 21, P = 0.0000008), while at the same time the charge transferred by sEPSCs increased from 1.3 ± 0.1 pC to 9 ± 1 pC (n = 21, P = 0.000003, Fig. 20a). The ammonium-induced increase of the charge transferred by sIPSCs (5000 ± 1000 %) was significantly greater than that of the sEPSCs (900 ± 200 %; P = 0.01318). Similar effects were observed during bath application of ACSF of pH 6.6. The acidified solution increased the charge transferred by sIPSCs from 2.1 ± 0.6 pC to 19 ± 3 pC (n = 9, P = 0.0005), while at the same time the charge transferred by sEPSCs increased from 2.0 ± 0.5 pC to 4.8 ± 0.6 pC (n = 9, P = 0.00003, Fig. 20b). Again, the difference between the increase of sIPSCs (1400 ± 400 %) and the

increase of sEPSCs (290 ± 30 %) was statistically significant (P = 0.00544). Thus, ASIC1a activation increases both GABAergic and glutamatergic spontaneous activity, but the increase of GABAergic activity is significantly greater than the increase of glutamatergic activity.

Next, we examined the effects of ASIC1a activation on BLA field potentials evoked by stimulation of the external capsule. The field potentials evoked in the BLA are not pure field EPSPs; they also contain population spiking activity and are under strong GABAergic inhibition. For this reason, any manipulation that increases inhibitory activity reduces the amplitude of the evoked field potential. Bath application of ammonium (8 mM) reduced the amplitude of the field potentials to 76.4 ± 4 % of the control values (from 0.46 ± 0.02 mV to 0.36 ± 0.01 mV, n = 4, *P = 0.008*; not shown). The reduction of the field potentials by ammonium suggested that ASIC1a activation suppresses excitability in the BLA network. To obtain more clear evidence of such an effect, we first induced epileptiform activity by increasing the concentration of K^+ in the ACSF to 7 mM and removing Mg^{++}, and then applied ammonium. Bath application of 8 mM ammonium reduced the evoked field potentials and eliminated the spontaneous epileptiform discharges (n = 5, Fig. 20c). The same concentration of ammonium had no significant effect on spontaneous epileptiform activity when flurbiprofen (2 mM) was present in the slice medium (n = 4; not shown), which is consistent with the involvement of ASIC1a channels in the suppressive effect of ammonium.

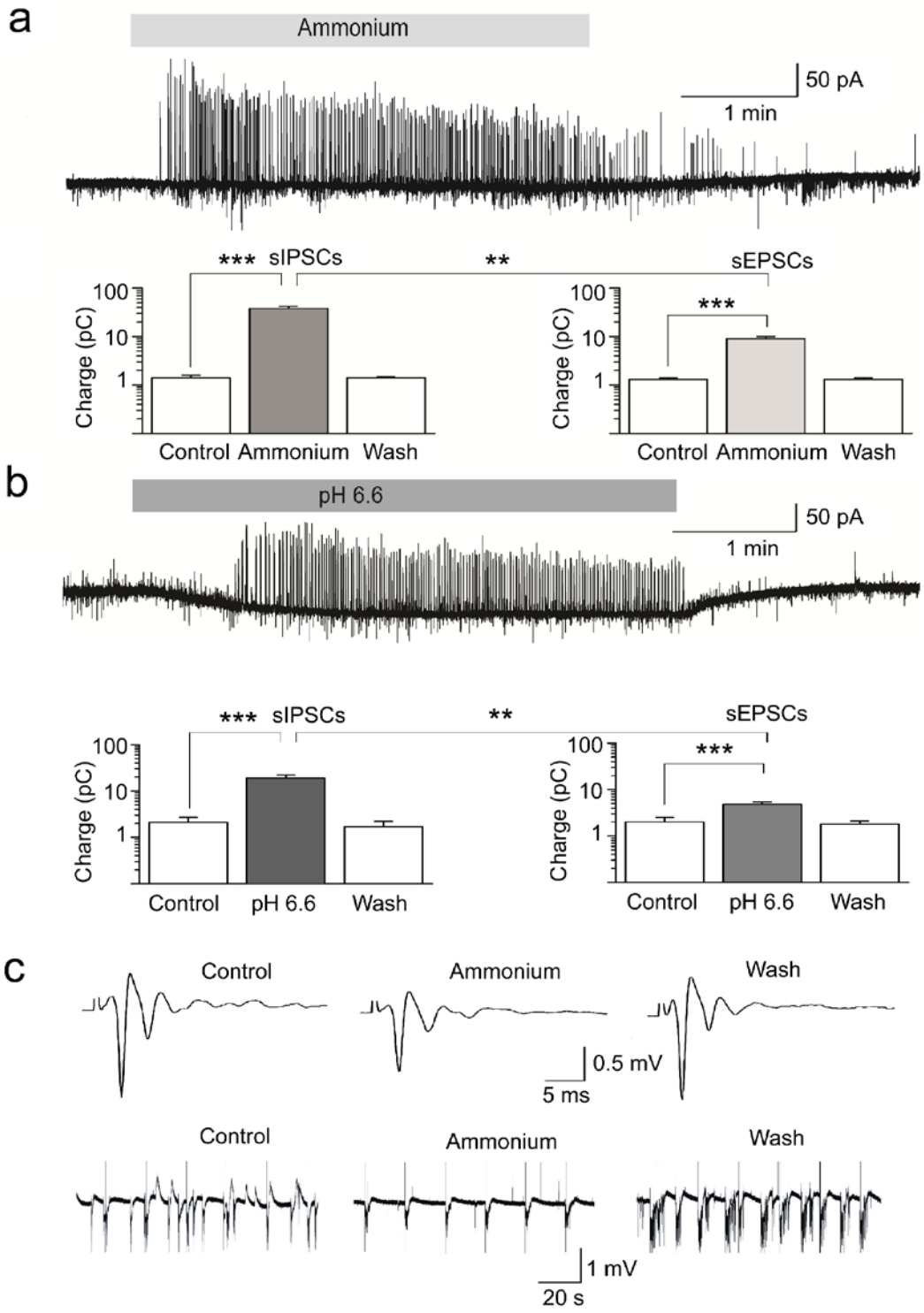

Figure 20. The net effect of ASIC1a activation is suppression of BLA excitability. (a) and (b) Simultaneous recordings of sIPSCs (outward currents) and sEPSCs (inward currents) were obtained from principal cells at V_h -58 mV, and in the presence of D-AP5 (50 μM) and SCH50911 (10 μM). Bath application of 5 mM

ammonium (a), or acidified solution (b) increased the charge transferred by sIPSCs and sEPSCs; the increase in the charge transferred by sIPSCs was significantly greater than the increase in charge transferred by sEPSCs. Example traces are shown in the upper panels of (a) and (b), and group data are shown in the bar graphs; n = 21 in (a) and n = 9 in (b), ***$P < 0.001$. (c) Upper panel shows field potentials evoked in the BLA by single-pulse stimulation of the external capsule, and lower panel shows spontaneous field activity recorded in gap-free mode. Recordings are in medium containing 7 mM K+ and zero Mg++, which induced epileptiform activity. Bath application of 8 mM ammonium reduced the evoked field potentials and blocked epileptiform activity. Each of the three field potentials shown in the upper panel is an average of 10 sweeps; the stimulus artifacts have been truncated for clarity. The equidistant vertical lines in the traces of spontaneous activity are stimulus artifacts, as evoked field potentials were sampled during gap-free recordings, by stimulation applied every 20 sec.

The net effect of ASIC1a blockade on BLA excitability

To determine whether the activity of ASIC1a channels favors enhancement of GABAergic inhibition over that of glutamatergic excitation also in the basal state, we examined the effect of ASIC1a blockade by flurbiprofen on sIPSCs and sEPSCs recorded simultaneously from principal cells (Fig. 21a). Flurbiprofen decreased the frequency of sIPSCs from 15 ± 1 Hz to 5 ± 1 Hz (n = 9, $P = 0.000004$), and the frequency of sEPSCs from 16 ± 1 Hz to 11 ± 1 Hz (n = 9, $P = 0.0002$). The reduction in the frequency of sIPSCs (70 ± 4 %) was significantly greater than the reduction in the frequency of sEPSCs (30 ± 4 %; $P = 0.000002$). We also tested the effects of flurbiprofen on evoked field potentials, in normal ACSF. Bath application of 2 mM flurbirpofen increased the amplitude of the field potentials from 0.61 ± 0.09 mV to 1.05 ± 0.19 mV (n = 5, $P = 0.020$, Fig. 21b). These results suggest that in the basal state the activity of ASIC1a in the BLA favors enhancement of inhibition over excitation.

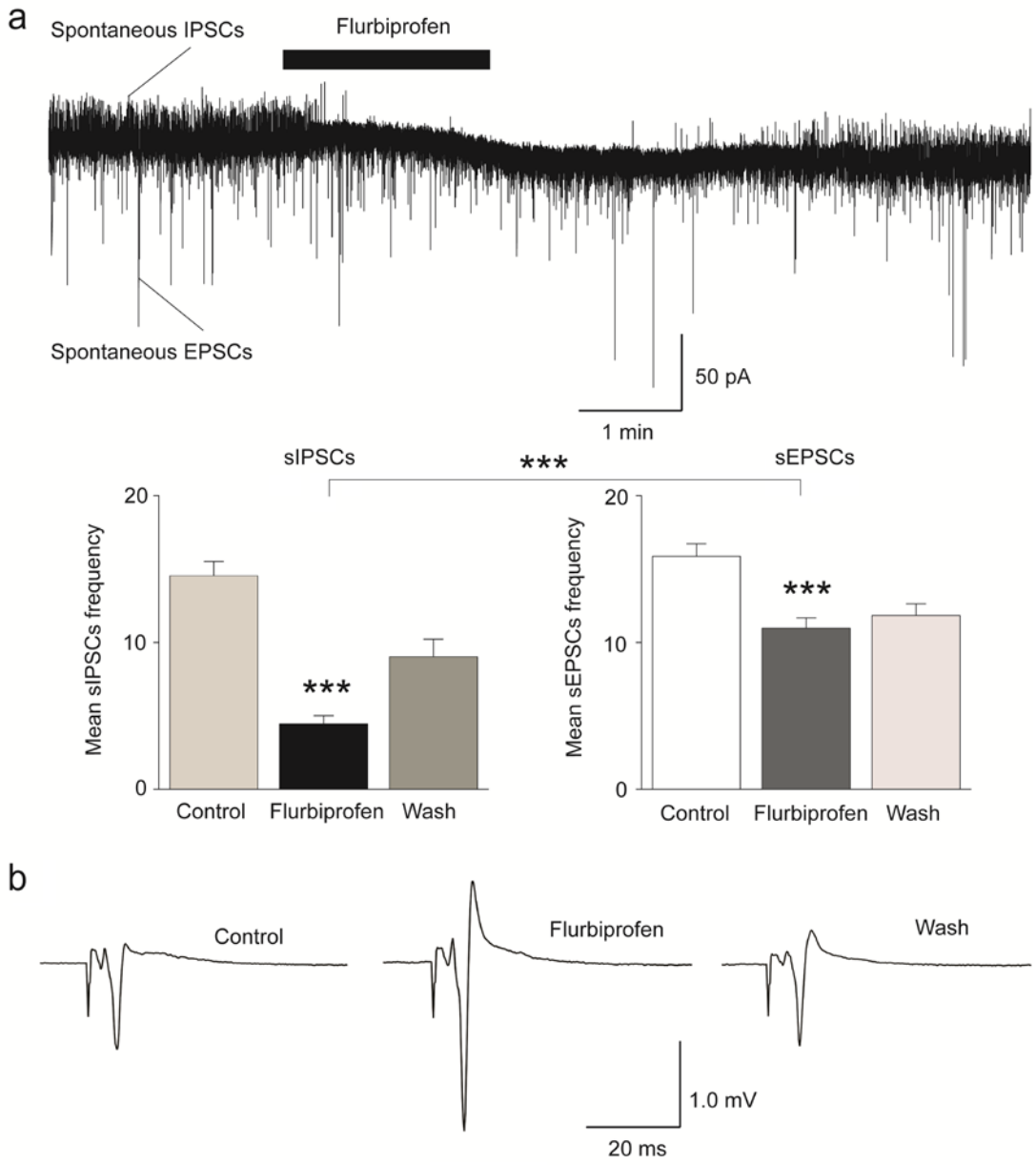

Figure 21. The net effect of ASIC1a antagonism is reduction of inhibition and increased excitability. (a) Simultaneous recordings of sIPSCs (outward currents) and sEPSCs (inward currents) were obtained from principal cells at V_h -58 mV, and in the presence of D-AP5 (50 μM) and SCH50911 (10 μM). Bath application of 2 mM flurbiprofen decreased the frequency of sIPSCs to a greater extent than that of sEPSCs. An example is shown in the upper panel, and group data in the bar graphs (n = 9, ***$P < 0.001$). (b) Field potentials evoked in the BLA by stimulation of the external capsule. Bath application of 2 mM flurbiprofen reversibly increased the amplitude of the evoked responses. Each trace is an average of 10 sweeps.

Effects of ASIC1a activation or blockade on anxiety-like behavior

Since the net role of ASIC1a in the BLA is primarily to enhance inhibition, activation of these channels could have an anxiolytic effect. One test of anxiety-like behavior in rodents is the open-field, where the more anxious the animal is, the less time it spends in the center of the field. Microinjection of ammonium (12 mMoles) bilaterally into the BLA significantly increased the time the rats spent in the center of the open field, from 9.7 ± 2.1 % of the total movement time (after vehicle microinjection) to 17.3 ± 2.6 % of the total movement time (P = 0.009, n = 8, Fig. 22a, left graph). We also examined the effect of blockade of ASIC1a on anxiety. The effects of the synthetic psalmotoxin (400 nMoles; n = 5) and the tarantula venom psalmotoxin (1 μl from a 1/1000 dilution of the 100 μl lyophilized milked venom; n = 4) were similar, therefore the results were combined. Psalmotoxin significantly reduced the time the rats spent in the center of the open field from 12.8 ± 1.6 % of the total movement time (after vehicle microinjection) to 6.8 ± 1.0 % of the total movement time (P = 0.013, n = 9, Fig. 22a, right graph). The distance the rats traveled in the open field was not significantly affected by activation or blockade of ASIC1a.

Another behavioral test that can assess the level of anxiety is the light/dark box. In this test, the less anxious the animal is, the longer the latency to enter the dark compartment and the longer the time it spends in the light compartment. Rats that received microinjection of ammonium (12 mMoles) bilaterally into the BLA displayed a longer latency (104.0 ± 22.0 s, n = 7) to enter the dark compartment – after placed in the light compartment – compared to rats that received the vehicle (35.8 ± 11.0 s; n = 6; P = 0.012; Fig. 22b, left graph). In addition, the time spent in the light compartment was

significantly longer in rats administered ammonium (138.4 ± 12.5 s) compared to vehicle-microinjected rats (48.2 ± 8.8 s; $P = 0.00013$; Fig. 22b, right graph).

Figure 22. In vivo activation of ASIC1a in the BLA suppresses anxiety-like behavior, while antagonism of ASIC1a increases anxiety. (a) In the open field test, the rats spent significantly more time in the center, after microinjection of ammonium bilaterally into the BLA (left graph), and significantly less time in the center, after microinjection of psalmotoxin into the BLA (right graph), compared to the time they spent in the center of the open field when injected with the vehicle. (b) In the light-dark box test, rats microinjected with ammonium bilaterally into the BLA took a significantly longer time to enter the dark compartment, and spent more total time in the light compartment compared to rats injected with the vehicle. *$P < 0.05$.

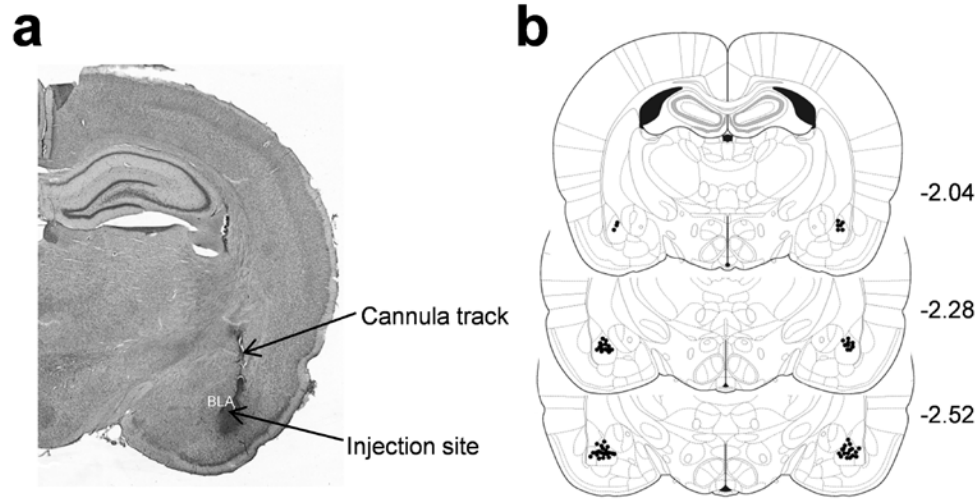

Open Field

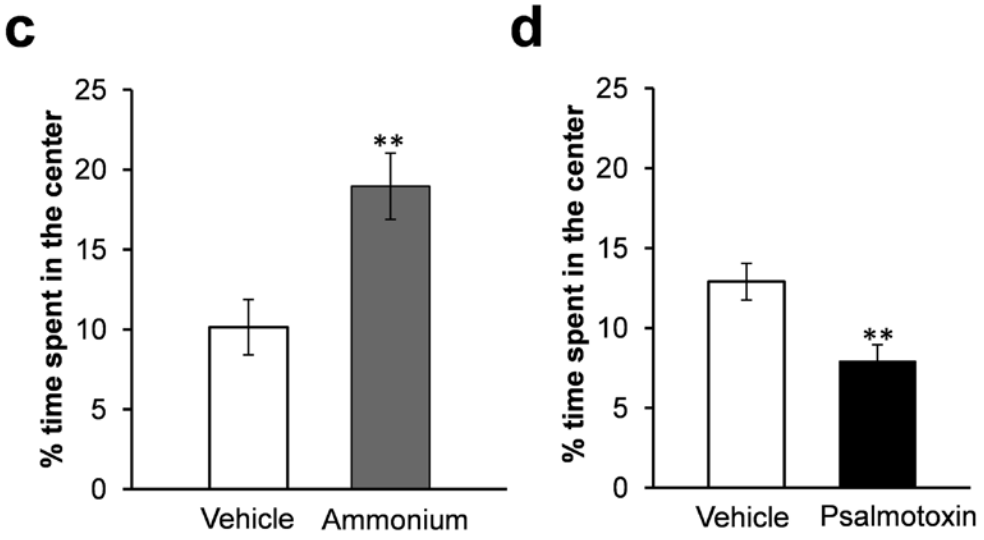

Light-Dark Box

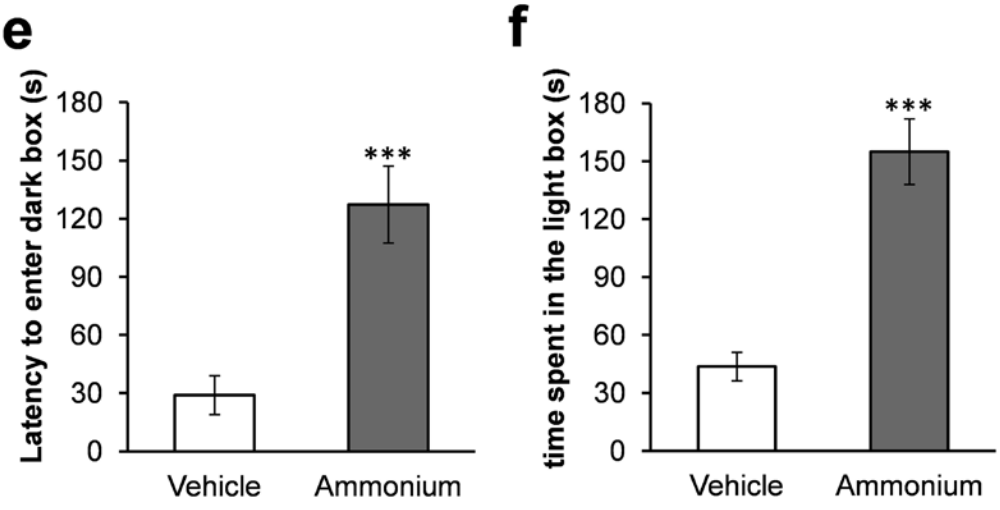

DISCUSSION

In the present study, we demonstrated that in the rat BLA, ASIC1a channels are present on both interneurons and principal cells, and their activation by ammonium, or by lowering extracellular pH, induces intense firing. When these channels are activated throughout the BLA network, spontaneous GABAergic inhibitory activity is increased significantly more than glutamatergic activity. Consistent with this finding, ammonium blocked epileptiform discharges *in vitro*, and reduced anxiety-like behavior when microinjected bilaterally into the BLA *in vivo*. Furthermore, ASIC1a channels are active in the basal state, enhancing background GABAergic inhibition, not only by direct depolarization of interneurons, but also by indirect excitation of interneurons secondary to ASIC1a-mediated depolarization of principal cells. Accordingly, *in vivo* blockade of ASIC1a in the BLA increased anxiety.

The BLA displays a markedly high expression of the ASIC1a subunit (73; 304), but it also expresses the ASIC2a and ASIC2b subunits (34; 160). It is unknown if the functional ASIC1a channels in the BLA are homomeric ASIC1a trimers, or if they co-assemble with the ASIC2a or 2b. From the two mechanisms that we employed to activate these channels, the low pH can activate any type of ASIC, while ammonium specifically activates ASIC1a currents as demonstrated in isolated sensory neurons (220), as well as in central dopaminergic neurons, hippocampal interneurons, and HEK 293 cells (223). The effects we observed when ASICs were activated by either low pH or ammonium application were blocked by flurbiprofen. In addition, both flurbiprofen and PcTX1 significantly reduced the frequency of sIPSCs in the BLA (Fig. 22). Flurbiprofen has been shown to inhibit PcTX1-sensitive currents (298), and PcTX1 specifically blocks

currents mediated by homomeric ASIC1a (27; 85). Thus, at least a portion of the ASIC1a channels in the BLA are probably homomeric trimers.

If we consider that ASIC1a channels are present on both interneurons and principal neurons, and their activation strongly depolarizes both types of neurons (Figs. 15 and 16), but also that interneurons constitute only a small percentage of the total neuronal population in the BLA (175; 241), then we have to ask why the predominant effect of ASIC1a activation in the BLA network is an increase of GABAergic inhibition rather than glutamatergic excitation. A possible explanation lies on the evidence that much of the excitatory input within the BLA circuitry is directed onto interneurons, while most of the inhibitory input is directed onto principal cells (154; 209; 226; 268). Our observations are in accordance with these findings, as only a small percentage of the interneurons we have recorded from have sIPSCs, while all of them display high activity of single sEPSCs and, occasionally, bursts of sEPSCs. An additional factor that can make BLA interneurons more excitable is that the $GABA_A$ receptor-mediated IPSPs recorded from them reverse at more depolarized potentials than the $GABA_A$ IPSPs of projection cells (170). Finally, the electrical coupling between BLA interneurons (191; 309) can enhance inhibitory strength in the BLA network. As a result, when both interneurons and principal cells are depolarized by ASIC1a activation, the inhibition of principal cells is stronger than their excitation, probably because principal cells receive strong inhibitory inputs, which are further reinforced due to concomitant strong excitation of interneurons (see Fig. 19).

Both the electrophysiological and the behavioral results suggested that the ASIC1a channels in the BLA are active in the basal state, preferentially increasing

background inhibition. Thus, flurbiprofen or PcTX1 reversibly decreased the frequency and amplitude of isolated sIPSCs (Fig. 22), and when sIPSCs and sEPSCs were recorded simultaneously, flurbiprofen preferentially reduced the sIPSCs (Fig. 21a). In addition, flurbiprofen reduced the basal excitatory drive of interneurons (Fig. 19d). These results are consistent with the increase of the evoked population response in the BLA by bath application of flurbiprofen (Fig. 21b; increased population spiking due to reduced inhibition), as well as with the increase in anxiety-like behavior in the open field, when psalmotoxin was injected bilaterally in the BLA (Fig. 22a). How can ASIC1a channels be active in the basal state? Extracellular pH can fluctuate during normal synaptic activity, and the nature of these fluctuations (alkalinization or acidification, and their time course relative to the intensity of synaptic activity) may differ in different brain regions (64; 313). The present data suggest that, in the BLA, pH shifts during spontaneous synaptic activity, maintain a sufficient number of ASIC1a channels open to have a significant effect on spontaneous inhibitory activity.

Previous studies have shown the involvement of ASIC1a activation in the suppression of seizures in vivo, and the blockade of epileptiform activity in hippocampal slices (321). A similar role of these channels was demonstrated in BLA slices, in the present study, where bath application of ammonium suppressed epileptiform activity. In agreement with the role of ASIC1a in suppressing excitatory activity in the BLA, we found increased anxiety-like behavior when these channels were blocked, and suppression of anxiety when they were activated. These results are in sharp contrast to previous studies which have indicated that activation of ASIC1a is necessary for the generation and expression of certain types of fear (320), and genetic elimination or

blockade of these channels have anxiolytic effects (73; 82). Species difference (mice versus rats) in the function of ASIC1a in the BLA is possible. Such species difference exists for the function of the GluK1 receptors in the BLA, the blockade of which is anxiogenic in mice (311), but anxiolytic in rats (17). It should also be considered that the strength and the temporal pattern of ASIC1a activation could play a determinant role in the effect it will have on the network excitability – and may have played a role in the discrepant results –, as strong or slow acidification can lead to fast desensitization of ASIC1a (38; 103), which can give way to other mechanisms that may produce hyperexcitability.

The present study clearly demonstrated that in the rat amygdala the primary function of ASIC1a channels is to increase inhibition, and, as a result, activation of these channels has an anxiolytic effect. It is apparent, however, that we are still at the early stages of understanding the roles that ASICa plays in the excitability of different brain regions, what parameters affect these roles, and if there are species differences. Delineating the functions of these channels can potentially have profound implications for the treatment of several neurological and mental illnesses.

APPENDIX 3: THE LIMITATIONS OF DIAZEPAM AS A TREATMENT FOR NERVE AGENT-INDUCED SEIZURES AND NEUROPATHOLOGY IN RATS; COMPARISON WITH UBP302

James P. Apland, Vassiliki Aroniadou-Anderjaska, Taiza H. Figueiredo, Franco Rossetti,

Steven L. Miller, Maria F.M. Braga*

Neurotoxicology Branch, U.S. Army Medical Research Institute of Chemical Defense,

Aberdeen Proving Ground, Maryland, 21010 (J.P.A.); Department of Anatomy,

Physiology, and Genetics (V.A-A., T.H.F., F.R., S.L.M., M.F.M.B.) and Department of

Psychiatry (V.A-A., M.F.M.B.), F. Edward Hébert School of Medicine, Uniformed

Services University of the Health Sciences, Bethesda, Maryland, 20814

*__Corresponding Author:__
Maria F.M. Braga, D.D.S., Ph.D.,
Department of Anatomy, Physiology, and Genetics,
F. Edward Hébert School of Medicine,
Uniformed Services University of the Health Sciences,
4301 Jones Bridge Road, Bethesda, MD 20814
Phone: (301) 295-3524
Fax: (301) 295-3566
Email: maria.braga@usuhs.edu

Abstract

Exposure to nerve agents induces prolonged status epilepticus (SE), causing brain damage or death. Diazepam (DZP) is the presently FDA-approved drug for the cessation of nerve agent-induced SE. Here, we compared the efficacy of DZP with that of UBP302–an antagonist of the kainate receptors that contain the GluK1 subunit–against seizures, neuropathology, and behavioral deficits induced by soman, in rats. DZP, administered 1 h or 2 h post-exposure, terminated the SE, but seizures returned; thus, the total duration of SE within 24 h after soman exposure was similar to (DZP at 1 h) or longer than (DZP at 2 h) that in the soman-exposed rats that did not receive anticonvulsant. Compared to DZP, UBP302 stopped SE with a slower time-course, but reduced dramatically the total duration of SE within 24 h. Neuropathology and behavior were assessed in the groups that received anticonvulsant treatment 1 h after exposure. UBP302, but not DZP, reduced neuronal degeneration in a number of brain regions, as well as neuronal loss in the basolateral amygdala and the CA1 hippocampal area, and prevented interneuronal loss in the basolateral amygdala. Anxiety-like behavior, assessed in the open field and by the acoustic startle response, 30 days after soman exposure, was increased in the group that did not receive anticonvulsant treatment and in the DZP-treated group, but not in the UBP302-treated group. The results argue against the use of DZP for the treatment of nerve agent-induced seizures and brain damage, and suggest that targeting GluK1-containing receptors is a more effective approach.

Introduction

The devastating effects of the sarin attack against civilians in Syria that the world witnessed in August of 2013 (81) brought again to the forefront the question of readiness and whether the existing medical countermeasures can save lives and protect against the long-term health consequences of exposure. The primary action of nerve agents is the inhibition of acetylcholinesterase (AChE). Without medical intervention, the ensuing cholinergic crisis can culminate in the collapse of the cardiorespiratory system and death (24). In addition to the peripheral effects, AChE inhibition in the brain produces convulsive seizures and status epilepticus (SE), initiated by the excessive stimulation of cholinergic receptors. If immediate death is prevented by adequate control of the peripheral symptoms, but SE is not controlled effectively, lives may still be lost from the prolonged SE, or severe brain damage can ensue with long-term behavioral consequences. The lasting behavioral deficits that follow nerve agent exposure are well-known from experimental studies in animals (74; 90; 155; 228), but also from studies in the victims of the sarin attacks in Japan, who present neurological and neuropsychiatric disturbances years after the exposure (118; 204; 315).

As the initiation of seizures after nerve agent exposure is due to excessive elevation of acetylcholine, acting primarily on muscarinic receptors, administration of muscarinic receptor antagonists can halt the development of SE, but only when administered within a short period of time after exposure (153; 261; 266), suggesting that seizures are sustained and reinforced by glutamatergic rather than cholinergic mechanisms (181). One way to suppress glutamatergic hyperactivity is by enhancing GABAergic inhibition. Benzodiazepines, which are positive allosteric modulators of $GABA_A$ receptors (48; 96), have long been the first line of treatment for the cessation of

SE triggered by various etiologies (266). Accordingly, the benzodiazepine diazepam (DZP) is also currently the only FDA-approved injectable drug for the control of seizures caused by nerve agents.

A number of concerns, however, are associated with the use of DZP for the cessation of nerve agent-induced SE. First, the efficacy of DZP decreases as the interval between the initiation of SE and the administration of DZP increases (183; 261; 288); this has also been documented in the lithium-pilocarpine model of SE (102; 130; 301), which has many similarities to the nerve agent-induced SE, in both the mechanisms of seizure initiation and the effects it produces (284). The development of resistance to DZP is concerning because in a terrorist attack with nerve agents, it may not be possible for medical assistance to arrive immediately; thus, when DZP is administered, the seizures may have already become resistant to benzodiazepines. Second, benzodiazepines are among the anticonvulsants with the most serious side effects (136; 185). Third, seizures often recur after termination of the initial SE by benzodiazepines (174; 264), and at least in the case of nerve agent-induced SE, it is unclear whether DZP compares favorably with other anticonvulsant treatments in the duration of its anti-seizure effects. This is particularly significant considering that the duration and intensity of seizures clearly correlate with the severity of the resulting neuropathology (227; 258).

We recently demonstrated that nerve agent-induced seizures can be effectively controlled by targeting the glutamatergic system. LY293558, which is an antagonist of both the AMPA receptors and the kainate receptor subtype that contains the GluK1 subunit (GluK1Rs; formerly known as GluR5 kainate receptors or GLU_{K5} receptors; see (66; 124)) was very efficacious in stopping seizures induced by the nerve agent soman

and protecting against neuronal damage (12; 89). In the present study, we used a rat model of nerve agent exposure in which the anticonvulsant treatment was delayed to at least 1 h, and compared the efficacy of DZP to that of another GluK1R antagonist, (S)-3-(2-carboxybenzyl)willardiine (UBP302), which antagonizes selectively the GluK1Rs (190), against soman-induced seizures, as well as acute and long-term neuropathology. We also examined the efficacy of DZP and UBP302 in preventing the development of anxiety, which is a prevalent behavioral deficit resulting from nerve agent-induced brain damage, in both animals (74; 155; 228) and humans (118; 204).

Materials and Methods

Animals

Male, Sprague-Dawley rats (Charles River Laboratories, Wilmington, MA), weighing 150-250 g (6 to 8-weeks-old) at the start of the experiments, were individually housed in an environmentally controlled room (20–23°C, 12-h light/12-h dark cycle, lights on 06:00 am), with food and water available *ad libitum*. The animal care and use programs at the U.S. Army Medical Research Institute of Chemical Defense (USAMRICD) and the Uniformed Services University of the Health Sciences (USUHS) are accredited by the Association for Assessment and Accreditation of Laboratory Animal Care International. All animal experiments were conducted following the Guide for the Care and Use of Laboratory Animals by the Institute of Laboratory Animal Resources, National Research Council and the Animal Welfare Act of 1966 (P.L. 89-544), as amended, and were approved by the Institutional Animal Care and Use Committees of the USAMRICD and the USUHS.

Soman administration and drug treatment

Soman (pinacolyl methylphosphonofluoridate) was obtained from the U.S. Army Edgewood Chemical Biological Center (Aberdeen Proving Ground, MD). The agent was diluted in cold saline, and administered via a single subcutaneous injection (154 µg/kg, which is approximately 1.4 X LD50; (126)) to rats that were 7 to 8-weeks-old. To increase survival rate, rats were administered HI-6 (1-(2-hydroxyiminomethylpyridinium)-3-(4-carbamoylpyridinium)-2-oxapropane dichloride; 125 mg/kg, i.p.; Starks Associates, Buffalo, NY) 30 min prior to soman exposure. HI-6 is a bispyridinium oxime that reactivates inhibited acetylcholinesterase, primarily in the

periphery (24). Within 1 min after soman exposure, rats also received an intramuscular injection of atropine sulfate (2 mg/kg; Sigma- Aldrich, St. Louis, MO) to minimize peripheral toxic effects. The soman-exposed rats were randomly divided into 3 groups: Those that did not receive any further treatment (except for the oxime pretreatment and the atropine; SOMAN group), those that received DZP (10 mg/kg, i.m.) at 1 h after exposure to soman (SOMAN+DZP group), and those that received UBP302 (250 mg/kg, i.p.) at 1 h after exposure to soman (SOMAN+UBP302 group). Some of the soman-exposed rats had been implanted with electrodes for electroencephalographic (EEG) monitoring (see next section for implantation procedure), 10 days before exposure. From the implanted rats, some were administered DZP or UBP302 (doses same as above) at 1h or 2 h after soman exposure; therefore, there were two SOMAN+DZP groups and two SOMAN+UBP302 groups for the electrode-implanted rats (for the two time points of anticonvulsant treatment; sample sizes are in the results section). DZP and UBP302 were purchased from Hospira Inc. (Lake Forest, IL) and Tocris Bioscience (Bristol, UK), respectively. Control animals received HI-6 and atropine, but were injected with saline instead of soman (CONTROL group). For the SOMAN+UBP302 groups, we had to decide on a dose based only on our own observations, as there are no previous studies in which UBP302 has been injected systemically. First, we tested 100 mg/kg; this concentration suppressed seizures, but with a very slow time course (it took more than 3 h to terminate seizure activity). We concluded with 250 mg/kg, after testing this concentration also in control rats (rats not exposed to soman). Unlike DZP which produces sedative effects even at 10 mg/kg, the 250 mg/kg of UBP302 administered to control rats produced only a mild reduction in overall activity.

In the rats that were not implanted with EEG electrodes, the occurrence and the progression of seizures were monitored behaviorally and classified according to the Racine scale (232), with minor modifications: Stage 0, no behavioral response; Stage 1, behavioral arrest; Stage 2, oral/facial movements, chewing, head nodding; Stage 3, unilateral/bilateral forelimb clonus without rearing, Straub tail, extended body posture; Stage 4, bilateral forelimb clonus plus rearing; Stage 5, rearing and falling; and Stage 6, full tonic-clonic seizures.

Electrode implantation and EEG recordings

Rats (6-week-old) were anesthetized with isoflurane using a gas anesthesia system (Kent Scientific, Torrington, CT). Five stainless steel, cortical screw electrodes were stereotaxically implanted, as described previously (89), using the following coordinates (from (215)): two frontal electrodes, 2.0 mm posterior from bregma and 2.5 mm lateral from the midline, and two parietal electrodes, 5.0 mm posterior from bregma and 2.5 mm lateral from the midline; a cerebellar reference electrode was implanted 1.0 mm posterior to lambda. Each screw electrode (Plastics One Inc., Roanoke, VA) was placed in a plastic pedestal (Plastics One Inc.) and fixed to the skull with dental acrylic cement. For EEG recordings (obtained 10 days after electrode implantation), rats were placed in the EEG chamber and connected to the EEG system (Stellate, Montreal, Canada; 200 Hz sampling rate). Video-EEG recordings were performed in the freely moving rats, as described previously (89). EEG was continuously recorded for 24 hours after soman injection; during that time the animals had free access to food and water. The termination of the soman-induced SE was defined as the disappearance of large amplitude, repetitive discharges (>1 Hz with at least double the amplitude of the background activity).

Fixation & tissue processing

Neuropathological analysis was performed in the amygdala, piriform cortex, entorhinal cortex, hippocampus, and a neocortical region of rats that were not implanted with EEG electrodes (the implantation procedure might cause some damage that could interfere with the neuropathology results). One day, 7 days, and 30 days after soman administration, rats were deeply anesthetized with pentobarbital (75-100 mg/kg, i.p.) and transcardially perfused with PBS (100 ml) followed by 4% paraformaldehyde (200 ml). The brains were removed and post-fixed overnight at 4º C, then transferred to a solution of 30% sucrose in PBS for 72 hours, and frozen with dry ice before storage at -80º C until sectioning. A 1-in-5 series of sections from the rostral extent of the amygdala to the caudal extent of the entorhinal cortex was cut at 40 µm on a sliding microtome. One series of sections was mounted on slides (Superfrost Plus, Daigger, Vernon Hills, IL) in PBS for Nissl staining with cresyl violet. Two adjacent series of sections were mounted on slides for Fluoro-Jade C (FJC) staining, or were stored at -20°C in a cryoprotectant solution for GAD-67 immunohistochemistry. All neuropathological analysis was done in a blind fashion.

Fluoro-Jade C staining and analysis

FJC (Histo-Chem, Jefferson, AR) was used to identify irreversibly degenerating neurons in all the amygdalar nuclei and the piriform cortex (-2.04 mm to -3.36 mm from bregma), a neocortical area (-2.04 and -6.36 mm from bregma), the entorhinal cortex and the CA1, CA3, and hilar areas of the ventral hippocampus (-5.4 and -6.36 mm from bregma; all coordinates from (215)); we studied the ventral hippocampus because it displays significantly more severe neurodegeneration after soman exposure than the dorsal

hippocampus (14). Mounted sections were air-dried overnight and then immersed in a solution of 1% sodium hydroxide in 80% ethanol for 5 min. The slides were then rinsed for 2 min in 70% ethanol and 2 min in distilled water (dH_20), and then incubated in 0.06% potassium permanganate solution for 10 min. After a 2 min rinse in dH_20, the slides were transferred to a 0.0001% solution of FJC dissolved in 0.1% acetic acid for 10 minutes. Following three 1-minute rinses in dH_20, the slides were dried on a slide warmer, cleared in xylene for at least 1 min, and coverslipped with DPX (Sigma-Aldrich).

To assess the extent of neurodegeneration, we used a series of adjacent Nissl-stained sections to trace the regions of interest. The tracings from the Nissl-stained sections were superimposed on the FJC-stained sections, using the Stereo Investigator 9.0 (MicroBrightField, Williston, VT). The following rating system was used to score the extent of neuronal degeneration in each structure and substructures: 0 = no damage, 1 = minimal damage (1-10%), 2 = mild damage (11-25%), 3 = moderate damage (26-45%) and 4 = severe damage (>45%). We have previously shown that qualitative assessment using this scale produces results that are in agreement with quantitative assessments (Qashu et al., 2010). The scores for neurodegeneration present on FJC-stained sections were assessed considering the density of cells from Nissl-stained sections, along the anterior to posterior extent, at 600 μm intervals.

Stereological quantification

Design-based stereology was used to quantify the total number of neurons in Nissl-stained sections in the basolateral amygdala (BLA) and CA1 area. Sections were viewed with a Zeiss Axioplan 2ie (Oberkochen, Germany) fluorescent microscope with a

motorized stage, interfaced with a computer running StereoInvestigator 9.0 (MicroBrightField). The BLA and CA1 regions were identified on slide-mounted sections, and delineated for each slide of each animal, under a 2.5× objective, based on the atlas of Paxinos and Watson (215). All sampling was done under a 63× oil immersion objective. Nissl-stained neurons were distinguished from glial cells by their larger size and pale nuclei surrounded by darkly-stained cytoplasm containing Nissl bodies. The total number of Nissl-stained neurons was estimated using the optical fractionator probe, and, along with the coefficient of error (CE), was calculated using Stereo Investigator 9.0 (MicroBrightField). The CE was calculated by the software according to Gundersen (m = 1; (105)) and Schmitz-Hof (2nd estimation; (246)) equations.

For Nissl-stained neurons in the BLA, a 1-in-5 series of sections was analyzed (8 sections on average). The counting frame was 35 × 35 µm, the counting grid was 190 × 190 µm, and the dissector height was 12 µm. Nuclei were counted when the cell body came into focus within the dissector which was placed 2 µm below the section surface. Section thickness was measured at every counting site, and the average mounted section thickness was 22.3 µm. An average of 365 neurons per rat was counted, and the average CE was 0.045 for both the Gunderson and Schmitz-Hof equations. For Nissl-stained neurons in the CA1 area, a 1-in-10 series of sections was analyzed (8 sections on average). The counting frame was 20 × 20 µm, the counting grid was 250 × 250 µm, and the dissector height was 10 µm. Nuclei were counted when the cell body came into focus within the dissector which was placed 2 µm below the section surface. Section thickness was measured at every counting site, and the average mounted section thickness was 18.3 µm. An average of 253 neurons per rat was counted, and the CE was 0.065 for

Gunderson (m = 1) and 0.060 for Schmitz-Hof (2nd estimation) equation. For GABAergic interneurons immuno-labeled for GAD-67 in the BLA (see procedure below), a 1-in-10 series of sections was analyzed (on average 6 sections). The counting frame was 60 x 60 µm, the counting grid was 100 × 100 µm, and the dissector height was 20 µm. Nuclei were counted when the top of the nucleus came into focus within the dissector which was placed 2 µm below the section surface. Section thickness was measured at every 5th counting site, and the average mounted section thickness was 30 µm. An average of 260 neurons per rat was counted, and the average CE was 0.07 for the Gunderson equation and 0.065 for Schmitz-Hof equation.

GAD67 immunohistochemistry

To label GAD-67 immunoreactive neurons, a l-in-5 series of free-floating sections was collected from the cryoprotectant solution, washed three times for 5 min each in 0.1 M PBS, and then incubated in a blocking solution containing 10% normal goat serum (NGS, Chemicon International, Temecula, CA) and 0.5% Triton X-100 in PBS for one hour at room temperature. The sections were then incubated with mouse anti-GAD67 serum (1:1000, MAB5406; Chemicon), 5% NGS, 0.3% Triton X-100, and 1% bovine serum albumin, overnight at 4º C. After rinsing three times for 10 min each in 0.1% Triton X-100 in PBS, the sections were incubated with Cy3-conjugated goat anti-mouse antibody (1:1000; Jackson ImmunoResearch, West Grove, PA) and 0.0001% DAPI (Sigma-Aldrich, St. Louis, MO) in PBS for one hour at room temperature. After a final rinse in PBS for 10 min, sections were mounted on slides, air dried for at least 30 min, and coverslipped with ProLong Gold antifade reagent (Life Technologies, Grand Island, NY).

Behavioral experiments

Animals from the SOMAN, SOMAN+DZP, SOMAN+UBP302 and CONTROL groups were tested in the open field and the acoustic startle apparatus, 30 days after soman. In the open field apparatus (40X40X30 cm clear Plexiglas arena), anxiety-like behavior was assessed as described previously ((17; 228)), following the procedure used by Grunberg and collaborators (87). One day prior to testing (on day 29 after soman exposure), animals were acclimated to the apparatus for 20 min. On the test day, the rats were placed in the center of the open field, and activity was measured and recorded for 20 min, using an Accuscan Electronics infrared photocell system (Accuscan Instruments Inc., Columbus, OH). Data were automatically collected and transmitted to a computer equipped with "Fusion" software (from Accuscan Electronics). Locomotion (distance traveled in cm), total movement time, and time spent in the center of the open field were analyzed. Anxiety behavior was measured as the ratio of the time spent in the center over the total movement time, expressed as a percentage of the total movement time. Subjects were exposed to an acclimation session on day 29 post-exposure, and followed next day for a test session.

Acoustic startle response (ASR) testing was conducted with the use of the Med Associates Acoustic Response Test System (Med Associates, Georgia, VT), which consists of weight-sensitive platforms inside individual sound-attenuating chambers. A ventilating fan built into the chamber provides background noise. Each rat was individually placed in a ventilated holding cage. The holding cages are small enough to restrict extensive locomotion, but large enough to allow the subject to turn around and make other small movements. Each cage was placed on a weight-sensitive platform. Subjects' movements in response to stimuli were measured as a voltage change by a

strain gauge inside each platform. All animals were acclimated to the apparatus in two sessions on post-soman days 28 and 29. Startle stimuli consisted of 120 or 110 dB sound pressure level noise bursts of 20-ms duration. Each stimulus had a 2 ms rise and decay time, such that the onset and offset were abrupt, which is a primary requirement for startle. Each trial type (110 dB or 120 dB stimulus) was presented eight times. Trial types were presented in random order to avoid effects and habituation, and inter-trial intervals ranged randomly from 15 to 25 s. Responses were recorded by an interfaced Pentium computer as the maximum response occurring during the no-stimulus periods and during the startle period, and were assigned a value based on an arbitrary scale used by the software of the test system.

Statistical analysis

Fisher exact test was used to compare the survival rate between the groups. Initial SE duration, total SE duration, number of convulsive seizures recurring during the 24 h period after termination of the initial SE, stereological estimations of the number of neurons and interneurons, and results from behavioral tests were compared between the SOMAN, the SOMAN+DZP and the SOMAN+UBP302 groups using analysis of variance (ANOVA) followed by post-hoc tests as described in the figure legends. The statistical values are presented as mean and standard error of the mean. Neurodegeneration scores were compared between groups for each structure separately using the Kruskal-Wallis test followed by Mann-Whitney U-test for comparisons between pairs of groups. The statistical values are presented as median and the interquartile range (IQR, the difference between the 75th and the 25th percentiles). For

all tests, differences were considered significant when $P < 0.05$. Sample sizes (n) refer to the number of animals.

Results

Behavioral SE (stage 3 seizures progressing to higher stages) developed within 5 to 15 min after soman injection. Eleven out of 124 rats that were exposed to soman did not develop seizures and were not included in the study. The survival rate for the animals that were non-implanted with EEG electrodes (92 rats) was 63% (22 out of 34) for the SOMAN group, which did not receive anticonvulsant treatment, 91% (21 out of 23) for the SOMAN+DZP group, which received DZP at 1 h after soman challenge, and 96% (24 out of 25) for the SOMAN+UBP302 group, which received UBP302 at 1 h after soman exposure. The higher survival rate of the DZP- and UBP302-treated rats, versus the SOMAN group, was statistically significant (Fisher exact test, $P = 0.018$ and $P = 0.003$, respectively).

For the rats that were implanted with EEG electrodes (n = 31), the survival rate was 44% for the SOMAN group (4 out of 9) and 100% for the animals that were administered DZP at 1 h (n = 6) or 2 h (n = 4) after exposure, as well as for the animals administered UBP302 at 1 h (n = 8) or 2 h (n = 4) after exposure. In the SOMAN+DZP group, the electrographic initial SE –the SE that started after soman injection and was terminated, at least temporarily, after anticonvulsant administration (Fig. 23A)– lasted for 113.6 ± 10.6 min (n = 6), when DZP was administered 1 h after soman, and 133.7 ± 10.9 min (n = 4) when DZP was administered at 2 h after soman. In the SOMAN+UBP302 group, the electrographic initial SE (Fig. 23B) lasted for 189.9 ± 6.2 min (n = 8) when UBP302 was administered 1 h after soman, and 236 ± 5.4 min (n = 4) when UBP302

was administered 2 h after soman. Compared to the duration of the SE in the SOMAN group (609.4 ± 37.3 min, n = 4), the initial SE duration in the SOMAN+DZP and the SOMAN+UBP302 groups was significantly lower ($P < 0.001$) whether the anticonvulsants were administered at 1 h after soman exposure (Fig. 23C, left set of bars) or at 2 h after soman exposure (Fig. 23D, left set of bars). The duration of the initial SE in the SOMAN+UBP302 group was significantly greater than in the SOMAN+DZP group ($P < 0.05$).

Seizures recurred in all of the rats that received DZP and in half of the rats that received UBP302. The total duration of electrographic seizures within the 24 h period after soman exposure (initial SE + recurring seizures) was significantly lower in rats administered UBP302 at 1 h (203.6 ± 4.4 min, n = 8, $P < 0.001$; Fig. 23C, right set of bars) or 2 h (237 ± 3.2 min, n = 4, $P = 0.003$; Fig. 23D, right set of bars) after exposure, compared to the SOMAN group (655.2 ± 36.9 min, n = 4). In contrast, rats treated with DZP at 1 h after exposure had similar total duration of SE (707.4 ± 62.5 min, n = 6) to the untreated SOMAN rats (Fig. 23C, right set of bars), while in rats treated with DZP at 2 h post-exposure, the total duration of SE (879 ± 59.2 min, n = 4) was significantly longer than that in the SOMAN group ($P < 0.05$; Fig. 23D, right set of bars). The total duration of SE in the SOMAN+UBP302 group was also significantly less than in the SOMAN+DZP group ($P < 0.01$).

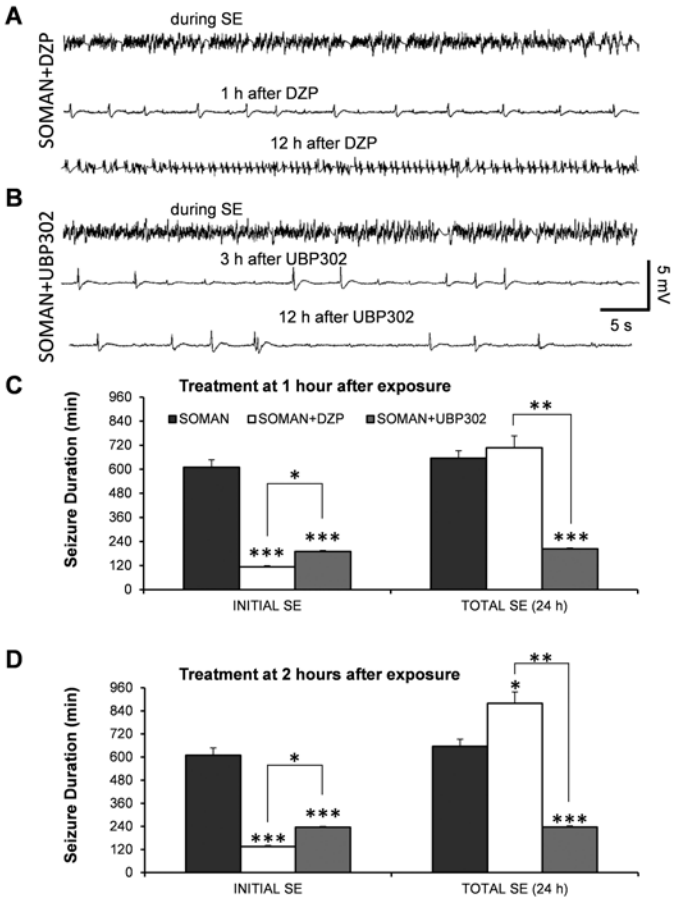

Figure 23. DZP terminates soman-induced SE, but does not reduce the total duration of SE within the 24 h period after soman exposure, as seizures return; UBP302 reduces the total duration of SE within 24 h. (A) and (B) Example traces from EEG recordings showing that both DZP and UBP302–administered 1h after soman–terminated the SE induced by soman, but seizure activity returned after DZP administration. (C) Duration of initial SE and total duration of SE within 24 h after soman exposure, when DZP and UBP302 were administered at 1 h after soman injection. The three bars on the left show the duration of the initial SE (the SE that started 5 to 15 min after soman exposure and was terminated by DZP or UBP302, or spontaneously in the SOMAN group), while the three bars on the right show the total duration of SE. SOMAN, n = 4; SOMAN+DZP, n = 6; SOMAN+UBP302, n = 8. (D) Duration of initial SE and total duration of SE within 24 h after soman exposure, when DZP and UBP302 were administered at 2 h after soman injection. The three bars on the left show the duration of the initial SE, while the three bars to the right show the total duration of SE. SOMAN, n = 4; SOMAN+DZP, n = 4; SOMAN+UBP302, n = 4. *$P < 0.05$, **$P < 0.01$ and ***$P < 0.001$ in comparison to the SOMAN group (ANOVA followed by Bonferroni post-hoc test for the initial SE and ANOVA followed by Games-Howell post-hoc test for total SE). *$P < 0.05$, **$P < 0.01$ for the comparisons between the DZP-treated and the UBP302-treated groups (ANOVA followed by Fisher's LSD test).

Using the video-EEG recording system, we also counted the number of convulsive seizures that recurred after termination of the initial SE and within the remaining time of the 24 h period after the exposure, in the SOMAN rats and the rats that received anticonvulsant treatment at 1 h after soman exposure. After the prolonged SE in the SOMAN group, the number of recurring convulsive seizures was very low (1.5 ± 0.86, n = 4; Fig. 24). The number of recurring convulsive seizures in the DZP-treated group (27.2 ± 6.89, n = 6) was significantly greater than in the UBP302-treated group (4.72 ± 2.10, n = 8, $P < 0.01$; Fig. 24).

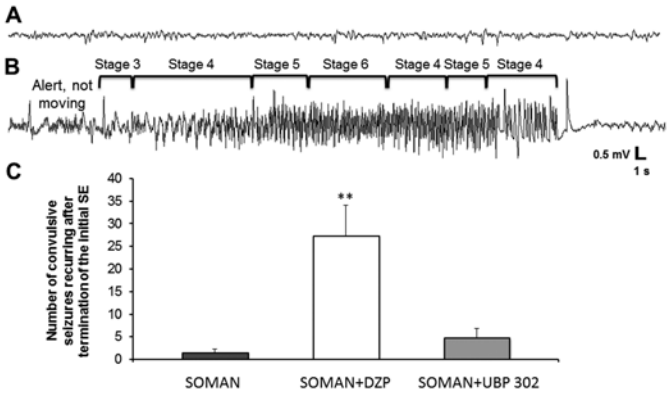

Figure 24. The number of convulsive seizures that recurred in the DZP-treated rats after termination of the initial SE was greater than in the UBP302-treated rats. (A) EEG baseline before soman exposure. (B) Representative recording of a convulsive seizure recurring after termination of the initial SE by DZP, and its correspondence with the behavioral seizure observations. (C) Number of convulsive seizures that occurred after cessation of the initial SE, within the remaining time of the 24 h period after soman exposure. SOMAN, n = 4; SOMAN+DZP, n = 6; SOMAN+UBP302, n = 8. $^{**}P < 0.01$, significantly higher compared to the SOMAN+UBP302 group and the SOMAN group (ANOVA followed by Holm-Sidak post-hoc test).

Neuronal loss and degeneration, 1 day after soman administration

Neuropathological analysis was performed in the SOMAN group and in the groups that received DZP or UBP302 at 1 h after soman exposure; neuronal loss was determined based on comparisons with the CONTROL group. The neurodegeneration score for the amygdala was moderate in the SOMAN group (median = 3, IQR = 3~4, n = 6), severe in

the SOMAN+DZP group (median = 4, IQR = 3~4, n = 6), and mild in the SOMAN+UBP302 group (median = 2, IQR = 2~3, n = 6; Fig. 25). Neuronal degeneration in the CA1, CA3 and hilar regions of the ventral hippocampus was severe in the SOMAN group (CA1, median = 4, IQR = 3~4; CA3, median = 4, IQR = 3~4; hilus, median = 4, IQR = 4~4), moderate in the SOMAN+DZP group (CA1, median = 3, IQR = 2.75~4; CA3, median = 3, IQR = 2.5~4; hilus, median = 3, IQR = 3~4), and mild to moderate in the SOMAN+UBP302 group (CA1, median = 2, IQR = 2~3; CA3, median = 2.5, IQR = 2~3; hilus, median = 2.5, IQR = 2~3). The neurodegeneration score for the neocortex was mild in the SOMAN group (median = 2.5, IQR = 2~3) and the SOMAN+DZP group (median = 2, IQR = 1~2), and minimal to mild in the SOMAN+UBP302 group (median=1.5, IQR = 1~2). The neuronal degeneration in the amygdala, ventral hippocampus, and neocortex of the SOMAN+UBP302 group was significantly less extensive compared to the SOMAN group (for the amygdala, $P = 0.026$; for the CA1 area, $P = 0.041$; for the CA3 area, $P = 0.015$; for the hilus, $P = 0.002$; for the cortex, $P = 0.026$; Fig. 25). In contrast, there were no significant differences between the SOMAN+DZP group and the SOMAN group in the neurodegeneration scores of the amygdala, hippocampus, and neocortex. In addition, neurodegeneration scores for the piriform cortex and entorhinal cortex did not differ significantly among the SOMAN group (piriform cortex, median = 3, IQR = 3~4; entorhinal cortex, median = 2, IQR = 2~2.25), the SOMAN+DZP group (piriform cortex, median = 4, IQR = 3~4; entorhinal cortex, median = 2, IQR = 2~3), and the SOMAN+UBP302 group (piriform cortex, median = 3, IQR = 3~3.25; entorhinal cortex, median = 2, IQR = 1.75~2). The control group did not show any FJC-positive staining.

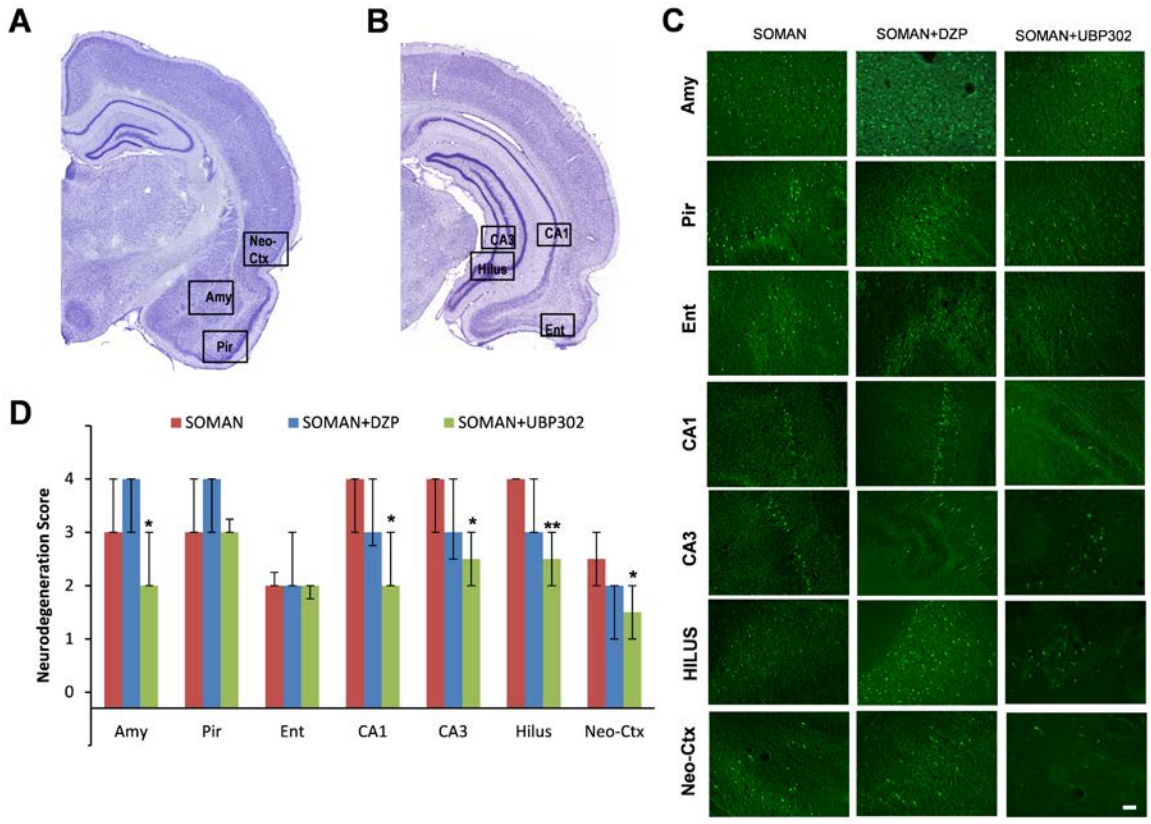

Figure 25. UBP302, but not DZP, administered 1 h after soman exposure, reduced neuronal degeneration in the amygdala, hippocampus, and neocortex, 1 day after the exposure. (A) and (B) Panoramic photomicrographs of Nissl-stained sections showing the brain regions evaluated by FJC staining. (C) Representative photomicrographs of FJC-stained sections from the brain regions where neuronal degeneration was evaluated, for the SOMAN, SOMAN+DZP, and SOMAN+UBP302 groups. Total magnification is 100x. Scale bar is 50 µm. (D) Neuropathology scores (median and interquartile range) for the SOMAN, SOMAN+DZP, and SOMAN+UBP groups (n = 6 for each group) for the amygdala (Amy), piriform cortex (Pir), entorhinal cortex (Ent), the CA1, CA3, and hilar areas of the ventral hippocampus, and neocortex (neo-Ctx). **P* < 0.05, ***P* < 0.01 in comparison to the SOMAN group (Mann-Whitney U test).

The total number of neurons in the BLA and the CA1 hippocampal area was estimated using an unbiased stereological method in Nissl-stained sections. The number of neurons in the SOMAN group (BLA, 78,027 ± 1,939; CA1, 463,976 ± 19,972; n = 6) was significantly lower than the number of neurons in the CONTROL group (BLA, 118,041 ± 4,281; CA1, 645,450 ± 28,232, n = 6), in both brain regions (*P* < 0.001; Fig. 26). The number of neurons in the SOMAN+DZP group (BLA, 87,893 ± 4,814; CA1,

439,186 ± 23,211; n = 6) did not differ significantly from that in the SOMAN group (*P* = 0.23 and *P* = 0.83 for the BLA and CA1, respectively; Fig. 26). In the SOMAN+UBP302 group, the number of neurons in the BLA (98,648 ± 4,513, n = 6) was significantly lower than in the controls (*P* = 0.008), but also significantly higher than in the SOMAN group (*P* = 0.005; Fig. 26C). The number of neurons in the CA1 area of the SOMAN+UBP302 group (588,100 ± 28,012, n = 6) did not differ from the control group (*P* = 0.276) and was significantly higher than in the SOMAN group (*P* = 0.006; Fig. 26D).

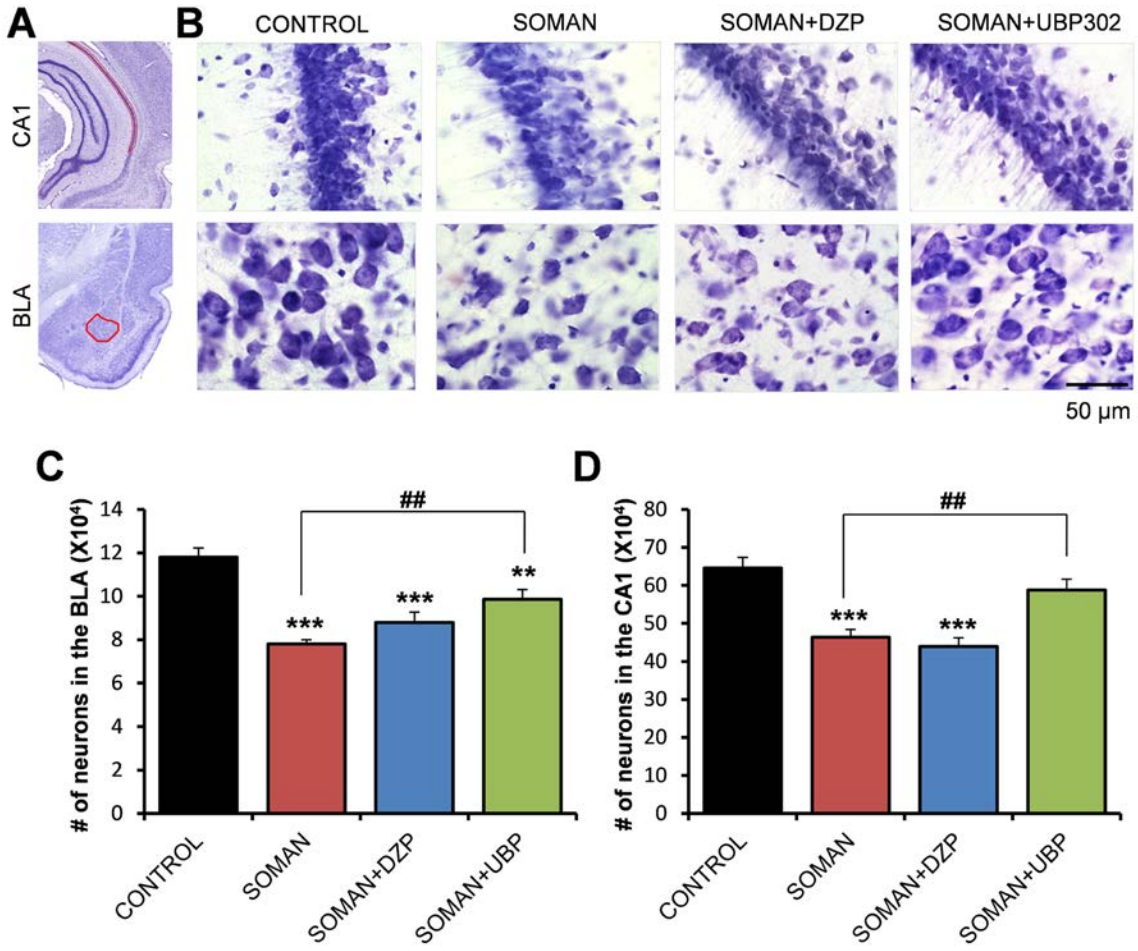

Figure 26. UBP302, but not DZP, administered 1 h after soman exposure, reduced neuronal loss in the BLA and the CA1 hippocampal area, 1 day after the exposure. (A) Panoramic photomicrographs of Nissl-stained half hemispheres outlining the amygdalar nucleus and the hippocampal subfield where stereological analysis was performed. (B) Representative photomicrographs of Nissl-stained sections showing BLA and CA1 cells from the CONTROL,

SOMAN, SOMAN+DZP and SOMAN+UBP302 groups. Total magnification is 630x and scale bar is 50 µm. (C) and (D) Group data (mean and standard error; n = 6 for each group) of stereological estimation of the total number of Nissl-stained neurons in the BLA (left) and CA1 area (right). $^{**}P < 0.01$, $^{***}P < 0.001$ in comparison to CONTROL, $^{\#\#}P < 0.01$ in comparison to the SOMAN group (ANOVA, Dunnett post-hoc test).

Neuronal loss and degeneration, 7 days after soman administration

The neurodegeneration results at 7 days after soman exposure are shown in Fig. 27. The SOMAN group (n = 6) had moderate to severe neurodegeneration in the amygdala (median = 3, IQR = 2.75~4), piriform cortex (median = 3, IQR = 3~4), entorhinal cortex (median = 3, IQR = 2~3), CA1 hippocampal area (median = 4, IQR = 3 ~4), and CA3 hippocampal area (median = 3, IQR = 1~3.5), and mild to moderate in the hilus (median = 2.5, IQR = 0~4) and neocortex (median = 2.5, IQR = 1~3). Similarly, in the SOMAN+DZP group (n = 6), neurodegeneration was moderate to severe in the amygdala (median = 3, IQR = 0.75~3.25), the piriform cortex (median = 3.5, IQR = 1.75~4), entorhinal cortex (median = 3, IQR = 1.5~3), CA1 hippocampal area (media = 3.5, IQR =2.5 ~4), and CA3 hippocampal area (median = 3, IQR = 0.75~3.25), and mild to moderate in the hilus (median = 2.5, IQR = 1.75~3.25) and neocortex (median = 2, IQR = 1~3). In the SOMAN+UBP302 group (n = 6), neurodegeneration was minimal to mild in the entorhinal cortex (median = 1.5, IQR = 0.75~2.25), CA3 hippocampal area (median = 0.5, IQR = 0~2), hilus (median = 1.5, IQR = 0~3), and neocortex (median = 1, IQR = 0.75~2), mild to moderate in the amygdala (median = 2, IQR = 1.5~3) and CA1 area (median = 2, IQR =0 ~ 3), and moderate to severe in the piriform cortex (median = 3, IQR = 1.5~4). Compared to the SOMAN group, neurodegeneration in the SOMAN+UBP302 group was significantly lower in the amygdala ($P = 0.041$), entorhinal cortex ($P = 0.041$), CA1 ($P = 0.009$) and CA3 ($P = 0.041$) hippocampal areas.

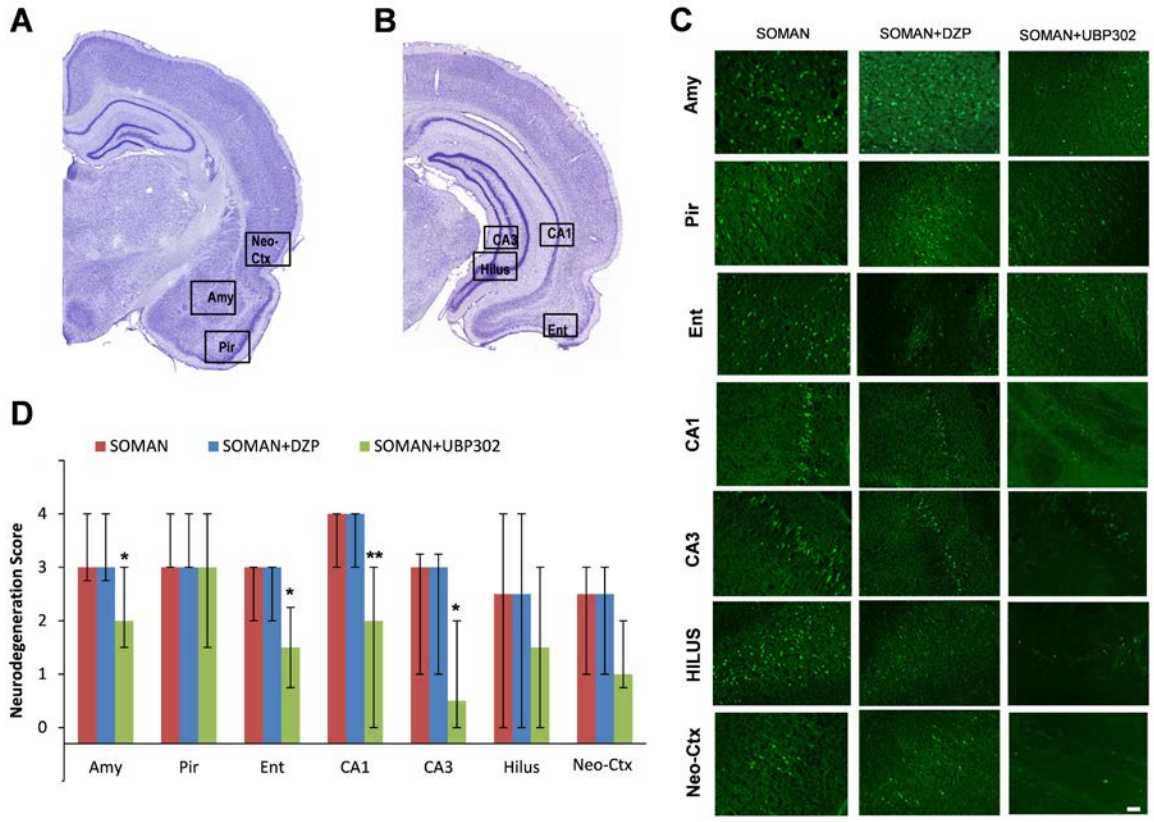

Figure 27. UBP302, but not DZP, administered 1 h after soman exposure, reduced neuronal degeneration in the amygdala, CA1 and CA3 dorsal hippocampal areas, and entorhinal cortex, 7 days after the exposure. (A) and (B) Panoramic photomicrographs of Nissl-stained sections showing the brain regions evaluated by FJC staining. (C) Representative photomicrographs of FJC-stained sections from the brain regions where neuronal degeneration was evaluated, for the SOMAN, SOMAN+DZP, and SOMAN+UBP302 groups. Total magnification is 100x. Scale bar is 50 μm. (D) Neuropathology scores (median and interquartile range) for the SOMAN, SOMAN+DZP, and SOMAN+UBP groups (n = 6 for each group), for the amygdala (Amy), piriform cortex (Pir), entorhinal cortex (Ent), the CA1, CA3 and hilar areas of the ventral hippocampus, and neocortex (neo-Ctx). *$P < 0.05$, **$P < 0.01$ in comparison to the SOMAN group (Mann-Whitney U test).

The total number of neurons in the BLA and the CA1 hippocampal area was estimated 7 days after soman exposure; the results are shown in Fig. 28. The number of neurons in the SOMAN group (BLA, 79,394 ± 3287; CA1, 440,698 ± 17,159; n = 6) was again significantly lower than the number of neurons in the CONTROL group (BLA, 115,108 ± 2,673; CA1, 639,701 ± 29,350, n = 6), in both brain regions ($P < 0.001$). The

number of neurons in the SOMAN+DZP group (BLA, 87,729 ± 6,032; CA1, 463,196 ± 25,729; n = 6) did not differ significantly from those in the SOMAN group (*P* = 0.424 and *P* = 0.841 for the BLA and CA1, respectively). The number of neurons in the SOMAN+UBP302 group (BLA, 99,678 ± 4,947; CA1, 568,098 ± 20,386; n = 6) was significantly higher than in the SOMAN group (*P* = 0.011 for the BLA and *P* = 0.003 for the CA1), but differed from the CONTROL group only in the BLA.

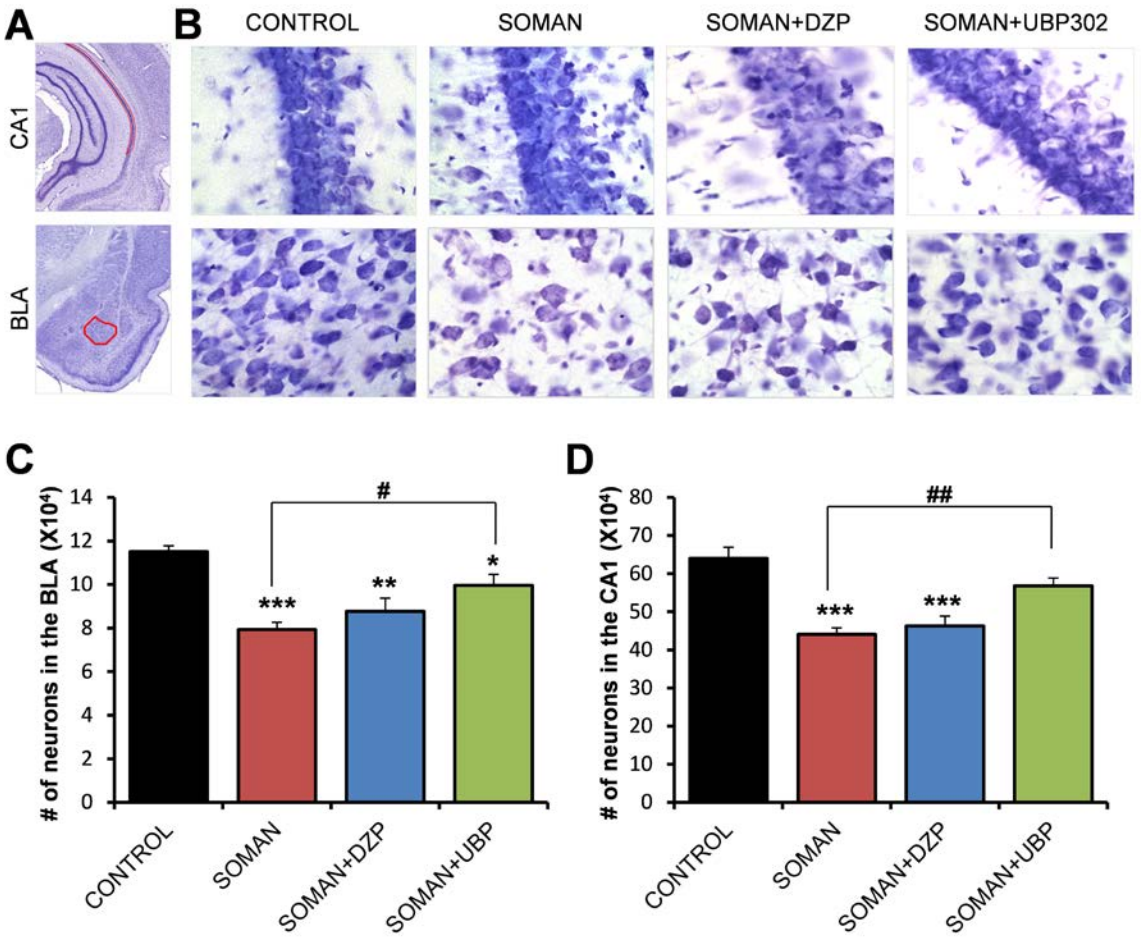

Figure 28. UBP302, but not DZP, administered 1 h after soman exposure, reduced neuronal loss in the BLA and the CA1 hippocampal area, 7 days after the exposure. (A) Panoramic photomicrographs of Nissl-stained half hemispheres outlining the amygdalar nucleus and the hippocampal subfield where stereological analysis was performed. (B) Representative photomicrographs of Nissl-stained sections showing BLA and CA1 cells from the CONTROL, SOMAN, SOMAN+DZP and SOMAN+UBP302 groups. Total magnification is 630x and scale bar is 50 µm. (C) and (D) Group data (mean and standard error; n = 6 for each group) of stereological estimation of the total number of

Nissl-stained neurons in the BLA (left) and CA1 area (right). *P < 0.05, **P < 0.01, ***P < 0.001 in comparison to CONTROL, $^{\#}P$ < 0.05 and $^{\#\#}P$ < 0.01 in comparison to the SOMAN group (ANOVA, Dunnett post-hoc test).

We have previously shown that the number of GABAergic interneurons in the BLA is not altered 1 day after soman exposure, but it is significantly reduced 7 days after the exposure (89; 228). Therefore, we examined whether DZP or UBP302 protected against GABAergic interneuronal loss. Stereological estimation of GAD67+ neurons in the BLA showed that, compared to the CONTROL group (10,837 ± 565, n = 6), there was a significantly lower number of GABAergic interneurons in both the SOMAN (7,260 ± 367; n = 6, P = 0.001) and the SOMAN+DZP (8,875 ± 293; n = 6, P = 0.012) groups. In contrast, the number of GABAergic interneurons in the SOMAN+UBP302 group (10,345 ± 633; n = 6) did not differ from the CONTROL group (P = 0.9; Fig. 29).

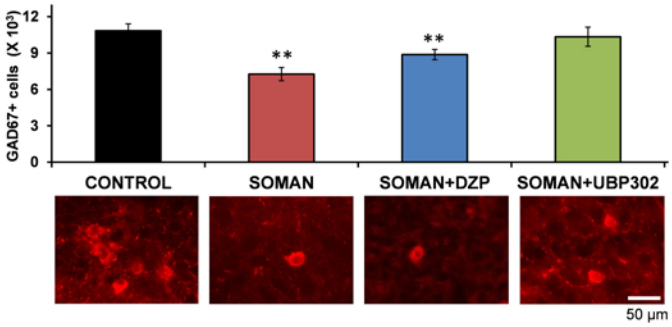

Figure 29. UBP302, but not DZP, administered 1 h after soman exposure, prevented GABAergic interneuronal loss in the BLA, 7 days after the exposure. Group data (mean and standard error; n = 6 for the each group) of stereological estimation of the total number of GAD67+ neurons in the BLA for the CONTROL, SOMAN, SOMAN+DZP and SOMAN+UBP302 groups. Representative photomicrographs of GAD67+ interneurons are shown in the lower panel. Total magnification is 630x and scale bar is 50 µm. **P < 0.01 in comparison to CONTROL (ANOVA, Dunnett post-hoc test).

Neuronal loss and degeneration, 30 days after soman administration

Thirty days after soman exposure, the analysis of ongoing neuronal degeneration showed that in the amygdala neurodegeneration was mild to moderate in the SOMAN group

(median = 2.5, IQR = 2~3.75, n = 6) and the SOMAN+DZP group (median = 2, IQR = 2~3, n = 6), but only minimal in the SOMAN+UBP302 (median = 1, IQR = 0~2, n = 6; $P < 0.001$ compared to SOMAN; Fig. 8). In the piriform cortex, neurodegeneration was mild to moderate in the SOMAN group (median = 2, IQR = 2~3.75) and the SOMAN+DZP group (median = 3, IQR = 2~4), but only minimal in the SOMAN+UBP302 group (median = 1, IQR = 1~2; $P = 0.002$ compared to SOMAN; Fig. 30). In the CA1 hippocampal area, neurodegeneration was moderate in the SOMAN group (median = 3, IQR = 3~4), and mild in the SOMAN+DZP group (median = 2, IQR = 0~3; $P = 0.002$ compared to SOMAN) and the SOMAN+UBP302 groups (median = 2, IQR = 0.5~3; $P = 0.001$). There were no significant differences between the three groups in the neurodegeneration scores for the entorhinal cortex (SOMAN group: median = 1.5, IQR = 1~2; SOMAN+DZP group: median = 2, IQR = 0~2; SOMAN+UBP302 group: median = 1, IQR = 1~2), CA3 hippocampal area (SOMAN group: median = 3, IQR = 0~3; SOMAN+DZP group: median = 1, IQR = 1~3; SOMAN+UBP302 group: median = 2, IQR = ~3), the hilus (SOMAN and SOMAN+DZP groups: median = 1, IQR = 0~2; SOMAN+UBP302 group: median = 0, IQR = 0~2), and the neocortex (SOMAN and SOMAN+DZP groups: median = 1, IQR = 0~1; SOMAN+UBP302 group: median = 0, IQR = 0~1).

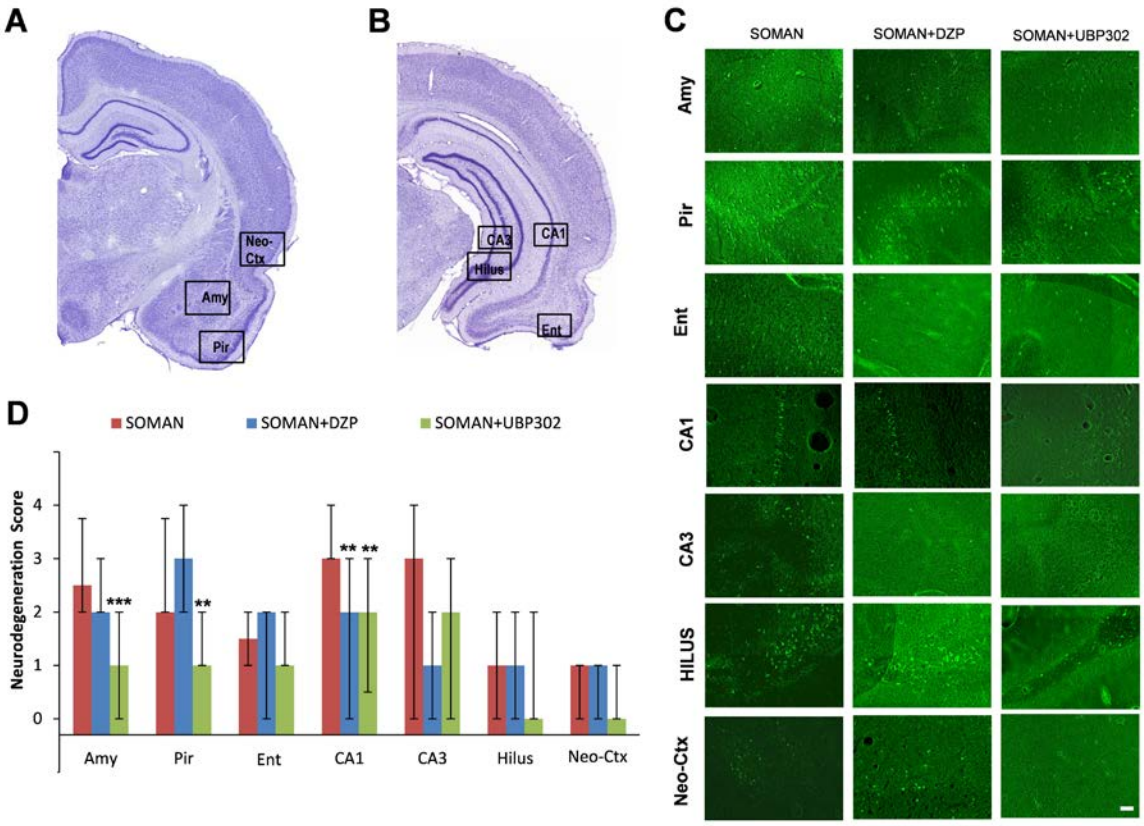

Figure 30. UBP302, administered 1 h after soman exposure, reduces neuronal degeneration in the amygdala, piriform cortex, and CA1 hippocampal area, while DZP reduces neurodegeneration in the CA1 area, 30 days after the exposure. (A) and (B) Panoramic photomicrographs of Nissl-stained sections showing the brain regions evaluated by FJC staining. (C) Representative photomicrographs of FJC-stained sections from the brain regions where neuronal degeneration was evaluated, for the SOMAN, SOMAN+DZP, and SOMAN+UBP302 groups. Total magnification is 100x. Scale bar is 50 μm. (D) Neuropathology scores (median and interquartile range) for the SOMAN , SOMAN+DZP, and SOMAN+UBP groups (n = 6 for each group), for the amygdala (Amy), piriform cortex (Pir), entorhinal cortex (Ent), the CA1, CA3 and hilar areas of the dorsal hippocampus, and neocortex (neo-Ctx). *$P < 0.05$ in comparison to the SOMAN group (Mann-Whitney U test).

Thirty days after soman exposure, neuronal loss was still present in the SOMAN group (n = 6), in which the total number of neurons (BLA, 82,119 ± 2099; CA1, 444,356 ± 21,045) was significantly lower ($P < 0.001$) than in the CONTROL group (BLA, 119,860 ± 2898; CA1, 684,738 ± 15,340; n = 6; Fig. 31). In the SOMAN+UBP302 group

(n = 6), the total number of neurons (BLA, 101,412 ± 1535; CA1, 553,583 ± 27,489) was significantly lower than in the CONTROL group, both in the BLA (P = 0.012; Fig. 31C) and in the CA1 area (P = 0.006; Fig. 31D), but also significantly higher than in the SOMAN group (P = 0.001). The number of neurons in the SOMAN+DZP group (BLA, 88,591 ± 7134; CA1, 463,211 ± 21,536; n = 6) was significantly lower than the CONTROL group (P < 0.001), and did not differ from the number of neurons in the SOMAN group (P = 0.55 and P = 0.34 for the BLA and the CA1 area, respectively; Fig. 31).

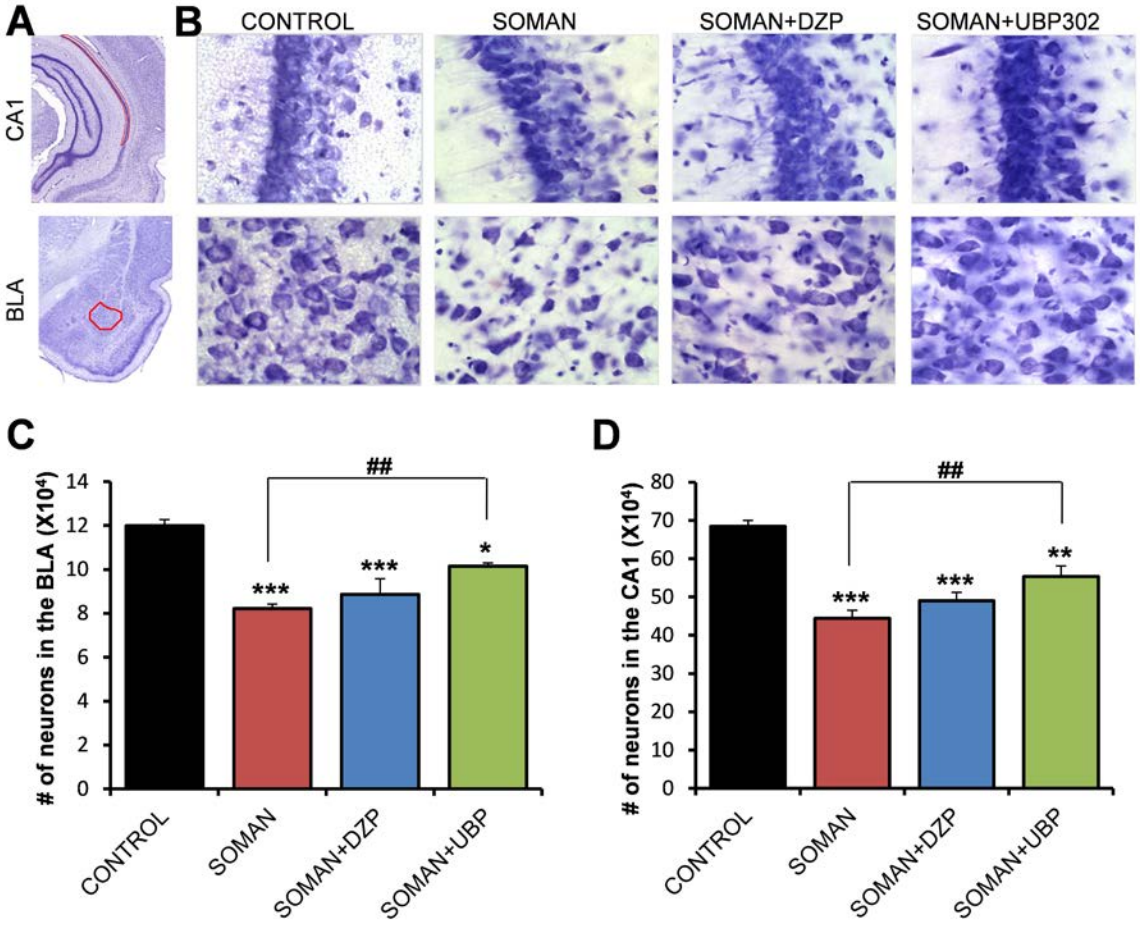

Figure 31. UBP302, but not DZP, administered 1 h after soman exposure, reduced neuronal loss in the BLA and the CA1 hippocampal area, 30 days after the exposure. (A) Panoramic photomicrographs of Nissl-stained half hemispheres outlining the amygdalar nucleus and the hippocampal subfield where stereological analysis was performed. (B) Representative photomicrographs of

Nissl-stained sections showing BLA and CA1 cells from the CONTROL, SOMAN, SOMAN+DZP and SOMAN+UBP302 groups. Total magnification is 630x and scale bar is 50 µm. (C) and (D) Group data (mean and standard error; n = 6 for each group) of stereological estimation of the total number of Nissl-stained neurons in the BLA (left) and CA1 area (right). *$P < 0.05$, **$P < 0.01$, ***$P < 0.001$ in comparison to CONTROL; $^{\#\#}P < 0.01$ in comparison to the SOMAN group (ANOVA, Dunnett post-hoc test).

Behavioral alterations 30 days after soman administration

To investigate whether the long-term neuropathology observed 30 days after soman exposure had translated into behavioral deficits, we examined anxiety-like behavior in all experimental groups, using the open field and the acoustic startle response (ASR) tests. The distance traveled in the open field by the groups exposed to soman (SOMAN: 2270 ± 265 cm, n = 10; SOMAN+DZP: 2290 ± 235 cm, n = 9; SOMAN+UBP302: 1329 ± 279 cm, n = 12) was not significantly different from that in the CONTROL group (1620 ± 219 cm, n = 8; Fig. 32A). However, both the SOMAN and the SOMAN+DZP groups spent significantly less time in the center of the open field (SOMAN group, 6.28 ± 1.56 % of the total movement time, n = 10, $P = 0.034$; SOMAN+DZP group, 6.88 ± 1.29 % of the total movement time, n = 9, $P = 0.027$) compared to the time spent by the CONTROL rats (15.22 ± 2.67 % of the total movement time, n = 8). The SOMAN+UBP302 rats spent 17.61 ± 2.27 % (n = 12) of the total movement time in the center of the open field, which was not different from the CONTROL group ($P = 0.73$; Fig. 32B).

In the ASR test, there was a significant increase in startle amplitude in the SOMAN (110 dB: 17.94 ± 0.83, n = 10, $P < 0.001$; 120 dB: 19.20 ± 0.35, $P = 0.001$) and the SOMAN+DZP (110 dB: 17.38 ± 0.95, n = 9, $P = 0.001$; 120 dB: 18.85 ± 0.41, $P = 0.003$) groups compared to the CONTROL group (110 dB: 10.99 ± 1.35; 120 dB: 14.09 ± 1.54, n = 8; Fig. 10C). Startle response amplitude in the SOMAN+UBP302 group (110

dB: 13.95 ± 0.99; 120 dB: 16.03 ± 0.91, n =12) did not differ from the CONTROL group (P = 0.123 for the 110 dB, and P = 0.291 for the 120 dB; Fig. 32C).

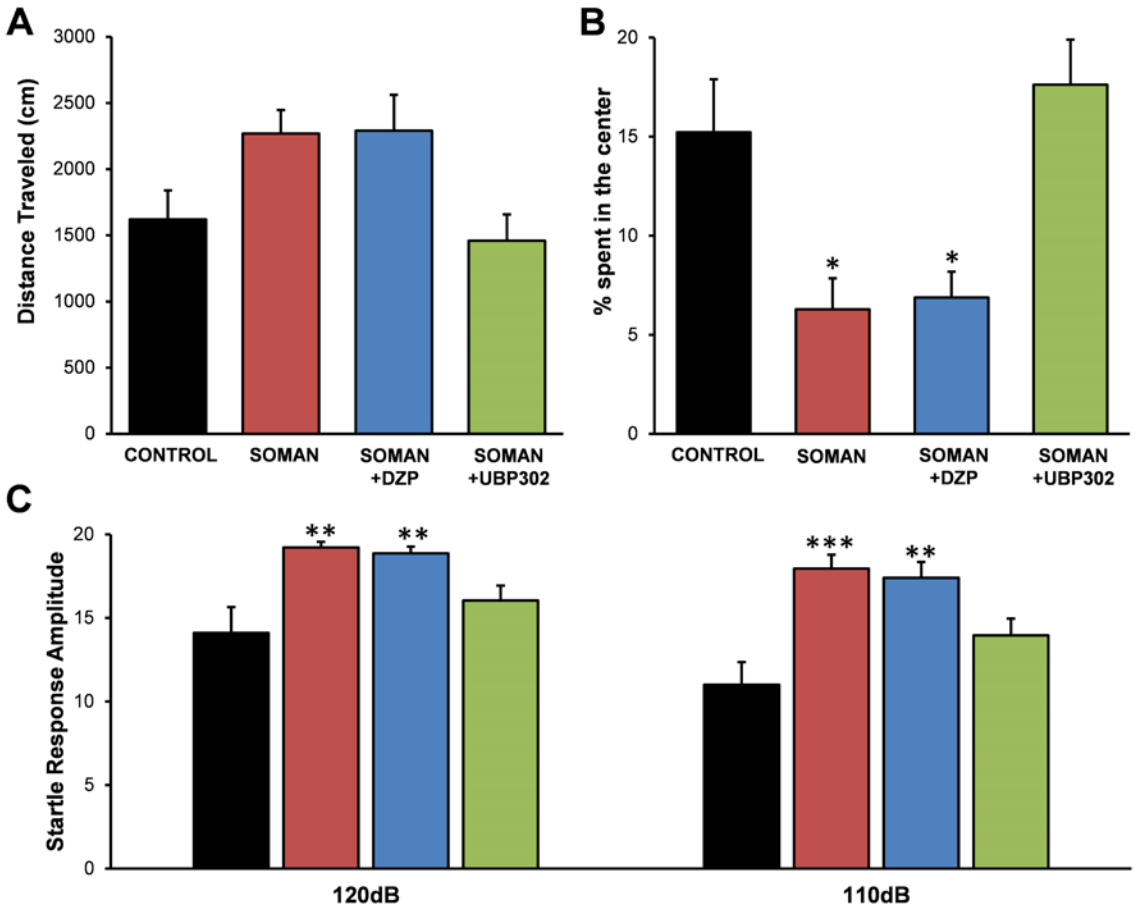

Figure 32. UBP302, but not DZP, administered 1 h after soman exposure, protected against the development of anxiety, 30 days after the exposure. (A) Distance traveled (Mean ± SE) in the open field. (B) Percentage of time spent in the center of the Open Field. (C) Amplitude of startle responses to 120 dB and 110 dB acoustic stimuli. CONTROL, n = 8; SOMAN, n = 10; SOMAN+DZP, n = 9; SOMAN+UBP302, n = 12. *P < 0.05, **P < 0.01 and ***P < 0.001 (ANOVA, Dunnett post-hoc comparison to CONTROL).

Discussion

Seizures induced by exposure to nerve agents require medical intervention, otherwise they can lead to severe brain damage or death. Administration of DZP is the presently FDA-approved treatment for nerve agent-induced seizures. The present study showed that if DZP is administered to soman-exposed rats at 1 hour post-exposure,

seizures are terminated effectively, but they soon return, resulting in a total duration of SE within 24 h after exposure that is no different from the total SE duration in the soman-exposed rats that do not receive anticonvulsant treatment. Moreover, if DZP is administered at 2 h after soman exposure, the total duration of SE in the DZP-treated rats is longer than in the rats that do not receive anticonvulsant treatment. The consequences of the return of seizures after DZP treatment were evident in the neuropathology analysis and the behavioral tests. Thus, DZP treatment provided no protection against neuronal degeneration and death, except for a lower number of degenerating neurons in the CA1 hippocampal area, 30 days after the exposure. In contrast, treatment with the GluK1 antagonist UBP302, which reduced the total duration of SE within 24 hours post-exposure, protected against neuronal damage in most of the brain regions examined. The anxiety tests also revealed that UBP302, but not DZP treatment, prevented an increase in anxiety-like behavior, 30 days after soman exposure.

The disadvantages of DZP treatment as an anticonvulsant

From the clinical experience and studies in human patients, as well as from experimental studies in animals, the efficacy of benzodiazepines in terminating status epilepticus has long been recognized to decrease as the latency between the initiation of SE and the time point of drug administration increases (78; 102; 130; 174; 262; 301). This is also the case with SE induced by nerve agents. Thus, in rats, Shih et al. (255) found that DZP was very effective in stopping seizures when administered 5 min after the onset of soman-induced SE, but was virtually ineffective when administration was delayed to 40 min after seizure initiation. The mechanisms underlying the development of refractoriness to benzodiazepines are not fully understood, but may involve internalization and

downregulation of $GABA_A$ receptors (78; 102; 199), or other dysfunctions in GABAergic synaptic transmission that manifest as the seizures progress. At least in hippocampal neurons, Goodkin et al. (102) have demonstrated that GABAergic inhibition displays a high degree of plasticity, in that, during prolonged epileptiform bursting, the rate of GABA receptor internalization increases rapidly, and the subunit composition of these receptors swiftly changes (as suggested by the changes in the kinetics of miniature IPSCs), perhaps due to movement of extrasynaptic $GABA_A$ receptors onto synaptic sites. Therefore, when DZP is administered at delayed time points, the function of the GABAergic system is already compromised, and, as a result, DZP may be ineffective. Nevertheless, the available evidence suggests that the progressive refractoriness to benzodiazepines is not an absolute phenomenon and can be partially overcome depending on the animal model used to induce SE, the dose of DZP, or other factors. For example, in a guinea pig model of nerve agent exposure, 10 mg/kg of DZP was effective against soman-induced seizures in a sizeable proportion of the animals, even when administration was delayed beyond 1 h after seizure onset, although its efficacy was still clearly reduced as the latency of administration increased (McDonough et al., 2010). In addition, kainic acid-induced SE can be stopped by 25 mg/kg DZP even when the drug is administered 3 h after the onset of seizures (231), and in the present study, 10 mg/kg DZP terminated SE at either the 1 h or the 2 h time point of administration.

Considering the above, one would conclude that DZP remains an effective anticonvulsant, but it is desirable to be used at early time points after seizure initiation, for greater effectiveness. What, however, has not received enough attention is the recurrence of intense seizures after cessation of the initial SE by DZP, and the impact that

such recurrence of SE has on the neuroprotective efficacy of DZP. Shih et al. (255) reported that 25% of the animals receiving 9 mg/kg DZP at 5 min after the onset of soman-induced seizures had seizures recurring within the 6 h monitoring period. In the present study, seizures recurred in all of the soman-exposed rats that received DZP, making the total duration of seizures within the 24 h period of video-EEG monitoring no different from (Fig. 23C), or even longer than (Fig. 23D) in the soman-exposed rats that did not receive anticonvulsant treatment. The mechanisms underlying the recurrence of seizures after cessation of the initial SE by DZP probably involve a severely compromised GABAergic system, in combination with the pharmacokinetics of the drug. Thus, intense seizure activity impairs the function of GABAergic inhibition (78; 102; 199). Then, the brain is exposed to DZP, which, on one hand, enhances $GABA_A$ receptor activity and thereby stops the SE temporarily, but on the other hand it may contribute to more desensitization and downregulation of $GABA_A$ receptors (292; 296), further impairing GABAergic synaptic transmission. As DZP is rapidly cleared from the animal's system (235), the brain remains with severely compromised GABAergic inhibition, and therefore neuronal networks intermittently enter into intense seizure activity, every time the unopposed glutamatergic activity intensifies.

Targeting the GluK1KRs to control seizures

While inhibition progressively weakens during SE, glutamatergic excitation is reinforced, probably not only because of disinhibition; during SE, there is upregulation of AMPA receptors (62; 234), as well as enhanced expression of the GluK1 subunit (291), which could significantly contribute to worsening hyperexcitability and excitotoxicity. Therefore, suppressing glutamatergic hyperactivity can be a more effective way to

control seizures, particularly if immediate treatment is not possible and the anticonvulsant is administered with a delay after seizure onset. Indeed, we have shown previously that the GluK1/AMPA receptor antagonist LY293558, administered 1 h after soman exposure, stops seizures and fully protects against neuronal damage (12; 89). In the present study, we tested UBP302, which is selective for the GluK1 receptors (190). It is uncertain at what concentrations UBP302 reached the brain and whether other glutamatergic receptors were also affected, however, this compound also suppresses soman-induced seizure-like activity, *in vitro*, at relatively low concentrations that are considered selective for GluK1 antagonism (11). UBP302 blocked the seizures induced by soman, and protected against neuropathology and anxiety-related behavioral deficits.

The time-course of termination of the initial SE by UBP302 was slow in comparison to that of DZP or LY293558. Although this may have to do with the type of receptors being targeted and their involvement in seizure activity, it is also possible that it relates to the pharmacokinetics of UBP302 which is not known. However, despite the apparently slow time-course of action of UBP302, the total duration of SE within the 24 h period after exposure was dramatically reduced in the UBP302-treated rats, compared to either the soman-exposed rats that did not receive anticonvulsant treatment or the rats that received DZP. The mechanisms by which a GluK1 antagonist may suppress hyperexcitability and stop seizures have been discussed previously (17; 89). GluK1Rs modulate both GABAergic and glutamatergic synaptic transmission, in a number of brain regions (124). At least in the BLA and the hippocampus, the net effect of their activation is excitatory. This is suggested by the findings that GluK1R antagonists block epileptiform activity in hippocampal slices and limbic seizures in vivo (269). In the BLA,

GluK1Rs are present on postsynaptic (somatodendritic) sites of both principal cells (Gryder and Rogawski, 2003) and interneurons (42), as well as on the presynaptic terminals of both cell types, where they mediate facilitation of glutamate release (17) and either facilitation or inhibition of GABA release, depending on the concentration of the agonist (42). The net effect of their activation in the BLA network is an increased excitation and excitability, as suggested by a greater enhancement of spontaneous EPSCs versus IPSCs, the reduction of anxiety-like behavior when these receptors are blocked by microinjection of UBP302 selectively into the BLA, and the increased anxiety or the induction of seizures when a GluK1R agonist is injected into the BLA (17). Although it remains to be determined what role GluK1Rs play in the overall excitation of other neuronal networks, the fact that activation of these receptors increases the excitation state of the BLA and the hippocampus, two highly seizurogenic brain regions, may explain why blockade of these receptors can terminate seizures. It should also be noted that in contrast to the downregulation and internalization of $GABA_A$ receptors after excessive neuronal/seizure activity (78; 102; 199), which can render DZP ineffective, the upregulation of the GluK1 subunit (291) may contribute to hyper-excitation, which further explains the efficacy of GluK1R antagonists.

Neuropathology and associated behavioral deficits

Depending on the extent of brain damage after prolonged SE, behavioral deficits may ensue. Increased anxiety is observed in animals that have been exposed to nerve agents (74; 155; 228). Similarly, the human victims of the sarin terrorist attack in Japan report enduring symptoms of anxiety disorders, long after the exposure (118; 204). The amygdala plays a central role in emotional behavior, and dysfunction with increased

excitability of the BLA is associated with anxiety (101; 221; 253; 318). The hippocampus is also significantly involved in the modulation of anxiety (84; 93). Both the amygdala and the hippocampus are severely damaged by nerve agent-induced SE, as shown in the present and previous studies (14; 15; 258). In the BLA, there is significant loss of GABAergic neurons by day 7 after exposure to soman (88; 228), and at 14 and 30 days after exposure the ratio of GABAergic interneurons to the total number of neurons in the BLA is significantly decreased (228). Reduction of inhibitory activity in the BLA, resulting from the interneuronal loss, will increase the excitability of the BLA network, which can lead to the development of anxiety.

In the present study, treatment with UBP302 significantly reduced neuronal loss and degeneration in a number of brain regions, including the hippocampus and the amygdala, and prevented the loss of GABAergic interneurons in the BLA, as assessed 30 days after the exposure. The neuroprotection provided by UBP302, despite its being only partial, was sufficient to prevent the development of anxiety-like behavior, as assessed in the open field and the acoustic startle response tests. In contrast, DZP had no neuroprotective effects, except for reduced neurodegeneration in the CA1 area at 30 days after exposure, and did not prevent the development of anxiety. Since the extent of nerve agent-induced neuropathology is solely or largely determined by the intensity and duration of seizures (227; 258), the failure of DZP to protect the brain can be attributed to the failure of this drug to reduce the total duration of seizures. Consistent with the present findings revealing the inefficacy of DZP to reduce neuropathology and prevent behavioral deficits, previous studies in which 10 mg/kg DZP was administered at 30 min

after soman-induced seizures show that this treatment did not prevent the development of anxiety-like behavior (155) or epileptogenesis (76).

The present data clearly argue against the use of DZP as a medical countermeasure for the treatment of SE induced by nerve agent exposure, at least when anticonvulsant treatment is delayed. DZP is likely to substantially increase the survival rate of exposed individuals, but because seizures recur, there is virtually no protection against neuropathology and the resulting behavioral deficits. Administering DZP repeatedly, every time intense seizures recur, not only may not be feasible, but may also be detrimental to the victims' health. The results suggest that targeting the glutamatergic system is a more effective approach to controlling nerve agent-induced SE, and antagonists of the GluK1Rs appear to be both safe and efficacious in this regard.

Authorship contributions

Participated in research design: Braga, Aroniadou-Anderjaska, Apland

Conducted experiments: Apland, Figueiredo, Rossetti, Miller

Performed data analysis: Figueiredo, Apland, Rossetti, Aroniadou-Anderjaska, Braga

Wrote or contributed to the writing of the manuscript: Aroniadou-Anderjaska, Figueiredo, Apland, Miller, Braga

APPENDIX 4: NEURO.TV: NEUROSCIENCE EDUCATION ON THE INTERNET

Xie Diana L[1], Miller Steven L[2], Boucher Leanne[3], Kubie John L[4], Gariépy Jean-Francois[1*]

[1]Duke Institute for Brain Sciences, Duke University, Box 91003, Levine Science Research Center, Room B107, 450 Research Drive, Durham, North Caroline 27708, United States of America
[2]Program in Neuroscience, Uniformed Services University of the Health Sciences, Bethesda, MD 20814, United States of America
[3]Farquhar Psychology Program, Nova Southeastern University, Davie-Fort Lauderdale, FL 33314, United States of America
[4]Department of Anatomy and Cell Biology, The Robert F. Furchgott Center for Neural and Behavioral Science, State University of New York Downstate Medical Center, Brooklyn, New York, USA

***Corresponding Author:**
Jean-Francois Gariepy, Ph.D.
Duke Institute for Brain Sciences
Duke University, Box 91003
Levine Science Research Center
Room B107, 450 Research Drive
Durham, North Carolina 27708, U.S.A.
Telephone: 919-688-0333
Email: jeanfrancois.garipey@gmail.com

ABSTRACT

NEURO.tv is a new educational project that seeks to bring advanced concepts in neuroscience to the general public. We film one-hour discussions with leading neuroscientists, philosophers, and psychologists who have had significant impact on our current understanding of brain function, and we publish these discussions on YouTube, iTunes, and other social media outlets. Here, we explain the motivations behind this new program.

AN ONLINE PROGRAM TO DISSEMINATE KNOWLEDGE ABOUT BRAIN AND MIND

The internet has an enormous impact on the way people learn. With the advent of Massive Open Online Courses (MOOCs), academic blogs, and online education tools, anyone can learn anything, from almost anywhere. While academics take part in this online education movement, we have not yet fully benefited from the educational opportunities that the internet can provide. Interactions between researchers in different fields and the general public typically happen in universities or through the publishing of textbooks and journal articles between academics are sometimes precluded by the monetary and physical costs of conferences, traveling, and visits to universities. New technologies offer an avenue for scientists to share their knowledge with colleagues and members of the general public in a more efficient and open manner.

Despite the progress that the internet has made in leveling the barriers between scientists and the general public, there exists a need for a forum in which advanced subjects at the heart of current neuroscience research can be discussed openly, with participation from the general public. A new internet-based program called NEURO.tv addresses this need, by airing one-hour discussions with scientists who have made

significant discoveries in neuroscience. We believe this program provides a platform for academics to present ideas and discoveries directly to the public in a setting that is not rushed or overly technical, and that remains accessible to individuals of all backgrounds. NEURO.tv's format is not merely a repetition of presentation content by a speaker, but rather a new type of interaction between scientists of different fields, discussing what they really think about the scientific methods used in their research, advances in medical treatment, and other important scientific problems that shape or limit current research.

Leading neuroscientists, philosophers, and psychologists have already volunteered their time to appear on the show. Our success in having many scientists commit to appearing on the program is due in part to the fact that filming an episode does not require travel, since physical presence is not required; scientists can simply connect to conversations with each other from their home or office computers. Within a one-hour discussion, they are able to convey their thoughts on neuroscience-related topics to a wide public on the scale of many thousands, which is advantageous compared to the number of students they would reach in a traditional conference room or lecture hall. The Internet-based, asynchronous delivery also provides broad and flexible access to these fascinating discussions, years after the filming. Free access is a particularly crucial aspect of NEURO.tv and may benefit developed as well as developing countries, which may help reduce the gap in global access to advanced scientific knowledge (2). In principle, there is no reason why individuals in one country ought to have access to discussions with leading minds in neuroscientific research, while others cannot. As such, there remains a major demand for higher level education to be made available to the public and anyone interested in the subject. With the advent of crowd-funding platforms such as

Kickstarter, we have seen that independently operated programs like NEURO.tv can be entirely funded by the individuals who are interested in such educational initiatives (312).

NEURO.tv is not just targeted at educating the public; those involved in its production learn from their experience in the program as well. The program trains young scientists in scientific communication by placing them in a panelist or co-host position, a role that requires several weeks of preparation leading up to the filming. This preparation includes reading scientific articles, formulating topics to discuss, and preparing questions that will allow anyone with minimal understanding of biology to understand the show. It is a rare, novel, firsthand learning experience in public science communication and education.

Public science education has experienced a remarkable transformation as the internet has grown, with many high quality podcasts, videos, and blogs now being available for free to anyone interested in learning about science. However, a specialised niche has not yet been filled, one in which listeners could learn about how research is conducted, with an in-depth discussion on the details of a scientific discovery along with the implications of a result or cutting-edge technique. NEURO.tv fills this niche, with content that does not avoid these details, but rather embraces them, producing episodes that do not only focus on the product of research, but also delve deeper into the thought process behind it and why scientists care about the questions being covered.

The internet has also created opportunities to improve transparency and honesty in academia. In an academic presentation setting, there is rarely room to discuss any of the doubts scientists naturally harbor about their research or techniques, or the works of others. Neuroscience is a work-in-progress, and as with all science, relies on the best

available techniques at the time the research is conducted, rather than the perfect ones. Discussions on NEURO.tv take place in an informal setting, which allows scientists to freely express their ideas and opinions about research and methods, without fearing being dismissed. Open conversations like these can only serve to better the field and improve the confidence of the general public in the scientific process and in the ability of scientists to question themselves.

With the advent of the internet, there has been a movement towards increasing the accessibility of scientific knowledge. We believe that programs such as NEURO.tv allow a novel interface between scientists and the general public. With this new experiment in scientific communication, we hope that highly-motivated individuals in the general public will develop a taste for a deeper understanding of neuroscience, and that neuroscientists will embrace the idea that part of the work lies on their shoulders, and that simplifying the explanation of their research will benefit the general public, the field, and themselves.

REFERENCES

1. 2000. Chemical-biological terrorism and its impact on children: a subject review. American Academy of Pediatrics. Committee on Environmental Health and Committee on Infectious Diseases. *Pediatrics* 105:662-70
2. 2003. Worldwide neuroscience. *Nature neuroscience* 6:901
3. 2014. *In situ Hybridization White Paper*. http://www.brain-map.org
4. Abdel-Rahman A, Shetty AK, Abou-Donia MB. 2002. Acute exposure to sarin increases blood brain barrier permeability and induces neuropathological changes in the rat brain: dose-response relationships. *Neuroscience* 113:721-41
5. Adhikari A. 2014. Distributed circuits underlying anxiety. *Frontiers in behavioral neuroscience* 8:112
6. Alderson RF, Alterman AL, Barde YA, Lindsay RM. 1990. Brain-derived neurotrophic factor increases survival and differentiated functions of rat septal cholinergic neurons in culture. *Neuron* 5:297-306
7. Amitai Y, Almog S, Singer R, Hammer R, Bentur Y, Danon YL. 1992. Atropine poisoning in children during the Persian Gulf crisis. A national survey in Israel. *Jama* 268:630-2
8. Andersen SL. 2003. Trajectories of brain development: point of vulnerability or window of opportunity? *Neuroscience and biobehavioral reviews* 27:3-18
9. Anderson DR, Harris LW, Chang FC, Baze WB, Capacio BR, et al. 1997. Antagonism of soman-induced convulsions by midazolam, diazepam and scopolamine. *Drug and chemical toxicology* 20:115-31
10. Andreollo NA, Santos EF, Araujo MR, Lopes LR. 2012. Rat's age versus human's age: what is the relationship? *Arquivos brasileiros de cirurgia digestiva : ABCD = Brazilian archives of digestive surgery* 25:49-51
11. Apland JP, Aroniadou-Anderjaska V, Braga MF. 2009. Soman induces ictogenesis in the amygdala and interictal activity in the hippocampus that are blocked by a GluR5 kainate receptor antagonist in vitro. *Neuroscience* 159:380-9
12. Apland JP, Aroniadou-Anderjaska V, Figueiredo TH, Green CE, Swezey R, et al. 2013. Efficacy of the GluK1/AMPA receptor antagonist LY293558 against seizures and neuropathology in a soman-exposure model without pretreatment and its pharmacokinetics after intramuscular administration. *The Journal of pharmacology and experimental therapeutics* 344:133-40
13. Apland JP, Aroniadou-Anderjaska V, Figueiredo TH, Rossetti F, Miller SL, Braga MF. 2014. The limitations of diazepam as a treatment for nerve agent-induced seizures and neuropathology in rats: comparison with UBP302. *The Journal of pharmacology and experimental therapeutics* 351:359-72
14. Apland JP, Figueiredo TH, Qashu F, Aroniadou-Anderjaska V, Souza AP, Braga MF. 2010. Higher susceptibility of the ventral versus the dorsal hippocampus and the posteroventral versus anterodorsal amygdala to soman-induced neuropathology. *Neurotoxicology* 31:485-92
15. Aroniadou-Anderjaska V, Figueiredo TH, Apland JP, Qashu F, Braga MF. 2009. Primary brain targets of nerve agents: the role of the amygdala in comparison to the hippocampus. *Neurotoxicology* 30:772-6

16. Aroniadou-Anderjaska V, Fritsch B, Qashu F, Braga MF. 2008. Pathology and pathophysiology of the amygdala in epileptogenesis and epilepsy. *Epilepsy research* 78:102-16
17. Aroniadou-Anderjaska V, Pidoplichko VI, Figueiredo TH, Almeida-Suhett CP, Prager EM, Braga MF. 2012. Presynaptic facilitation of glutamate release in the basolateral amygdala: a mechanism for the anxiogenic and seizurogenic function of GluK1 receptors. *Neuroscience* 221:157-69
18. Aroniadou-Anderjaska V, Qashu F, Braga MF. 2007. Mechanisms regulating GABAergic inhibitory transmission in the basolateral amygdala: implications for epilepsy and anxiety disorders. *Amino acids* 32:305-15
19. Ashani Y, Catravas GN. 1981. Seizure-induced changes in the permeability of the blood-brain barrier following administration of anticholinesterase drugs to rats. *Biochemical pharmacology* 30:2593-601
20. Askwith CC, Benson CJ, Welsh MJ, Snyder PM. 2001. DEG/ENaC ion channels involved in sensory transduction are modulated by cold temperature. *Proceedings of the National Academy of Sciences of the United States of America* 98:6459-63
21. Atlas ADMB. 2009. Allen Developing Mouse Brain Atlas [Internet]. *Allen Institute for Brain Science, Seattle (WA)(Available from: http://www. developingmouse. brain-map. org)*
22. Bahn S, Volk B, Wisden W. 1994. Kainate receptor gene expression in the developing rat brain. *The Journal of neuroscience : the official journal of the Society for Neuroscience* 14:5525-47
23. Baille V, Clarke PG, Brochier G, Dorandeu F, Verna JM, et al. 2005. Soman-induced convulsions: the neuropathology revisited. *Toxicology* 215:1-24
24. Bajgar J. 2005. Complex view on poisoning with nerve agents and organophosphates. *Acta medica* 48:3-21
25. Bajgar J. 2010. Optimal choice of acetylcholinesterase reactivators for antidotal treatment of nerve agent intoxication. *Acta medica* 53:207-11
26. Balali-Mood M, Saber H. 2012. Recent advances in the treatment of organophosphorous poisonings. *Iranian journal of medical sciences* 37:74-91
27. Baron A, Waldmann R, Lazdunski M. 2002. ASIC-like, proton-activated currents in rat hippocampal neurons. *The Journal of physiology* 539:485-94
28. Bassler EL, Ngo-Anh TJ, Geisler HS, Ruppersberg JP, Grunder S. 2001. Molecular and functional characterization of acid-sensing ion channel (ASIC) 1b. *The Journal of biological chemistry* 276:33782-7
29. Beck KD, Knusel B, Hefti F. 1993. The nature of the trophic action of brain-derived neurotrophic factor, des(1-3)-insulin-like growth factor-1, and basic fibroblast growth factor on mesencephalic dopaminergic neurons developing in culture. *Neuroscience* 52:855-66
30. Ben-Ari Y, Holmes GL. 2006. Effects of seizures on developmental processes in the immature brain. *The Lancet. Neurology* 5:1055-63
31. Ben-Ari Y, Zigmond RE, Shute CC, Lewis PR. 1977. Regional distribution of choline acetyltransferase and acetylcholinesterase within the amygdaloid complex and stria terminalis system. *Brain research* 120:435-44
32. Bernasconi N, Natsume J, Bernasconi A. 2005. Progression in temporal lobe epilepsy: differential atrophy in mesial temporal structures. *Neurology* 65:223-8

33. Betz AL, Goldstein GW. 1981. Developmental changes in metabolism and transport properties of capillaries isolated from rat brain. *The Journal of physiology* 312:365-76
34. Biagini G, Babinski K, Avoli M, Marcinkiewicz M, Seguela P. 2001. Regional and subunit-specific downregulation of acid-sensing ion channels in the pilocarpine model of epilepsy. *Neurobiology of disease* 8:45-58
35. Bickler PE, Gallego SM, Hansen BM. 1993. Developmental changes in intracellular calcium regulation in rat cerebral cortex during hypoxia. *Journal of cerebral blood flow and metabolism : official journal of the International Society of Cerebral Blood Flow and Metabolism* 13:811-9
36. Bleakman R, Schoepp DD, Ballyk B, Bufton H, Sharpe EF, et al. 1996. Pharmacological discrimination of GluR5 and GluR6 kainate receptor subtypes by (3S,4aR,6R,8aR)-6-[2-(1(2)H-tetrazole-5-yl)ethyl]decahyd roisdoquinoline-3 carboxylic-acid. *Molecular pharmacology* 49:581-5
37. Bokonjic D, Rosic N. 1991. Anticonvulsive and protective effects of diazepam and midazolam in rats poisoned by highly toxic organophosphorus compounds. *Arhiv za higijenu rada i toksikologiju* 42:359-65
38. Bolshakov KV, Essin KV, Buldakova SL, Dorofeeva NA, Skatchkov SN, et al. 2002. Characterization of acid-sensitive ion channels in freshly isolated rat brain neurons. *Neuroscience* 110:723-30
39. Boskovic B. 1981. The treatment of Soman poisoning and its perspectives. *Fundamental and applied toxicology : official journal of the Society of Toxicology* 1:203-13
40. Bradford MM. 1976. A rapid and sensitive method for the quantitation of microgram quantities of protein utilizing the principle of protein-dye binding. *Analytical biochemistry* 72:248-54
41. Braga MF, Aroniadou-Anderjaska V, Li H, Rogawski MA. 2009. Topiramate reduces excitability in the basolateral amygdala by selectively inhibiting GluK1 (GluR5) kainate receptors on interneurons and positively modulating GABAA receptors on principal neurons. *The Journal of pharmacology and experimental therapeutics* 330:558-66
42. Braga MF, Aroniadou-Anderjaska V, Xie J, Li H. 2003. Bidirectional modulation of GABA release by presynaptic glutamate receptor 5 kainate receptors in the basolateral amygdala. *The Journal of neuroscience : the official journal of the Society for Neuroscience* 23:442-52
43. Braitman DJ, Sparenborg S. 1989. MK-801 protects against seizures induced by the cholinesterase inhibitor soman. *Brain research bulletin* 23:145-8
44. Buckley NJ, Bonner TI, Brann MR. 1988. Localization of a family of muscarinic receptor mRNAs in rat brain. *The Journal of neuroscience : the official journal of the Society for Neuroscience* 8:4646-52
45. Bunemann M, Hosey MM. 2001. Novel signalling events mediated by muscarinic receptor subtypes. *Life sciences* 68:2525-33
46. Burback BL, Cabell LA, Johnson JD, McDonough JA, Osheroff MR. 2013. International Journal of Toxicology special edition volume of MMB4 DMS. *International journal of toxicology* 32:3S-4S

47. Bymaster FP, McKinzie DL, Felder CC, Wess J. 2003. Use of M1-M5 muscarinic receptor knockout mice as novel tools to delineate the physiological roles of the muscarinic cholinergic system. *Neurochemical research* 28:437-42
48. Campo-Soria C, Chang Y, Weiss DS. 2006. Mechanism of action of benzodiazepines on GABAA receptors. *British journal of pharmacology* 148:984-90
49. Capacio BR, Byers CE, Merk KA, Smith JR, McDonough JH. 2004. Pharmacokinetic studies of intramuscular midazolam in guinea pigs challenged with soman. *Drug and chemical toxicology* 27:95-110
50. Capacio BR, Shih TM. 1991. Anticonvulsant actions of anticholinergic drugs in soman poisoning. *Epilepsia* 32:604-15
51. Carlsen J, Heimer L. 1986. A correlated light and electron microscopic immunocytochemical study of cholinergic terminals and neurons in the rat amygdaloid body with special emphasis on the basolateral amygdaloid nucleus. *The Journal of comparative neurology* 244:121-36
52. Carpentier P, Delamanche IS, Le Bert M, Blanchet G, Bouchaud C. 1990. Seizure-related opening of the blood-brain barrier induced by soman: possible correlation with the acute neuropathology observed in poisoned rats. *Neurotoxicology* 11:493-508
53. Carpentier P, Testylier G, Dorandeu F, Segebarth C, Montigon O, et al. 2008. Hyperosmolar treatment of soman-induced brain lesions in mice: evaluation of the effects through diffusion-weighted magnetic resonance imaging and through histology. *Toxicology* 253:97-103
54. Carta M, Fievre S, Gorlewicz A, Mulle C. 2014. Kainate receptors in the hippocampus. *The European journal of neuroscience* 39:1835-44
55. Cascino GD. 1995. Clinical correlations with hippocampal atrophy. *Magnetic resonance imaging* 13:1133-6
56. Cascino GD, Jack CR, Jr., Parisi JE, Sharbrough FW, Hirschorn KA, et al. 1991. Magnetic resonance imaging-based volume studies in temporal lobe epilepsy: pathological correlations. *Annals of neurology* 30:31-6
57. Cendes F, Andermann F, Dubeau F, Gloor P, Evans A, et al. 1993. Early childhood prolonged febrile convulsions, atrophy and sclerosis of mesial structures, and temporal lobe epilepsy: an MRI volumetric study. *Neurology* 43:1083-7
58. Cendes F, Andermann F, Gloor P, Gambardella A, Lopes-Cendes I, et al. 1994. Relationship between atrophy of the amygdala and ictal fear in temporal lobe epilepsy. *Brain : a journal of neurology* 117 (Pt 4):739-46
59. Cendes F, Andermann F, Gloor P, Lopes-Cendes I, Andermann E, et al. 1993. Atrophy of mesial structures in patients with temporal lobe epilepsy: cause or consequence of repeated seizures? *Annals of neurology* 34:795-801
60. Chatterjee S, Riaz H. 2013. Death by insecticide. *Bmj* 346:f2029
61. Chen CC, England S, Akopian AN, Wood JN. 1998. A sensory neuron-specific, proton-gated ion channel. *Proceedings of the National Academy of Sciences of the United States of America* 95:10240-5

62. Chen Y. 2012. Organophosphate-induced brain damage: mechanisms, neuropsychiatric and neurological consequences, and potential therapeutic strategies. *Neurotoxicology* 33:391-400
63. Cheng B, Mattson MP. 1994. NT-3 and BDNF protect CNS neurons against metabolic/excitotoxic insults. *Brain research* 640:56-67
64. Chesler M. 2003. Regulation and modulation of pH in the brain. *Physiological reviews* 83:1183-221
65. Clement JG, Broxup B. 1993. Efficacy of diazepam and avizafone against soman-induced neuropathology in brain of rats. *Neurotoxicology* 14:485-504
66. Collingridge GL, Olsen RW, Peters J, Spedding M. 2009. A nomenclature for ligand-gated ion channels. *Neuropharmacology* 56:2-5
67. Collombet JM. 2011. Nerve agent intoxication: recent neuropathophysiological findings and subsequent impact on medical management prospects. *Toxicology and applied pharmacology* 255:229-41
68. Collombet JM, Carpentier P, Baille V, Four E, Bernabe D, et al. 2006. Neuronal regeneration partially compensates the delayed neuronal cell death observed in the hippocampal CA1 field of soman-poisoned mice. *Neurotoxicology* 27:201-9
69. Collombet JM, Four E, Bernabe D, Masqueliez C, Burckhart MF, et al. 2005. Soman poisoning increases neural progenitor proliferation and induces long-term glial activation in mouse brain. *Toxicology* 208:319-34
70. Collombet JM, Pierard C, Beracochea D, Coubard S, Burckhart MF, et al. 2008. Long-term consequences of soman poisoning in mice Part 1. Neuropathology and neuronal regeneration in the amygdala. *Behavioural brain research* 191:88-94
71. Cortes R, Palacios JM. 1986. Muscarinic cholinergic receptor subtypes in the rat brain. I. Quantitative autoradiographic studies. *Brain research* 362:227-38
72. Coryell MW, Wunsch AM, Haenfler JM, Allen JE, Schnizler M, et al. 2009. Acid-sensing ion channel-1a in the amygdala, a novel therapeutic target in depression-related behavior. *The Journal of neuroscience : the official journal of the Society for Neuroscience* 29:5381-8
73. Coryell MW, Ziemann AE, Westmoreland PJ, Haenfler JM, Kurjakovic Z, et al. 2007. Targeting ASIC1a reduces innate fear and alters neuronal activity in the fear circuit. *Biological psychiatry* 62:1140-8
74. Coubard S, Beracochea D, Collombet JM, Philippin JN, Krazem A, et al. 2008. Long-term consequences of soman poisoning in mice: part 2. Emotional behavior. *Behavioural brain research* 191:95-103
75. Coyle JT, Yamamura HI. 1976. Neurochemical aspects of the ontogenesis of cholinergic neurons in the rat brain. *Brain research* 118:429-40
76. de Araujo Furtado M, Lumley LA, Robison C, Tong LC, Lichtenstein S, Yourick DL. 2010. Spontaneous recurrent seizures after status epilepticus induced by soman in Sprague-Dawley rats. *Epilepsia* 51:1503-10
77. de Araujo Furtado M, Rossetti F, Chanda S, Yourick D. 2012. Exposure to nerve agents: from status epilepticus to neuroinflammation, brain damage, neurogenesis and epilepsy. *Neurotoxicology* 33:1476-90
78. Deeb TZ, Maguire J, Moss SJ. 2012. Possible alterations in GABAA receptor signaling that underlie benzodiazepine-resistant seizures. *Epilepsia* 53 Suppl 9:79-88

79. Deshpande LS, Carter DS, Phillips KF, Blair RE, DeLorenzo RJ. 2014. Development of status epilepticus, sustained calcium elevations and neuronal injury in a rat survival model of lethal paraoxon intoxication. *Neurotoxicology* 44:17-26
80. Diochot S, Salinas M, Baron A, Escoubas P, Lazdunski M. 2007. Peptides inhibitors of acid-sensing ion channels. *Toxicon : official journal of the International Society on Toxinology* 49:271-84
81. Dolgin E. 2013. Syrian gas attack reinforces need for better anti-sarin drugs. *Nature medicine* 19:1194-5
82. Dwyer JM, Rizzo SJ, Neal SJ, Lin Q, Jow F, et al. 2009. Acid sensing ion channel (ASIC) inhibitors exhibit anxiolytic-like activity in preclinical pharmacological models. *Psychopharmacology* 203:41-52
83. Ellman GL, Courtney KD, Andres V, Jr., Feather-Stone RM. 1961. A new and rapid colorimetric determination of acetylcholinesterase activity. *Biochemical pharmacology* 7:88-95
84. Engin E, Treit D. 2007. The role of hippocampus in anxiety: intracerebral infusion studies. *Behavioural pharmacology* 18:365-74
85. Escoubas P, De Weille JR, Lecoq A, Diochot S, Waldmann R, et al. 2000. Isolation of a tarantula toxin specific for a class of proton-gated Na+ channels. *The Journal of biological chemistry* 275:25116-21
86. Etkin A, Wager TD. 2007. Functional neuroimaging of anxiety: a meta-analysis of emotional processing in PTSD, social anxiety disorder, and specific phobia. *The American journal of psychiatry* 164:1476-88
87. Faraday MM, Elliott BM, Grunberg NE. 2001. Adult vs. adolescent rats differ in biobehavioral responses to chronic nicotine administration. *Pharmacology, biochemistry, and behavior* 70:475-89
88. Figueiredo TH, Aroniadou-Anderjaska V, Qashu F, Apland JP, Pidoplichko V, et al. 2011. Neuroprotective efficacy of caramiphen against soman and mechanisms of its action. *British journal of pharmacology* 164:1495-505
89. Figueiredo TH, Qashu F, Apland JP, Aroniadou-Anderjaska V, Souza AP, Braga MF. 2011. The GluK1 (GluR5) Kainate/{alpha}-amino-3-hydroxy-5-methyl-4-isoxazolepropionic acid receptor antagonist LY293558 reduces soman-induced seizures and neuropathology. *The Journal of pharmacology and experimental therapeutics* 336:303-12
90. Filliat P, Coubard S, Pierard C, Liscia P, Beracochea D, et al. 2007. Long-term behavioral consequences of soman poisoning in mice. *Neurotoxicology* 28:508-19
91. Fisahn A, Yamada M, Duttaroy A, Gan JW, Deng CX, et al. 2002. Muscarinic induction of hippocampal gamma oscillations requires coupling of the M1 receptor to two mixed cation currents. *Neuron* 33:615-24
92. Foltin G, Tunik M, Curran J, Marshall L, Bove J, et al. 2006. Pediatric nerve agent poisoning: medical and operational considerations for emergency medical services in a large American city. *Pediatric emergency care* 22:239-44
93. Fournier NM, Duman RS. 2013. Illuminating hippocampal control of fear memory and anxiety. *Neuron* 77:803-6
94. Gale GD, Anagnostaras SG, Godsil BP, Mitchell S, Nozawa T, et al. 2004. Role of the basolateral amygdala in the storage of fear memories across the adult

lifetime of rats. *The Journal of neuroscience : the official journal of the Society for Neuroscience* 24:3810-5
95. Garcia SJ, Abu-Qare AW, Meeker-O'Connell WA, Borton AJ, Abou-Donia MB. 2003. Methyl parathion: a review of health effects. *Journal of toxicology and environmental health. Part B, Critical reviews* 6:185-210
96. Gielen MC, Lumb MJ, Smart TG. 2012. Benzodiazepines modulate GABAA receptors by regulating the preactivation step after GABA binding. *The Journal of neuroscience : the official journal of the Society for Neuroscience* 32:5707-15
97. Gilat E, Kadar T, Levy A, Rabinovitz I, Cohen G, et al. 2005. Anticonvulsant treatment of sarin-induced seizures with nasal midazolam: an electrographic, behavioral, and histological study in freely moving rats. *Toxicology and applied pharmacology* 209:74-85
98. Giniatullin R, Nistri A, Yakel JL. 2005. Desensitization of nicotinic ACh receptors: shaping cholinergic signaling. *Trends in neurosciences* 28:371-8
99. Gisabella B, Bolshakov VY, Benes FM. 2012. Kainate receptor-mediated modulation of hippocampal fast spiking interneurons in a rat model of schizophrenia. *PloS one* 7:e32483
100. Goel A, Aggarwal P. 2007. Pesticide poisoning. *The National medical journal of India* 20:182-91
101. Gonzalez LE, Andrews N, File SE. 1996. 5-HT1A and benzodiazepine receptors in the basolateral amygdala modulate anxiety in the social interaction test, but not in the elevated plus-maze. *Brain research* 732:145-53
102. Goodkin HP, Liu X, Holmes GL. 2003. Diazepam terminates brief but not prolonged seizures in young, naive rats. *Epilepsia* 44:1109-12
103. Grunder S, Chen X. 2010. Structure, function, and pharmacology of acid-sensing ion channels (ASICs): focus on ASIC1a. *International journal of physiology, pathophysiology and pharmacology* 2:73-94
104. Guerreiro C, Cendes F, Li LM, Jones-Gotman M, Andermann F, et al. 1999. Clinical patterns of patients with temporal lobe epilepsy and pure amygdalar atrophy. *Epilepsia* 40:453-61
105. Gundersen HJ, Jensen EB, Kieu K, Nielsen J. 1999. The efficiency of systematic sampling in stereology--reconsidered. *Journal of microscopy* 193:199-211
106. Gupta A, Agarwal R, Shukla GS. 1999. Functional impairment of blood-brain barrier following pesticide exposure during early development in rats. *Human & experimental toxicology* 18:174-9
107. Halley SA, Wrench JM, Reutens DC, Wilson SJ. 2010. The amygdala and anxiety after epilepsy surgery. *Epilepsy & behavior : E&B* 18:431-6
108. Hamilton MG, Posavad C. 1991. Alteration of calcium influx in rat cortical synaptosomes by soman. *Neuroreport* 2:273-6
109. Hamilton SE, Loose MD, Qi M, Levey AI, Hille B, et al. 1997. Disruption of the m1 receptor gene ablates muscarinic receptor-dependent M current regulation and seizure activity in mice. *Proceedings of the National Academy of Sciences of the United States of America* 94:13311-6
110. Harris LW, Gennings C, Carter WH, Anderson DR, Lennox WJ, et al. 1994. Efficacy comparison of scopolamine (SCP) and diazepam (DZ) against soman-induced lethality in guinea pigs. *Drug and chemical toxicology* 17:35-50

111. Harrison PK, Sheridan RD, Green AC, Scott IR, Tattersall JE. 2004. A guinea pig hippocampal slice model of organophosphate-induced seizure activity. *The Journal of pharmacology and experimental therapeutics* 310:678-86
112. Hauser WA. 1994. The prevalence and incidence of convulsive disorders in children. *Epilepsia* 35 Suppl 2:S1-6
113. Haut SR, Veliskova J, Moshe SL. 2004. Susceptibility of immature and adult brains to seizure effects. *The Lancet. Neurology* 3:608-17
114. Haut SR, Veliškova J, Moshé SL. 2004. Susceptibility of immature and adult brains to seizure effects. *The Lancet Neurology* 3:608-17
115. Hayward IJ, Wall HG, Jaax NK, Wade JV, Marlow DD, Nold JB. 1990. Decreased brain pathology in organophosphate-exposed rhesus monkeys following benzodiazepine therapy. *Journal of the neurological sciences* 98:99-106
116. Henretig FM, Cieslak TJ, Eitzen EM, Jr. 2002. Biological and chemical terrorism. *The Journal of pediatrics* 141:311-26
117. Hill JA, Jr., Zoli M, Bourgeois JP, Changeux JP. 1993. Immunocytochemical localization of a neuronal nicotinic receptor: the beta 2-subunit. *The Journal of neuroscience : the official journal of the Society for Neuroscience* 13:1551-68
118. Hoffman A, Eisenkraft A, Finkelstein A, Schein O, Rotman E, Dushnitsky T. 2007. A decade after the Tokyo sarin attack: a review of neurological follow-up of the victims. *Military medicine* 172:607-10
119. Holmes GL. 2005. Effects of seizures on brain development: lessons from the laboratory. *Pediatric neurology* 33:1-11
120. Holmes GL. 2009. The 2008 Judith Hoyer lecture: epilepsy in children: listening to mothers. *Epilepsy & behavior : E&B* 16:193-202
121. Holmes GL, Ben-Ari Y. 1998. Seizures in the developing brain: perhaps not so benign after all. *Neuron* 21:1231-4
122. Hyman C, Juhasz M, Jackson C, Wright P, Ip NY, Lindsay RM. 1994. Overlapping and distinct actions of the neurotrophins BDNF, NT-3, and NT-4/5 on cultured dopaminergic and GABAergic neurons of the ventral mesencephalon. *The Journal of neuroscience : the official journal of the Society for Neuroscience* 14:335-47
123. International Program on Chemical Safety. The WHO recommended classification of pesticides by hazard and guidelines to classification. p. v. Geneva: World Health Organization
124. Jane DE, Lodge D, Collingridge GL. 2009. Kainate receptors: pharmacology, function and therapeutic potential. *Neuropharmacology* 56:90-113
125. Jett DA. 2007. Neurological aspects of chemical terrorism. *Annals of neurology* 61:9-13
126. Jimmerson VR, Shih TM, Mailman RB. 1989. Variability in soman toxicity in the rat: correlation with biochemical and behavioral measures. *Toxicology* 57:241-54
127. Johansen JP, Cain CK, Ostroff LE, LeDoux JE. 2011. Molecular mechanisms of fear learning and memory. *Cell* 147:509-24
128. Johnson DD, Lowndes HE. 1974. Reduction by diazepam of repetitive electrical activity and toxicity resulting from soman. *European journal of pharmacology* 28:245-50

129. Johnson DD, Wilcox WC. 1975. Studies on the mechanism of the protective and antidotal actions of diazepam in organophosphate poisoning. *European journal of pharmacology* 34:127-32
130. Jones DM, Esmaeil N, Maren S, Macdonald RL. 2002. Characterization of pharmacoresistance to benzodiazepines in the rat Li-pilocarpine model of status epilepticus. *Epilepsy research* 50:301-12
131. Joosen MJ, van der Schans MJ, van Dijk CG, Kuijpers WC, Wortelboer HM, van Helden HP. 2011. Increasing oxime efficacy by blood-brain barrier modulation. *Toxicology letters* 206:67-71
132. Kadar T, Cohen G, Sahar R, Alkalai D, Shapira S. 1992. Long-term study of brain lesions following soman, in comparison to DFP and metrazol poisoning. *Human & experimental toxicology* 11:517-23
133. Kadar T, Shapira S, Cohen G, Sahar R, Alkalay D, Raveh L. 1995. Sarin-induced neuropathology in rats. *Human & experimental toxicology* 14:252-9
134. Kawana N, Ishimatsu S, Kanda K. 2001. Psycho-physiological effects of the terrorist sarin attack on the Tokyo subway system. *Military medicine* 166:23-6
135. Kegley S, Hill B, Orme S, Choi A. 2010. Parathion-Identification, toxicity, use, water pollution potential, ecological toxicity and regulatory information. *Pesticide Action Network*
136. Kellinghaus C, Stogbauer F. 2012. Treatment of status epilepticus in a large community hospital. *Epilepsy & behavior : E&B* 23:235-40
137. Kim JE, Kang TC. 2011. The P2X7 receptor-pannexin-1 complex decreases muscarinic acetylcholine receptor-mediated seizure susceptibility in mice. *The Journal of clinical investigation* 121:2037-47
138. Kim JJ, Fanselow MS. 1992. Modality-specific retrograde amnesia of fear. *Science* 256:675-7
139. King D, Spencer SS, McCarthy G, Spencer DD. 1997. Surface and depth EEG findings in patients with hippocampal atrophy. *Neurology* 48:1363-7
140. Koliatsos VE, Martin LJ, Walker LC, Richardson RT, DeLong MR, Price DL. 1988. Topographic, non-collateralized basal forebrain projections to amygdala, hippocampus, and anterior cingulate cortex in the rhesus monkey. *Brain research* 463:133-9
141. Kornblum HI, Sankar R, Shin DH, Wasterlain CG, Gall CM. 1997. Induction of brain derived neurotrophic factor mRNA by seizures in neonatal and juvenile rat brain. *Molecular brain research* 44:219-28
142. Kozer E, Mordel A, Haim SB, Bulkowstein M, Berkovitch M, Bentur Y. 2005. Pediatric poisoning from trimedoxime (TMB4) and atropine automatic injectors. *The Journal of pediatrics* 146:41-4
143. Kozhemyakin M, Rajasekaran K, Kapur J. 2010. Central cholinesterase inhibition enhances glutamatergic synaptic transmission. *Journal of neurophysiology* 103:1748-57
144. Krieger RI. 2001. *Handbook of pesticide toxicology*. San Diego: Academic Press
145. Krieger RI, Hayes WJ. 2010. *Hayes' handbook of pesticide toxicology*. Amsterdam ; Boston: Elsevier : Academic Press
146. Krishtal OA, Pidoplichko VI. 1980. A receptor for protons in the nerve cell membrane. *Neuroscience* 5:2325-7

147. Kruse AC, Kobilka BK, Gautam D, Sexton PM, Christopoulos A, Wess J. 2014. Muscarinic acetylcholine receptors: novel opportunities for drug development. *Nature reviews. Drug discovery* 13:549-60
148. Kubova H, Mares P. 2013. Are morphologic and functional consequences of status epilepticus in infant rats progressive? *Neuroscience* 235:232-49
149. Kwon OY, Park SP. 2014. Depression and anxiety in people with epilepsy. *Journal of clinical neurology* 10:175-88
150. Lallement G, Carpentier P, Collet A, Baubichon D, Pernot-Marino I, Blanchet G. 1992. Extracellular acetylcholine changes in rat limbic structures during soman-induced seizures. *Neurotoxicology* 13:557-67
151. Lallement G, Carpentier P, Collet A, Pernot-Marino I, Baubichon D, Blanchet G. 1991. Effects of soman-induced seizures on different extracellular amino acid levels and on glutamate uptake in rat hippocampus. *Brain research* 563:234-40
152. Lallement G, Clarencon D, Masqueliez C, Baubichon D, Galonnier M, et al. 1998. Nerve agent poisoning in primates: antilethal, anti-epileptic and neuroprotective effects of GK-11. *Archives of toxicology* 72:84-92
153. Lallement G, Dorandeu F, Filliat P, Carpentier P, Baille V, Blanchet G. 1998. Medical management of organophosphate-induced seizures. *Journal of physiology, Paris* 92:369-73
154. Lang EJ, Pare D. 1997. Similar inhibitory processes dominate the responses of cat lateral amygdaloid projection neurons to their various afferents. *Journal of neurophysiology* 77:341-52
155. Langston JL, Wright LK, Connis N, Lumley LA. 2012. Characterizing the behavioral effects of nerve agent-induced seizure activity in rats: increased startle reactivity and perseverative behavior. *Pharmacology, biochemistry, and behavior* 100:382-91
156. Lapchak PA, Araujo DM, Dugich-Djordjevic MM, Hefti F. 1992. The role of neurotrophins in the central nervous system: significance for the treatment of neurodegenerative diseases. In *Treatment of Dementias*:99-111: Springer. Number of 99-111 pp.
157. Lein ES, Hawrylycz MJ, Ao N, Ayres M, Bensinger A, et al. 2006. Genome-wide atlas of gene expression in the adult mouse brain. *Nature* 445:168-76
158. Lemercier G, Carpentier P, Sentenac-Roumanou H, Morelis P. 1983. Histological and histochemical changes in the central nervous system of the rat poisoned by an irreversible anticholinesterase organophosphorus compound. *Acta neuropathologica* 61:123-9
159. Liang LP, Ho YS, Patel M. 2000. Mitochondrial superoxide production in kainate-induced hippocampal damage. *Neuroscience* 101:563-70
160. Lingueglia E, de Weille JR, Bassilana F, Heurteaux C, Sakai H, et al. 1997. A modulatory subunit of acid sensing ion channels in brain and dorsal root ganglion cells. *The Journal of biological chemistry* 272:29778-83
161. Lipp JA. 1968. Cerebral electrical activity following soman administration. *Archives internationales de pharmacodynamie et de therapie* 175:161-9
162. Lipp JA. 1972. Effect of diazepam upon soman-induced seizure activity and convulsions. *Electroencephalography and clinical neurophysiology* 32:557-60

163. Lipp JA. 1973. Effect of benzodiazepine derivatives on soman-induced seizure activity and convulsions in the monkey. *Archives internationales de pharmacodynamie et de therapie* 202:244-51
164. Litchfield JT, Jr., Wilcoxon F. 1949. A simplified method of evaluating dose-effect experiments. *The Journal of pharmacology and experimental therapeutics* 96:99-113
165. Liu Z, Stafstrom CE, Sarkisian M, Tandon P, Yang Y, et al. 1996. Age-dependent effects of glutamate toxicity in the hippocampus. *Brain research. Developmental brain research* 97:178-84
166. Mamczarz J, Pereira EF, Aracava Y, Adler M, Albuquerque EX. 2010. An acute exposure to a sub-lethal dose of soman triggers anxiety-related behavior in guinea pigs: interactions with acute restraint. *Neurotoxicology* 31:77-84
167. Marks JD, Friedman JE, Haddad GG. 1996. Vulnerability of CA1 neurons to glutamate is developmentally regulated. *Brain research. Developmental brain research* 97:194-206
168. Marrs TC, Rice P, Vale JA. 2006. The role of oximes in the treatment of nerve agent poisoning in civilian casualties. *Toxicological reviews* 25:297-323
169. Martin LJ, Doebler JA, Shih TM, Anthony A. 1985. Protective effect of diazepam pretreatment on soman-induced brain lesion formation. *Brain research* 325:287-9
170. Martina M, Royer S, Pare D. 2001. Cell-type-specific GABA responses and chloride homeostasis in the cortex and amygdala. *Journal of neurophysiology* 86:2887-95
171. Mash DC, Potter LT. 1986. Autoradiographic localization of M1 and M2 muscarine receptors in the rat brain. *Neuroscience* 19:551-64
172. Mash DC, White WF, Mesulam MM. 1988. Distribution of muscarinic receptor subtypes within architectonic subregions of the primate cerebral cortex. *The Journal of comparative neurology* 278:265-74
173. Matsuoka Y, Okazaki M, Kitamura Y, Taniguchi T. 1999. Developmental expression of P-glycoprotein (multidrug resistance gene product) in the rat brain. *Journal of neurobiology* 39:383-92
174. Mayer SA, Claassen J, Lokin J, Mendelsohn F, Dennis LJ, Fitzsimmons BF. 2002. Refractory status epilepticus: frequency, risk factors, and impact on outcome. *Archives of neurology* 59:205-10
175. McDonald AJ, Mascagni F. 2002. Immunohistochemical characterization of somatostatin containing interneurons in the rat basolateral amygdala. *Brain research* 943:237-44
176. McDonough JH, Jr., Clark TR, Slone TW, Jr., Zoeffel D, Brown K, et al. 1998. Neural lesions in the rat and their relationship to EEG delta activity following seizures induced by the nerve agent soman. *Neurotoxicology* 19:381-91
177. McDonough JH, Jr., Dochterman LW, Smith CD, Shih TM. 1995. Protection against nerve agent-induced neuropathology, but not cardiac pathology, is associated with the anticonvulsant action of drug treatment. *Neurotoxicology* 16:123-32
178. McDonough JH, Jr., Jaax NK, Crowley RA, Mays MZ, Modrow HE. 1989. Atropine and/or diazepam therapy protects against soman-induced neural and

cardiac pathology. *Fundamental and applied toxicology : official journal of the Society of Toxicology* 13:256-76
179. McDonough JH, Jr., McLeod CG, Jr., Nipwoda MT. 1987. Direct microinjection of soman or VX into the amygdala produces repetitive limbic convulsions and neuropathology. *Brain research* 435:123-37
180. McDonough JH, Jr., Shih TM. 1993. Pharmacological modulation of soman-induced seizures. *Neuroscience and biobehavioral reviews* 17:203-15
181. McDonough JH, Jr., Shih TM. 1997. Neuropharmacological mechanisms of nerve agent-induced seizure and neuropathology. *Neuroscience and biobehavioral reviews* 21:559-79
182. McDonough JH, Jr., Zoeffel LD, McMonagle J, Copeland TL, Smith CD, Shih TM. 2000. Anticonvulsant treatment of nerve agent seizures: anticholinergics versus diazepam in soman-intoxicated guinea pigs. *Epilepsy research* 38:1-14
183. McDonough JH, McMonagle JD, Shih TM. 2010. Time-dependent reduction in the anticonvulsant effectiveness of diazepam against soman-induced seizures in guinea pigs. *Drug and chemical toxicology* 33:279-83
184. McDonough JH, Shih T-M. 2007. 14 ATROPINE AND OTHER ANTICHOLINERGIC DRUGS. *Chemical warfare agents: toxicology and treatment*:287
185. Mehta V, Singhi P, Singhi S. 2007. Intravenous sodium valproate versus diazepam infusion for the control of refractory status epilepticus in children: a randomized controlled trial. *Journal of child neurology* 22:1191-7
186. Mercey G, Verdelet T, Renou J, Kliachyna M, Baati R, et al. 2012. Reactivators of acetylcholinesterase inhibited by organophosphorus nerve agents. *Accounts of chemical research* 45:756-66
187. Mesulam MM, Mufson EJ, Levey AI, Wainer BH. 1983. Cholinergic innervation of cortex by the basal forebrain: cytochemistry and cortical connections of the septal area, diagonal band nuclei, nucleus basalis (substantia innominata), and hypothalamus in the rhesus monkey. *The Journal of comparative neurology* 214:170-97
188. Moffett MC, Schultz MK, Schwartz JE, Stone MF, Lumley LA. 2011. Impaired auditory and contextual fear conditioning in soman-exposed rats. *Pharmacology, biochemistry, and behavior* 98:120-9
189. Moorcraft PM, Peter. 2008. *The Rhodesian War: A Military History*. Pen & Sword. 208 pp.
190. More JC, Nistico R, Dolman NP, Clarke VR, Alt AJ, et al. 2004. Characterisation of UBP296: a novel, potent and selective kainate receptor antagonist. *Neuropharmacology* 47:46-64
191. Muller JF, Mascagni F, McDonald AJ. 2005. Coupled networks of parvalbumin-immunoreactive interneurons in the rat basolateral amygdala. *The Journal of neuroscience : the official journal of the Society for Neuroscience* 25:7366-76
192. Muller JF, Mascagni F, McDonald AJ. 2011. Cholinergic innervation of pyramidal cells and parvalbumin-immunoreactive interneurons in the rat basolateral amygdala. *The Journal of comparative neurology* 519:790-805
193. Muller JF, Mascagni F, Zaric V, McDonald AJ. 2013. Muscarinic cholinergic receptor M1 in the rat basolateral amygdala: ultrastructural localization and

synaptic relationships to cholinergic axons. *The Journal of comparative neurology* 521:1743-59
194. Murata K, Araki S, Yokoyama K, Okumura T, Ishimatsu S, et al. 1997. Asymptomatic sequelae to acute sarin poisoning in the central and autonomic nervous system 6 months after the Tokyo subway attack. *Journal of neurology* 244:601-6
195. Murphy MR, Blick DW, Dunn MA, Fanton JW, Hartgraves SL. 1993. Diazepam as a treatment for nerve agent poisoning in primates. *Aviation, space, and environmental medicine* 64:110-5
196. Myhrer T, Andersen JM, Nguyen NH, Aas P. 2005. Soman-induced convulsions in rats terminated with pharmacological agents after 45 min: neuropathology and cognitive performance. *Neurotoxicology* 26:39-48
197. Nagai T, Kimura H, Maeda T, McGeer PL, Peng F, McGeer EG. 1982. Cholinergic projections from the basal forebrain of rat to the amygdala. *The Journal of neuroscience : the official journal of the Society for Neuroscience* 2:513-20
198. Nakajima T, Ohta S, Fukushima Y, Yanagisawa N. 1999. Sequelae of sarin toxicity at one and three years after exposure in Matsumoto, Japan. *Journal of epidemiology / Japan Epidemiological Association* 9:337-43
199. Naylor DE, Liu H, Wasterlain CG. 2005. Trafficking of GABA(A) receptors, loss of inhibition, and a mechanism for pharmacoresistance in status epilepticus. *The Journal of neuroscience : the official journal of the Society for Neuroscience* 25:7724-33
200. Nishiwaki Y, Maekawa K, Ogawa Y, Asukai N, Minami M, et al. 2001. Effects of sarin on the nervous system in rescue team staff members and police officers 3 years after the Tokyo subway sarin attack. *Environmental health perspectives* 109:1169-73
201. Nitecka L, Frotscher M. 1989. Organization and synaptic interconnections of GABAergic and cholinergic elements in the rat amygdaloid nuclei: single- and double-immunolabeling studies. *The Journal of comparative neurology* 279:470-88
202. Nozaki H, Aikawa N, Shinozawa Y, Hori S, Fujishima S, et al. 1995. Sarin poisoning in Tokyo subway. *Lancet* 345:980-1
203. Ohbu S, Yamashina A, Takasu N, Yamaguchi T, Murai T, et al. 1997. Sarin poisoning on Tokyo subway. *Southern medical journal* 90:587-93
204. Ohtani T, Iwanami A, Kasai K, Yamasue H, Kato T, et al. 2004. Post-traumatic stress disorder symptoms in victims of Tokyo subway attack: a 5-year follow-up study. *Psychiatry and clinical neurosciences* 58:624-9
205. Okumura T, Takasu N, Ishimatsu S, Miyanoki S, Mitsuhashi A, et al. 1996. Report on 640 victims of the Tokyo subway sarin attack. *Annals of emergency medicine* 28:129-35
206. Organization WH. 1995. The International Programme on Chemical Safety.
207. Padilla S, Lassiter TL, Hunter D. 1999. Biochemical measurement of cholinesterase activity. *Methods in molecular medicine* 22:237-45

208. Padou V, Boyet S, Nehlig A. 1995. Changes in transport of [14C] alpha-aminoisobutyric acid across the blood-brain barrier during pentylenetetrazol-induced status epilepticus in the immature rat. *Epilepsy research* 22:175-83
209. Pan BX, Dong Y, Ito W, Yanagawa Y, Shigemoto R, Morozov A. 2009. Selective gating of glutamatergic inputs to excitatory neurons of amygdala by presynaptic GABAb receptor. *Neuron* 61:917-29
210. Parent JM, Yu TW, Leibowitz RT, Geschwind DH, Sloviter RS, Lowenstein DH. 1997. Dentate granule cell neurogenesis is increased by seizures and contributes to aberrant network reorganization in the adult rat hippocampus. *The Journal of neuroscience : the official journal of the Society for Neuroscience* 17:3727-38
211. Parish C. 2013. Agency for toxic substances and disease registry.
212. Park JH, Cho H, Kim H, Kim K. 2006. Repeated brief epileptic seizures by pentylenetetrazole cause neurodegeneration and promote neurogenesis in discrete brain regions of freely moving adult rats. *Neuroscience* 140:673-84
213. Park K, Lee S, Kang SJ, Choi S, Shin KS. 2007. Hyperpolarization-activated currents control the excitability of principal neurons in the basolateral amygdala. *Biochemical and biophysical research communications* 361:718-24
214. Patel M, Li QY. 2003. Age dependence of seizure-induced oxidative stress. *Neuroscience* 118:431-7
215. Paxinos G, Watson C. 2005. *The rat brain in stereotaxic coordinates*. Amsterdam ; Boston: Elsevier Academic Press
216. Petras JM. 1994. Neurology and neuropathology of Soman-induced brain injury: an overview. *Journal of the experimental analysis of behavior* 61:319-29
217. Phelps EA, LeDoux JE. 2005. Contributions of the amygdala to emotion processing: from animal models to human behavior. *Neuron* 48:175-87
218. Philippens IH, Melchers BP, de Groot DM, Wolthuis OL. 1992. Behavioral performance, brain histology, and EEG sequela after immediate combined atropine/diazepam treatment of soman-intoxicated rats. *Pharmacology, biochemistry, and behavior* 42:711-9
219. Phillips RG, LeDoux JE. 1992. Differential contribution of amygdala and hippocampus to cued and contextual fear conditioning. *Behavioral neuroscience* 106:274-85
220. Pidoplichko VI. 1992. Ammonia and proton gated channel populations in trigeminal ganglion neurons. *General physiology and biophysics* 11:39-48
221. Pidoplichko VI, Aroniadou-Anderjaska V, Prager EM, Figueiredo TH, Almeida-Suhett CP, et al. 2014. ASIC1a activation enhances inhibition in the basolateral amygdala and reduces anxiety. *The Journal of neuroscience : the official journal of the Society for Neuroscience* 34:3130-41
222. Pidoplichko VI, Dani JA. 2005. Applying small quantities of multiple compounds to defined locations of in vitro brain slices. *Journal of neuroscience methods* 142:55-66
223. Pidoplichko VI, Dani JA. 2006. Acid-sensitive ionic channels in midbrain dopamine neurons are sensitive to ammonium, which may contribute to hyperammonemia damage. *Proceedings of the National Academy of Sciences of the United States of America* 103:11376-80

224. Pidoplichko VI, Prager EM, Aroniadou-Anderjaska V, Braga MF. 2013. alpha7-Containing nicotinic acetylcholine receptors on interneurons of the basolateral amygdala and their role in the regulation of the network excitability. *Journal of neurophysiology* 110:2358-69
225. Pinheiro PS, Lanore F, Veran J, Artinian J, Blanchet C, et al. 2013. Selective block of postsynaptic kainate receptors reveals their function at hippocampal mossy fiber synapses. *Cerebral cortex* 23:323-31
226. Popescu AT, Pare D. 2011. Synaptic interactions underlying synchronized inhibition in the basal amygdala: evidence for existence of two types of projection cells. *Journal of neurophysiology* 105:687-96
227. Prager EM, Aroniadou-Anderjaska V, Almeida-Suhett CP, Figueiredo TH, Apland JP, Braga MF. 2013. Acetylcholinesterase inhibition in the basolateral amygdala plays a key role in the induction of status epilepticus after soman exposure. *Neurotoxicology* 38:84-90
228. Prager EM, Aroniadou-Anderjaska V, Almeida-Suhett CP, Figueiredo TH, Apland JP, et al. 2014. The recovery of acetylcholinesterase activity and the progression of neuropathological and pathophysiological alterations in the rat basolateral amygdala after soman-induced status epilepticus: relation to anxiety-like behavior. *Neuropharmacology* 81:64-74
229. Prager EM, Figueiredo TH, Long RP, 2nd, Aroniadou-Anderjaska V, Apland JP, Braga MF. 2014. LY293558 prevents soman-induced pathophysiological alterations in the basolateral amygdala and the development of anxiety. *Neuropharmacology* 89C:11-8
230. Pressler R, Auvin S. 2013. Comparison of Brain Maturation among Species: An Example in Translational Research Suggesting the Possible Use of Bumetanide in Newborn. *Frontiers in neurology* 4:36
231. Qashu F, Figueiredo TH, Aroniadou-Anderjaska V, Apland JP, Braga MF. 2010. Diazepam administration after prolonged status epilepticus reduces neurodegeneration in the amygdala but not in the hippocampus during epileptogenesis. *Amino acids* 38:189-97
232. Racine RJ. 1972. Modification of seizure activity by electrical stimulation. II. Motor seizure. *Electroencephalography and clinical neurophysiology* 32:281-94
233. Raffaele K, Hughey D, Wenk G, Olton D, Modrow H, McDonough J. 1987. Long-term behavioral changes in rats following organophosphonate exposure. *Pharmacology, biochemistry, and behavior* 27:407-12
234. Rajasekaran K, Joshi S, Kozhemyakin M, Todorovic MS, Kowalski S, et al. 2013. Receptor trafficking hypothesis revisited: plasticity of AMPA receptors during established status epilepticus. *Epilepsia* 54 Suppl 6:14-6
235. Ramsay RE, Hammond EJ, Perchalski RJ, Wilder BJ. 1979. Brain uptake of phenytoin, phenobarbital, and diazepam. *Archives of neurology* 36:535-9
236. Rauch SL, Whalen PJ, Shin LM, McInerney SC, Macklin ML, et al. 2000. Exaggerated amygdala response to masked facial stimuli in posttraumatic stress disorder: a functional MRI study. *Biological psychiatry* 47:769-76
237. Rogawski MA, Gryder D, Castaneda D, Yonekawa W, Banks MK, Lia H. 2003. GluR5 kainate receptors, seizures, and the amygdala. *Annals of the New York Academy of Sciences* 985:150-62

238. Rogers MA, Yamasue H, Abe O, Yamada H, Ohtani T, et al. 2009. Smaller amygdala volume and reduced anterior cingulate gray matter density associated with history of post-traumatic stress disorder. *Psychiatry research* 174:210-6
239. Rolls ET. 2015. Limbic systems for emotion and for memory, but no single limbic system. *Cortex; a journal devoted to the study of the nervous system and behavior* 62C:119-57
240. Romano JA, Lukey BJ, Salem H. 2008. *Chemical warfare agents : chemistry, pharmacology, toxicology, and therapeutics*. Boca Raton: CRC Press. xxv, 723 p. pp.
241. Sah P, Faber ES, Lopez De Armentia M, Power J. 2003. The amygdaloid complex: anatomy and physiology. *Physiological reviews* 83:803-34
242. Salmen B, Beed PS, Ozdogan T, Maier N, Johenning FW, et al. 2012. GluK1 inhibits calcium dependent and independent transmitter release at associational/commissural synapses in area CA3 of the hippocampus. *Hippocampus* 22:57-68
243. Saunders NR, Knott GW, Dziegielewska KM. 2000. Barriers in the immature brain. *Cellular and molecular neurobiology* 20:29-40
244. Saunders NR, Liddelow SA, Dziegielewska KM. 2012. Barrier mechanisms in the developing brain. *Frontiers in pharmacology* 3:46
245. Sax NI, Lewis RJ. 1992. *Sax's dangerous properties of industrial materials*. New York, N.Y.: Van Nostrand Reinhold
246. Schmitz C, Hof PR. 2000. Recommendations for straightforward and rigorous methods of counting neurons based on a computer simulation approach. *Journal of chemical neuroanatomy* 20:93-114
247. Schmued LC, Stowers CC, Scallet AC, Xu L. 2005. Fluoro-Jade C results in ultra high resolution and contrast labeling of degenerating neurons. *Brain research* 1035:24-31
248. Segal M, Dudai Y, Amsterdam A. 1978. Distribution of an alpha-bungarotoxin-binding cholinergic nicotinic receptor in rat brain. *Brain research* 148:105-19
249. Segerstrale M, Juuri J, Lanore F, Piepponen P, Lauri SE, et al. 2010. High firing rate of neonatal hippocampal interneurons is caused by attenuation of afterhyperpolarizing potassium currents by tonically active kainate receptors. *The Journal of neuroscience : the official journal of the Society for Neuroscience* 30:6507-14
250. Sengupta P. 2013. The Laboratory Rat: Relating Its Age With Human's. *International journal of preventive medicine* 4:624-30
251. Shafferman A, Ordentlich A, Barak D, Stein D, Ariel N, Velan B. 1996. Aging of phosphylated human acetylcholinesterase: catalytic processes mediated by aromatic and polar residues of the active centre. *The Biochemical journal* 318 (Pt 3):833-40
252. Sheffler DJ, Williams R, Bridges TM, Xiang Z, Kane AS, et al. 2009. A novel selective muscarinic acetylcholine receptor subtype 1 antagonist reduces seizures without impairing hippocampus-dependent learning. *Molecular pharmacology* 76:356-68

253. Shekhar A, Sajdyk TJ, Gehlert DR, Rainnie DG. 2003. The amygdala, panic disorder, and cardiovascular responses. *Annals of the New York Academy of Sciences* 985:308-25
254. Sherwood TW, Lee KG, Gormley MG, Askwith CC. 2011. Heteromeric acid-sensing ion channels (ASICs) composed of ASIC2b and ASIC1a display novel channel properties and contribute to acidosis-induced neuronal death. *The Journal of neuroscience : the official journal of the Society for Neuroscience* 31:9723-34
255. Shih T, McDonough JH, Jr., Koplovitz I. 1999. Anticonvulsants for soman-induced seizure activity. *Journal of biomedical science* 6:86-96
256. Shih TM. 1990. Anticonvulsant effects of diazepam and MK-801 in soman poisoning. *Epilepsy research* 7:105-16
257. Shih TM. 1991. Cholinergic actions of diazepam and atropine sulfate in soman poisoning. *Brain research bulletin* 26:565-73
258. Shih TM, Duniho SM, McDonough JH. 2003. Control of nerve agent-induced seizures is critical for neuroprotection and survival. *Toxicology and applied pharmacology* 188:69-80
259. Shih TM, Koviak TA, Capacio BR. 1991. Anticonvulsants for poisoning by the organophosphorus compound soman: pharmacological mechanisms. *Neuroscience and biobehavioral reviews* 15:349-62
260. Shih TM, McDonough JH. 2000. Efficacy of biperiden and atropine as anticonvulsant treatment for organophosphorus nerve agent intoxication. *Archives of toxicology* 74:165-72
261. Shih TM, McDonough JH, Jr. 1999. Organophosphorus nerve agents-induced seizures and efficacy of atropine sulfate as anticonvulsant treatment. *Pharmacology, biochemistry, and behavior* 64:147-53
262. Shorvon S. 2001. The management of status epilepticus. *Journal of neurology, neurosurgery, and psychiatry* 70 Suppl 2:II22-7
263. Silman I, Sussman JL. 2008. Acetylcholinesterase: how is structure related to function? *Chemico-biological interactions* 175:3-10
264. Singhi S, Murthy A, Singhi P, Jayashree M. 2002. Continuous midazolam versus diazepam infusion for refractory convulsive status epilepticus. *Journal of child neurology* 17:106-10
265. Sirin GS, Zhou Y, Lior-Hoffmann L, Wang S, Zhang Y. 2012. Aging mechanism of soman inhibited acetylcholinesterase. *The journal of physical chemistry. B* 116:12199-207
266. Skovira JW, McDonough JH, Shih TM. 2010. Protection against sarin-induced seizures in rats by direct brain microinjection of scopolamine, midazolam or MK-801. *Journal of molecular neuroscience : MN* 40:56-62
267. Smith TD, Annis SJ, Ehlert FJ, Leslie FM. 1991. N-[3H]methylscopolamine labeling of non-M1, non-M2 muscarinic receptor binding sites in rat brain. *The Journal of pharmacology and experimental therapeutics* 256:1173-81
268. Smith Y, Pare JF, Pare D. 1998. Cat intraamygdaloid inhibitory network: ultrastructural organization of parvalbumin-immunoreactive elements. *The Journal of comparative neurology* 391:164-79

269. Smolders I, Bortolotto ZA, Clarke VR, Warre R, Khan GM, et al. 2002. Antagonists of GLU(K5)-containing kainate receptors prevent pilocarpine-induced limbic seizures. *Nature neuroscience* 5:796-804
270. Snoy P. 2010. Establishing Efficacy of Human Products Using Animals The US Food and Drug Administration's "Animal Rule". *Veterinary Pathology Online* 47:774-8
271. Song X, Pope C, Murthy R, Shaikh J, Lal B, Bressler JP. 2004. Interactive effects of paraoxon and pyridostigmine on blood-brain barrier integrity and cholinergic toxicity. *Toxicological sciences : an official journal of the Society of Toxicology* 78:241-7
272. Soreq H, Seidman S. 2001. Acetylcholinesterase--new roles for an old actor. *Nature reviews. Neuroscience* 2:294-302
273. Sosulina L, Graebenitz S, Pape HC. 2010. GABAergic interneurons in the mouse lateral amygdala: a classification study. *Journal of neurophysiology* 104:617-26
274. Spanedda F, Cendes F, Gotman J. 1997. Relations between EEG seizure morphology, interhemispheric spread, and mesial temporal atrophy in bitemporal epilepsy. *Epilepsia* 38:1300-14
275. Spencer DG, Jr., Horvath E, Traber J. 1986. Direct autoradiographic determination of M1 and M2 muscarinic acetylcholine receptor distribution in the rat brain: relation to cholinergic nuclei and projections. *Brain research* 380:59-68
276. Stafstrom CE. 2002. Assessing the behavioral and cognitive effects of seizures on the developing brain. *Progress in brain research* 135:377-90
277. Stafstrom CE, Holmes GL. 2002. Effects of uncontrolled seizures. Neural changes in animal models. *Advances in experimental medicine and biology* 497:171-94
278. Stein MB, Stein DJ. 2008. Social anxiety disorder. *Lancet* 371:1115-25
279. Sterri SH, Berge G, Fonnum F. 1985. Esterase activities and soman toxicity in developing rat. *Acta pharmacologica et toxicologica* 57:136-40
280. Sugita S, Uchimura N, Jiang ZG, North RA. 1991. Distinct muscarinic receptors inhibit release of gamma-aminobutyric acid and excitatory amino acids in mammalian brain. *Proceedings of the National Academy of Sciences of the United States of America* 88:2608-11
281. Swanson LW, Simmons DM, Whiting PJ, Lindstrom J. 1987. Immunohistochemical localization of neuronal nicotinic receptors in the rodent central nervous system. *The Journal of neuroscience : the official journal of the Society for Neuroscience* 7:3334-42
282. Talbot BG, Anderson DR, Harris LW, Yarbrough LW, Lennox WJ. 1988. A comparison of in vivo and in vitro rates of aging of soman-inhibited erythrocyte acetylcholinesterase in different animal species. *Drug and chemical toxicology* 11:289-305
283. Tandon P, Yang Y, Das K, Holmes G, Stafstrom C. 1999. Neuroprotective effects of brain-derived neurotrophic factor in seizures during development. *Neuroscience* 91:293-303
284. Tetz LM, Rezk PE, Ratcliffe RH, Gordon RK, Steele KE, Nambiar MP. 2006. Development of a rat pilocarpine model of seizure/status epilepticus that mimics chemical warfare nerve agent exposure. *Toxicology and industrial health* 22:255-66

285. Thiermann H, Worek F, Kehe K. 2013. Limitations and challenges in treatment of acute chemical warfare agent poisoning. *Chemico-biological interactions* 206:435-43
286. Timbrell J. 1999. *Principles of biochemical toxicology*. CRC Press
287. Timbrell J. 2001. *Introduction to toxicology*. CRC Press
288. Todorovic MS, Cowan ML, Balint CA, Sun C, Kapur J. 2012. Characterization of status epilepticus induced by two organophosphates in rats. *Epilepsy research* 101:268-76
289. Tubbs RS, Miller JH, Cohen-Gadol AA, Spencer DD. 2010. Intraoperative anatomic landmarks for resection of the amygdala during medial temporal lobe surgery. *Neurosurgery* 66:974-7
290. Ugawa S, Ishida Y, Ueda T, Inoue K, Nagao M, Shimada S. 2007. Nafamostat mesilate reversibly blocks acid-sensing ion channel currents. *Biochemical and biophysical research communications* 363:203-8
291. Ullal G, Fahnestock M, Racine R. 2005. Time-dependent effect of kainate-induced seizures on glutamate receptor GluR5, GluR6, and GluR7 mRNA and Protein Expression in rat hippocampus. *Epilepsia* 46:616-23
292. Uusi-Oukari M, Korpi ER. 2010. Regulation of GABA(A) receptor subunit expression by pharmacological agents. *Pharmacological reviews* 62:97-135
293. van der Zee EA, Luiten PG. 1999. Muscarinic acetylcholine receptors in the hippocampus, neocortex and amygdala: a review of immunocytochemical localization in relation to learning and memory. *Progress in neurobiology* 58:409-71
294. Vannucci SJ, Simpson IA. 2003. Developmental switch in brain nutrient transporter expression in the rat. *American journal of physiology. Endocrinology and metabolism* 285:E1127-34
295. Vazdarjanova A, Cahill L, McGaugh JL. 2001. Disrupting basolateral amygdala function impairs unconditioned freezing and avoidance in rats. *The European journal of neuroscience* 14:709-18
296. Vinkers CH, Olivier B. 2012. Mechanisms Underlying Tolerance after Long-Term Benzodiazepine Use: A Future for Subtype-Selective GABA(A) Receptor Modulators? *Advances in pharmacological sciences* 2012:416864
297. Voicu VA, Bajgar J, Medvedovici A, Radulescu FS, Miron DS. 2010. Pharmacokinetics and pharmacodynamics of some oximes and associated therapeutic consequences: a critical review. *Journal of applied toxicology : JAT* 30:719-29
298. Voilley N, de Weille J, Mamet J, Lazdunski M. 2001. Nonsteroid anti-inflammatory drugs inhibit both the activity and the inflammation-induced expression of acid-sensing ion channels in nociceptors. *The Journal of neuroscience : the official journal of the Society for Neuroscience* 21:8026-33
299. Waldmann R, Champigny G, Bassilana F, Heurteaux C, Lazdunski M. 1997. A proton-gated cation channel involved in acid-sensing. *Nature* 386:173-7
300. Waldmann R, Lazdunski M. 1998. H(+)-gated cation channels: neuronal acid sensors in the NaC/DEG family of ion channels. *Current opinion in neurobiology* 8:418-24

301. Walton NY, Treiman DM. 1988. Response of status epilepticus induced by lithium and pilocarpine to treatment with diazepam. *Experimental neurology* 101:267-75
302. Wasterlain CG, Niquet J, Thompson KW, Baldwin R, Liu H, et al. 2002. Seizure-induced neuronal death in the immature brain. *Progress in brain research* 135:335-53
303. Weissman BA, Raveh L. 2008. Therapy against organophosphate poisoning: the importance of anticholinergic drugs with antiglutamatergic properties. *Toxicology and applied pharmacology* 232:351-8
304. Wemmie JA, Askwith CC, Lamani E, Cassell MD, Freeman JH, Jr., Welsh MJ. 2003. Acid-sensing ion channel 1 is localized in brain regions with high synaptic density and contributes to fear conditioning. *The Journal of neuroscience : the official journal of the Society for Neuroscience* 23:5496-502
305. Wess J. 2003. Novel insights into muscarinic acetylcholine receptor function using gene targeting technology. *Trends in pharmacological sciences* 24:414-20
306. Wolfensberger SP, Veltman DJ, Hoogendijk WJ, Boomsma DI, de Geus EJ. 2008. Amygdala responses to emotional faces in twins discordant or concordant for the risk for anxiety and depression. *NeuroImage* 41:544-52
307. Womble MD, Moises HC. 1992. Muscarinic inhibition of M-current and a potassium leak conductance in neurones of the rat basolateral amygdala. *The Journal of physiology* 457:93-114
308. Womble MD, Moises HC. 1993. Hyperpolarization-activated currents in neurons of the rat basolateral amygdala. *Journal of neurophysiology* 70:2056-65
309. Woodruff AR, Sah P. 2007. Networks of parvalbumin-positive interneurons in the basolateral amygdala. *The Journal of neuroscience : the official journal of the Society for Neuroscience* 27:553-63
310. World Health Organization IPoCS. 2010. The WHO recommended classification of pesticides by hazard and guidelines to classification 2009. p. 78: Geneva : World Health Organization
311. Wu LJ, Ko SW, Toyoda H, Zhao MG, Xu H, et al. 2007. Increased anxiety-like behavior and enhanced synaptic efficacy in the amygdala of GluR5 knockout mice. *PloS one* 2:e167
312. Xie DL. 2013. *NEURO.tv - Discussion among scientists and philosophers*. http://www.kickstarter.com/projects/410389794/neurotv-discussion-among-scientists-and-philosophe
313. Xiong ZQ, Stringer JL. 2000. Extracellular pH responses in CA1 and the dentate gyrus during electrical stimulation, seizure discharges, and spreading depression. *Journal of neurophysiology* 83:3519-24
314. Yamasue H, Abe O, Kasai K, Suga M, Iwanami A, et al. 2007. Human brain structural change related to acute single exposure to sarin. *Annals of neurology* 61:37-46
315. Yanagisawa N, Morita H, Nakajima T. 2006. Sarin experiences in Japan: acute toxicity and long-term effects. *Journal of the neurological sciences* 249:76-85
316. Yermolaieva O, Leonard AS, Schnizler MK, Abboud FM, Welsh MJ. 2004. Extracellular acidosis increases neuronal cell calcium by activating acid-sensing

ion channel 1a. *Proceedings of the National Academy of Sciences of the United States of America* 101:6752-7
317. Zhou J, Bradford HF, Stern GM. 1994. The stimulatory effect of brain-derived neurotrophic factor on dopaminergic phenotype expression of embryonic rat cortical neurons in vitro. *Developmental brain research* 81:318-24
318. Zhou R, Wang S, Zhu X. 2010. Prenatal ethanol exposure attenuates GABAergic inhibition in basolateral amygdala leading to neuronal hyperexcitability and anxiety-like behavior of adult rat offspring. *Neuroscience* 170:749-57
319. Zhu PJ, Stewart RR, McIntosh JM, Weight FF. 2005. Activation of nicotinic acetylcholine receptors increases the frequency of spontaneous GABAergic IPSCs in rat basolateral amygdala neurons. *Journal of neurophysiology* 94:3081-91
320. Ziemann AE, Allen JE, Dahdaleh NS, Drebot, II, Coryell MW, et al. 2009. The amygdala is a chemosensor that detects carbon dioxide and acidosis to elicit fear behavior. *Cell* 139:1012-21
321. Ziemann AE, Schnizler MK, Albert GW, Severson MA, Howard MA, 3rd, et al. 2008. Seizure termination by acidosis depends on ASIC1a. *Nature neuroscience* 11:816-22